Fisheries and Oceans Canada | Pêches et Océans Canada
Ecosystems and Oceans Science | Sciences des écosystèmes et des océans

Canadian Science Advisory Secretariat (CSAS)

Research Document 2026/065

Quebec Region

Capelin in the Estuary and Gulf of St. Lawrence (NAFO Divisions 4RST) in 2025

Mathieu Boudreau, Geneviève J. Parent, Christelle Leung, Nellie Gagné, Mélanie Boudreau, Laurence Lévesque and Elisabeth Van Beveren

Fisheries and Oceans Canada
Maurice Lamontagne Institute
850, route de la Mer
Mont-Joli, Québec
G5H 3Z4

September 2026

Canada

Foreword

This series documents the scientific basis for the evaluation of aquatic resources and ecosystems in Canada. As such, it addresses the issues of the day in the time frames required and the documents it contains are not intended as definitive statements on the subjects addressed but rather as progress reports on ongoing investigations.

Published by:

Fisheries and Oceans Canada
Canadian Science Advisory Secretariat
200 Kent Street
Ottawa ON K1A 0E6

http://www.dfo-mpo.gc.ca/csas-sccs/
DFO.CSAS-SCAS.MPO@dfo-mpo.gc.ca



His Majesty the King in Right of Canada, as represented by the Minister of the Department of Fisheries and Oceans, 2026

This report is published under the Open Government Licence - Canada

ISSN 1919-5044
ISBN 978-1-100-00404-4 Cat. No. Fs70-5/2026-065E-PDF

Correct citation for this publication:

Boudreau, M., Parent, G.J., Leung, C., Gagné, N., Boudreau, M., Lévesque, L. and Van Beveren, E. 2026. Capelin in the Estuary and Gulf of St. Lawrence (NAFO Divisions 4RST) in 2025. DFO Can. Sci. Advis. Sec. Res. Doc. 2026/065. v + 106 p.

Aussi disponible en français :

*Boudreau, M., Parent, G.J., Leung, C., Gagné, N., Boudreau, M., Lévesque, L., et Van Beveren, E. 2026. Évaluation de stock de capelan (*Mallotus villosus*) de l'estuaire et du golfe du Saint-Laurent (4RST) en 2025. Secr. can. des avis sci. du MPO. Doc. de rech. 2026/065. v + 108 p.*

TABLE OF CONTENTS

ABSTRACT v
1. INTRODUCTION 1
1.1. STOCK STRUCTURE 1
1.2. ECOLOGY 2
1.3. REPRODUCTIVE CYCLE 2
1.3.1. Spawning phenology and distribution 3
1.3.2. Larval emergence and distribution 3
1.4. COMMERCIAL FISHERY 3
2. METHODS 4
2.1. COMMERCIAL FISHERY 4
2.1.1. Landings 4
2.2. COMMERCIAL SAMPLING 4
2.2.1. Size distribution 4
2.2.2. Relative condition factor, sex ratio and gonadosomatic index 4
2.3. INDEX OF STOCK STATUS 5
2.3.1. Trawl survey 5
2.3.2. Original mature biomass index 5
2.3.3. Original age-1 abundance index 7
2.3.4. Proposed mature biomass and age-1 abundance indices 8
2.3.5. Absolute mature biomass 10
2.4. FISHING MORTALITY 11
2.5. ASSESSING THE RELIABILITY OF CAPELIN DETECTION IN BOTTOM TRAWL SURVEYS 11
2.5.1. Predator stomach content 12
2.5.2. Environmental DNA 13
2.6. ECOSYSTEM AND CLIMATE CHANGE CONSIDERATIONS 14
3. RESULTS AND DISCUSSION 14
3.1. COMMERCIAL LANDINGS 14
3.2. COMMERCIAL SAMPLING 15
3.2.1. Mean total length 15
3.2.2. Condition, sex ratio and GSI 15
3.3. STOCK STATUS INDICATORS 16
3.3.1. Original mature biomass index 16
3.3.2. Original age-1 abundance index 16
3.3.3. Proposed mature biomass index 16
3.3.4. Proposed age-1 abundance index 18
3.4. SCALE OF FISHING MORTALITY 18
3.5. ASSESSING THE RELIABILITY OF CAPELIN DETECTION IN BOTTOM TRAWL SURVEYS 19

3.5.1. Predator stomach 19
3.5.2. Environmental DNA 19
3.6. ECOSYSTEM AND CLIMATE CHANGE CONSIDERATIONS 20
4. SOURCE OF UNCERTAINTY 20
5. CONCLUSION 21
6. ACKNOWLEDGEMENTS 22
7. REFERENCES CITED 23
TABLES 30
FIGURES 42

ABSTRACT

The 2024–2025 4RST Capelin fisheries were characterized by relatively low landings compared with 2018–2021, with less than 50% of the total allowable catch harvested. Fishing occurred primarily off western Newfoundland and Labrador and was dominated by the tuck seine and trap net fleets. Biological characteristics of the catch, including length composition, condition, sex ratio, and gonadosomatic index, remained consistent with observations from the past decade and showed no clear temporal trends. Revised mature biomass indices, which account for spatial and spatiotemporal autocorrelation as well as depth and diel effects on Capelin availability to bottom trawls, exhibited lower interannual variability and reduced uncertainty relative to previous estimates. Mature biomass in the northern Gulf of St. Lawrence has remained persistently low since 2013, whereas the southern Gulf has maintained higher levels with episodic increases. The fishing mortality index has generally remained at or below 0.25, below expected natural mortality and levels considered sustainable for a short-lived species. In the absence of approved Reference Points, stock status in 2025 remains uncertain. However, given the relatively low fishing mortality and the absence of a declining biomass trend since 2013 in the northern Gulf, combined with recent increases in the southern Gulf, harvest levels within the range observed since 2013 are unlikely to jeopardize the stock during the 2026 and 2027 fishing seasons.

1. INTRODUCTION

This research document presents biological indicators used to assess capelin (*Mallotus villosus*) stock status in 2025 in the Estuary and Gulf of St. Lawrence (GSL; NAFO[1] Divisions 4RST; Figure 1) and provides a description of the fishery. Results were presented for peer review at a Canadian Science Advisory Secretariat (CSAS) process held by Fisheries and Oceans Canada (DFO) on February 17-18, 2026 to provide science advice for the 2026-2027 Capelin fishing seasons (DFO 2026). Stock assessment of 4RST Capelin is normally undertaken every two years by DFO at the Maurice Lamontagne Institute (MLI) in Mont-Joli, Quebec. The last stock assessment took place in the winter of 2024 and provided advice for the 2024-2025 fishing seasons (DFO 2024). Previous science advisory processes concluded that fishery exploitation rates were unlikely to pose a risk to the stock. The Total Allowable Catch (TAC) remained at 10,225 t for the 2024-2025 fishing seasons, as it was in 2022 and 2023. The Capelin stock assessment is indicator-based and no reference points have been established under DFO's Precautionary Approach Policy (DFO 2009) or the recently amended Fisheries Act (Bill C-68). The stock has been encouraged to be included in the Fish Stock Provisions, which requires that a Limit Reference Point (LRP) be established. To fulfil this requirement, candidate LRPs based on an indicator of mature biomass were evaluated during the previous stock assessment (Boudreau et al. 2026). However, the level of uncertainty associated with the main stock status indicator has delayed the adoption of an LRP. For the 2026 stock assessment, we focused on improving our level of confidence in this main indicator.

1.1. STOCK STRUCTURE

Capelin have a circumpolar distribution and are mostly found in coastal and continental shelf waters with major populations occurring in the Northwest Atlantic Ocean, the northern Pacific Ocean, the waters around Iceland and in the Barents Sea. While Capelin are considered a single species, morphological, genetic, and genomic evidence indicate that there are multiple parapatric ecotypes (Dodson et al. 2007; Kenchington et al. 2015; Mecklenburg and Steinke 2015; Mecklenburg et al. 2018; Cayuela et al. 2020). Capelin found in the Arctic and Atlantic Oceans are divided into three distinct clades, including the Northeast/Central Atlantic clade, the Arctic clade, and the Northwest Atlantic clade. Within the Northwest Atlantic clade, three distinct haplotypes have been identified but all are intermixed across the Newfoundland and Labrador Shelf, the GSL, and the St. Lawrence Estuary (Cayuela et al. 2020). Previous attempts to examine the stock structure of Capelin in the Northwest Atlantic, including the GSL have highlighted multiple instances of phenotypic variation between spawning sites for traits such as spawning behaviour, diet, colour, morphology, number of vertebrae, and other life-history traits (Templeman 1948; O'Boyle and Lett 1977; Sharp et al. 1978; Carscadden 1979; Carscadden and Misra 1979; Lambert and Bernier 1989; Dodson et al. 2007; Praebel et al. 2008; Kenchington et al. 2015). Recent baseline work on adult otolith edge (Jac et al. 2026), rather than larval otolith microchemistry (Coussau et al. 2026), shows potential for better understanding migration patterns across the GSL.

[1] Northwest Atlantic Fisheries Organization

1.2. ECOLOGY

Capelin are a small schooling pelagic forage fish in the Osmeridae family (smelts). They can live up to 6 years and reach sexual maturity after 2–3 years. The sexes are indistinguishable until after their second winter, whereupon sexual dimorphism begins to appear. Males grow larger and reach sexual maturity at a larger size relative to females. Males also develop secondary sexual characteristics such as enlarged pectoral fins and two pairs of ridges, or spawning carina (one dorso-lateral and one at the base of the anal fins; Templeman 1948).

Capelin are cold water species generally found at temperatures from -1 °C to 4 °C but can also be observed over a wider range of temperatures (-2 °C – 14 °C, Carcadden 1979; Mowbray 2002; Simard, Lavoie and Saucier 2002; Rose 2005; Ingvaldsen and Gjøsæter 2013). Capelin feed almost exclusively on zooplankton, the composition of which varies seasonally, spatially, and with respect to the size of the individual (e.g., Murphy et al. 2025). Larvae (< 71 mm) mostly consume the early stages of small calanoid copepods (90–130 µm) while juveniles and adults (> 75 mm) consume larger prey generally dominated by late stages of *Calanus* species, euphausiids and hyperiid amphipods (Vesin 1981; Dalpadado and Mowbray 2013). Their diel vertical migrations coincide with those of their zooplankton prey, and most feeding occurs in the water column during nighttime (Templeman 1948; Vesin 1981; Courtois and Dodson 1986; Dalpadado and Mowbray 2013; Aarflot, Dalpadado and Fiksen 2020). However, these patterns can differ according to season and may be disrupted by changes in the physical environment or the presence of predators (Bailey et al. 1977; Rose 1988; Mowbray 2002).

Capelin are widely distributed throughout the GSL (Carscadden 1979; McQuinn et al. 2012) and can be important prey for fishes such as Greenland Halibut (*Reinhardtius hippoglossoides*) and Atlantic Cod (*Gadus morhua*; Ouellette-Plante et al. 2020), marine mammals, and seabirds (Buren, Koen-Alonso and Montevecchi 2012). Predation was estimated to be the main source of Capelin mortality in the GSL during the mid-1980s and the mid-1990s with variations in overall mortality being associated with the abundance of predators (Savenkoff, Grégoire et Chabot 2004). Variations of the amount of Capelin caught in the bottom-trawl surveys conducted in August in the northern (nGSL) and September in the southern GSL (sGSL) were found to be associated with several environmental and biological variables known to influence capelin survival and cohort strength (Lehoux et al. 2022), including body condition, sea surface temperatures, the timing of ice retreat in the GSL, as well as the abundance and phenology of one of the major prey items of capelin (*Calanoid* copepods). The findings of Lehoux et al. (2022) reinforced the hypothesis that capelin abundance is regulated by bottom-up processes in the first few years of their lives (Lewis et al. 2019).

1.3. REPRODUCTIVE CYCLE

Capelin are broadcast spawners, have determinate fecundity, and spawn only once a year. During the spring and summer, sexually segregated schools of mature Capelin migrate inshore to spawn on beaches or at demersal sites with suitable substrates (sand and fine gravel) and water temperatures of 2 °C – 12 °C (Templeman 1948; de Lafontaine et al. 1991; Davoren and Montevecchi 2006; Purchase 2018). The timing and location of those reproductive migrations are highly variable both within and among regions (Penton et al. 2012). Similar to beach spawners, demersal spawners tend to spawn on sites composed of sandy or fine gravel substrate, but are exposed to generally lower, more constant temperatures and higher salinities than on beaches. Post-spawning mortality is significant and is higher for males than females for both beach and demersal spawners (Penton et al. 2012). Iteroparity predominates among beach spawners, whereas semelparity is more common among demersal spawners (Christiansen et al. 2008). Post-spawning survival for females ranges interannually from 10-60%

and post-spawning mortality that may be ongoing for months after spawning was 80% for females and 98.5% for males 10 months after spawning in tank environment (Flynn, Nakashima and Burton 2001; Christiansen et al. 2008). Post-spawning mortality in females can occur until at least November (Burton and Flynn 1998).

1.3.1. Spawning phenology and distribution

The spawning season begins in late April–early May in the St. Lawrence estuary and progresses eastwards and northwards, reaching the Strait of Belle Isle in July and August as temperatures increase throughout the GSL (Boudreau et al. 2026). Capelin have been observed beach spawning along Quebec's North and South shore, the Saguenay Fjord, the Baie des Chaleurs, around Anticosti Island, in St. George's Bay (Nova Scotia), and off the west coast of Newfoundland (Templeman 1948; Carscadden 1979; Courtois, Simoneau and Dodson 1982; Nakashima et al. 1982; Ouellet 1987; Lambert and Bernier 1989; Sirois et al. 2009).

1.3.2. Larval emergence and distribution

Egg incubation time varies according to temperature and salinity, but typically takes 15–20 days at 10°C (Frank and Leggett 1981; Penton et al. 2012). Upon emerging from beaches or the ocean bottom, Capelin larvae are approximately 3–5 mm long. In the northwestern GSL, Capelin larvae can grow to 43–56 mm by their first winter. Larvae will metamorphose after their first winter at lengths of approximately 66–71 mm and juveniles will grow to approximately 80–110 mm by their second winter (Bailey et al. 1977; Jacquaz et al. 1977).

Capelin larvae are distributed broadly throughout the GSL (de Lafontaine et al. 1991). Upon rising to surface waters (0–20 m) following their emergence, larvae are quickly dispersed by the prevailing water currents, tides, and winds (Bailey et al. 1977; Jacquaz et al. 1977; Fortier and Leggett 1983, 1985; Ouellet et al. 2013). Areas of high larval density include the Saguenay Fjord (Sirois et al. 2009), the Estuary and northwestern GSL (Jacquaz et al. 1977; Ouellet et al. 2013), the mouth of the Baie des Chaleurs and the Shediac Valley (O'Boyle and Lett 1977; Grégoire and Girard 2014), all along Quebec's North Shore, St. George's Bay, Nova Scotia (Carscadden 1979; Lambert and Bernier 1989), and in the large bays along the west coast of Newfoundland (Carscadden 1979; Grégoire et al. 2013).

1.4. COMMERCIAL FISHERY

The commercial fishery for Capelin in the GSL is co-managed by DFO's Newfoundland and Labrador, Gulf, and Quebec regions under an evergreen Integrated Fishery Management Plan (IFMP) that was approved in 2017 and updated in 2021. The majority of the commercial fleet is based on the west coast of Newfoundland (NAFO Division 4R). Fishing seasons are generally short and coincide with the inshore Capelin spring spawning migration. The opening date for the commercial fishery is chosen based on the availability of Capelin to fishing gear, the weather, and recommendations from the industry. While females and their roe are largely sold for human consumption, males have traditionally been released, discarded, or used as fertilizer. The TAC for Capelin in the GSL has rarely been limiting and landings have historically been market-driven (Grégoire et al. 2013). The TAC is currently split by fleet and NAFO Division (Table 1). The 4R fixed gear fleet, which includes tuck seiners, has an allocation of 37.82% of the total TAC under a fully competitive quota. The 4R mobile gear fleet includes large (vessels > 19.81 m or 65 ft.) and small (vessels < 19.81 m) purse seiners, each with an allocation of 24.15% of the total TAC. Small seiners are managed through individual quotas, while larger seiners are managed as a competitive fishery. The allocation for 4ST is 13.88% of the total TAC and is managed as a competitive fishery across all gear types. All licence holders are required to have their catch monitored at dockside and the return of logbooks is mandatory.

2. METHODS

2.1. COMMERCIAL FISHERY

2.1.1. Landings

Detailed commercial fisheries landing data (1985–2025) were extracted from the most recent Zonal Interchange File Format database (ZIFF) compiled by MLI's data management and DFO's regional statistics bureaus. At the time of this assessment, landing data for the 2021 to 2025 fishing seasons were still preliminary.

Landings data were summarized by year, NAFO Division and gear type. The seasonality of the Capelin fishery was summarized yearly by calculating the cumulative daily percentage of the annual total landings. The spatial distribution of landed catches was not mapped because the majority of Capelin ZIFF data between 1985 and 2025 lacks geographic coordinates. Landings by NAFO Division were deemed more appropriate for this purpose.

2.2. COMMERCIAL SAMPLING

2.2.1. Size distribution

DFO's port sampling program provides data on the length and sex composition of commercial landings in the GSL (Lambert and Ménager 1998, Daigle et Benoît 2007). Each sample consists of total length measurements and sex determinations for 150 randomly selected fish from a single fishing trip. From 1984 to 1987, fish were measured with a precision of 5 mm, but subsequently, a 1 mm precision was used. These data were used to estimate the size distribution of female and male Capelin caught in Divisions 4R and 4ST for the 1984–2025 period.

A subsample of one Capelin per sex per 5 mm bin from each port sample was analyzed in the laboratory at MLI (hereafter, commercial biological data). Measurements taken at MLI included: total length (nearest mm), mass (nearest 0.1 g), sex, gonad mass (nearest 0.1 g) and maturity stage (immature, maturing, pre-spawning, spawning or recovering). Age reading was carried out in the past (1976–1993) and a renewed program is being developed.

2.2.2. Relative condition factor, sex ratio and gonadosomatic index

Mean body condition of male and female Capelin was estimated by calculating the relative condition factor (*Kn*; Le Cren 1951) for each sex and NAFO division using the commercial biological data with the following equation:

$$\text{(eq. 1)}\quad Kn_i = W_i / aL_i^b$$

where a and b are the coefficients of the sex and NAFO-specific length-weight relationship, L_i is the individual fish (i) length in millimetres and W is the somatic weight of the i th fish in grams. The effects of different factors on the relative condition of both sexes were assessed by fitting generalized linear models (GLM) with an identity link, with Kn as the response variable and year, month, and fishing gear included as categorical independent variables. Standardized Kn time series were developed from the model estimates by fixing the month to June and the fishing gear to purse seiners, which represent the most commonly observed categories.

Annual sex ratios were calculated for NAFO Divisions 4R, 4S, and 4T using the commercial biological data (May-July). Gonadosomatic indices (GSI; %) were also calculated for males and

females using gonad weight$GW$$W$) of Capelin in the commercial biological data according to the following equation :

$$\text{(eq. 2) } GSI = \frac{GW}{W} * 100$$

Individuals whose sex could not be identified, those weighing less than 5 g, and males with a GSI greater than 10% were considered outliers in the data and were excluded from the analysis. Data were pooled across fishing gears because GSI did not differ significantly between them. Annual means and 95% confidence intervals were computed for each sex.

2.3. INDEX OF STOCK STATUS

2.3.1. Trawl survey

Multi-species bottom-trawl surveys have taken place every year in the nGSL in August (1990-2025) and in the sGSL in September (1971-2025). The sGSL survey used a Western IIA trawl from 1971 to 2022 and a Northeast Fisheries Science Center Ecosystem Survey Trawl (NEST) from 2022 onward (Chadwick et al. 2007; Benoît and Yin 2023). The nGSL survey used a University of Rhode Island (URI) trawl from 1990 to 2005 and then a Campelen shrimp trawl from 2006 onward (Bourdages et al. 2019; Chamberland et al. 2025). Both surveys followed a stratified-random design with an annual mean number of successful tows of 180 for the nGSL and 170 for the sGSL. The use of different gear and standard trawl duration for the nGSL (15 min) and the sGSL (20 min) has so far precluded the development of a single standardized index for the entire GSL.

Data obtained from each tow in the sGSL and nGSL surveys included total Capelin catch (kg) and tow characteristics (duration, start and end location, etc.). In the sGSL, lengths (total length, cm) were measured for all individuals in small catches or for a random sample of up to 200 individuals in large catches. Length-stratified subsamples were used to obtain individual weights (1 fish per 1 cm bin). In the nGSL, 30 randomly selected fish were measured for total length (mm) and weight (g). For each region (sGSL and nGSL), annual length frequencies were obtained by scaling tow-level length distributions to the corresponding catch size (in numbers), averaging across all tows in the region, and converting the result into frequencies. Results of the estimated frequencies showed that capelin caught in the nGSL are larger on average than in the sGSL (Figure 2).

Biological samples from the nGSL (2018-2025) and the sGSL (2020-2025) surveys were also preserved for subsequent length and maturity measurements at MLI. Maturity stages were assigned according to criteria established by Winters (1970). Capelin classified as “resting” or “maturation” were considered mature.

2.3.2. Original mature biomass index

A survey design-based approach was developed by Chamberland et al. (2022) to estimate relative mature biomass indices for the nGSL and sGSL from their corresponding bottom trawl surveys described above (section 2.3.1). This original approach was applied and refined during the 2024 assessment (Boudreau et al. 2026). For the 2026 assessment, we present this original method alongside a newly developed indicator based on the same data.

Capelin are associated with cold conditions and perform vertical migrations that affect their availability to the trawl. There is clear evidence that the bottom trawl has a higher probability of capturing Capelin when sampling their preferred thermal habitat (PTH) bottom temperature; -1 to 3.2 °C in the nGSL and 0 to 2 °C in the sGSL) relative to when sampling unfavourable thermal habitats (UTH). Therefore, survey strata were first classified by habitat type. The

definition of PTH and UTH were based on cumulative frequencies of Capelin catch in relation to bottom temperatures recorded when the gear touched the seafloor (Chamberland et al. 2022, Figure 3). Removing UTH strata because of their low catchability results in the need to extrapolate Capelin abundance over a large area. Keeping them might be more appropriate if the data from these UTH strata are still informative on stock trends. Therefore, indices of mature Capelin and age-1 abundance were estimated for each combination of survey and habitat type (nGSL-PTH, nGSL-UTH, sGSL-PTH and sGSL-UTH) from 1995 to 2025 in the nGSL and from 1990 to 2025 in the sGSL. It was not possible to estimate the mature biomass nor the age-1 abundance before 1995 in the nGSL since Capelin were not previously measured.

The original indices were estimated in units of survey-specific mean number of mature Capelin caught per tow (MNPT, Chamberland et al. 2022), before a spatial model was applied to impute missing strata, and the regional indicators were converted into mature biomass. Here, we directly transformed the number of capelin caught per tow into mature weight to improve statistical properties (i.e., stabilise interannual variance) and to work directly with the stock unit of interest to management.

The annual (y) mature biomass of capelin caught per tow t ($MB_{t,y}$) was calculated as:

$$\text{(eq. 3) } MB_{t,y} = \sum_{l=1} \frac{N^{e}_{l,t,y}}{\sum_{l=1} N^{e}_{l,t,y}} * N^{c}_{t,y} * M_{l,t} * W_{l,t,y}$$

Length-frequency distributions were first estimated for each tow using the numbers at length l in the random sample ($N^{e}_{l,t,y}$) divided by the total sample size. These frequencies were then scaled by the total number of capelin caught ($N^{c}_{t,y}$) to estimate total numbers-at-length for each tow. Numbers-at-length were converted to mature biomass by applying length-specific maturity proportions ($M_{l,t}$) and weights ($W_{l,t,y}$). Values for $M_{l,t}$ were derived from biological samples collected during surveys conducted between 2018 and 2025. Since there were no major differences between the lengths at which 50% of Capelin were mature among sexes (males:12 cm; females:10.8 cm; undetermined sex: 11.4 cm) or among years (Boudreau et al. 2026), all sexes and years were pooled together to calculate $M_{l,t}$ (Figure 4). $W_{l,t,y}$ was predicted annually using length–weight relationships (Table 2, sGSL: 1990-2025; nGSL: 1995-2025). Total tow-specific mature capelin biomass was calculated by summing the mature biomass across all length classes.

Next, we reapplied the model of Chamberland et al. (2022) per survey-habitat combination, except that a Tweedie distribution was used instead of a negative binomial distribution, as annual tow-specific biomasses rather than numbers were used as input. Following the previous research recommendations of the last stock assessment (Boudreau et al. 2026), we also evaluated the effect of diurnal migration of Capelin on $MB_{t,y}$ by testing two different covariates: time of the day in hours and time of the day in categories (day and night).

For each survey-habitat combination (4 models), the annual mature biomasses ($MB_{t,s,y}$) per tow and stratum (s) were predicted according to the equations below:

$$\text{(eq. 4) } MB_{t,s,y} \sim Tweedie(\mu_{s,y}, p, \phi)$$

$$\text{(eq. 5) } \log(\mu_{s,y}) = \lambda_s + \delta_{s,y} + offset + T_{t,s,y}, \text{ where } \delta_{s,y} = \rho\delta_{s,y-1} + \varepsilon_{s,y} \text{ and } \varepsilon_{s,y} \sim N(0, \sigma^2)$$

where

- $MB_{t,s,y}$ is the mature biomass (kg) caught in tow *t*, stratum *s* and year *y*,
- $\mu_{s,y}$ is the mean biomass density (kg/km^2) in stratum *s* and year *y*,

- p, ϕ are the power and dispersion parameters of the Tweedie distribution,
- λ_s is the overall stratum effect,
- $\delta_{s,y}$ is the stratum-year effect that follows an Autoregressive Order 1 (AR(1)) process with autocorrelation parameter ρ and error variance σ^2,
- $offset$ is the swept area (km^2),
- $T_{t,s,y}$ is the time of day in hours or in categories associated with each observation.

As in Chamberland et al. (2022), tow duration was included as a model offset because sample duration should be proportional to the total biomass of Capelin caught.

For each of the four models, the estimated mean capelin biomass density per stratum $\mu_{s,y}$ was extracted for 10AM, when tow catches are highest (Chamberland et al. 2022). These densities were multiplied by the corresponding stratum surface area (A_s; km^2) and then summed across all strata to estimate total survey-habitat (SH) capelin biomass:

$$\text{(eq. 6) } MB_y^{SH} = \sum_S \mu_{s,y} * A_s$$

The areas represented by the different survey-habitat combination (SH) were 41,076 km^2 (nGSL-PTH), 75,039 km^2 (nGSL-UTH), 51,502 km^2 (sGSL-PTH), and 15,704 km^2 (sGSL-UTH).

Mature biomasses estimated in each survey-habitat combination were summed without any correction for catchability to obtain the annual trawlable mature biomass of the stock:

$$\text{(eq. 7) } MB_y = \sum_{SH} MB_y^{SH}$$

2.3.3. Original age-1 abundance index

A number at age-1 index ($N1_{t,y}$) was estimated following the same steps employed for the mature biomass index (see 2.3.2). Total numbers-at-length for each tow were converted to numbers at age-1 rather than mature biomass, by multiplying by the proportion of age-1 fish for each length bin ($PA1_{l,t}$, Figure 4):

$$\text{(eq. 8) } N1_{t,y} = \sum_{l=1} \frac{N^e_{l,t,y}}{\sum_{l=1} N^e_{l,t,y}} * N^c_{t,y} * PA1_{l,t}$$

The proportion of age-1 Capelin at length ($PA1_{l,t}$) was estimated from age at length data obtained from samples collected during the 2017 and 2018 surveys. The lack of age information precludes the inclusion of interannual variability in this parameter.

When fitting the SH-specific models, the negative binomial distribution was employed since the response variable is a count. The annual age-1 Capelin abundance in year y for each survey-habitat combination was estimated following:

$$\text{(eq. 9) } N1_{t,s,y} \sim NB\left(\mu_{s,y}, \phi\right)$$

$$\text{(eq. 10) } \log(\mu_{s,y}) = \lambda_s + \delta_{s,y} + offset + T_{t,s,y}, \text{ where } \delta_{a,y} = \rho\delta_{a,y-1} + \varepsilon_{a,y}$$

$$\text{(eq. 11) } MNPT_y = \frac{\sum_{a=1}^{L} N_y \mu_{a,y}}{N} \text{ where } N = \sum_{a=1}^{L} N_a$$

$$\text{(eq. 12) } R_y = MNPT_y \times SH$$

where

- $A1_{s,a,y}$ is the age 1 fish abundance caught in tow *t*, stratum *s* and year *y*

- ϕ is the negative binomial dispersion parameter.

Estimated averages ($\mu_{s,y}$) at 10AM were again multiplied by the corresponding stratum surface to obtain SH-specific indices, which were subsequently summed to estimate total abundance at age 1. The index is considered an age-1 abundance index rather than a recruitment index, as estimating recruitment would require larval survey data, which are not currently available. However, age-1 capelin abundance can still provide valuable insight into overall population trends.

2.3.4. Proposed mature biomass and age-1 abundance indices

During the 2024 stock assessment, concerns were raised that trends in mature Capelin biomass might be strongly influenced by one or a few unusually large catches, which carry high uncertainty (Boudreau et al. 2026). To address this, research recommendations included examining the spatial distribution of these catches and their consistency across the years to determine if they reflect recurring patterns or random events unlikely to indicate true local biomass. First, Capelin catches above the annual 99th percentile of non-zero values were mapped to explore their spatiotemporal patterns visually. Second, a new model was developed to better capture fine-scale spatial and temporal structure. In fisheries science, spatiotemporal generalized linear mixed models (GLMMs) are increasingly utilized to model species distributions and standardize abundance or biomass indices. A key benefit of these models is that they account for latent spatial and temporal autocorrelation through random effects, allowing infrequent large catches to be interpreted in the context of the stock's spatiotemporal distribution patterns. For example, these models have been used to estimate density, sex ratio, and female length of northern shrimp from Baffin Island to the Grand Banks of Newfoundland and Labrador (Baker et al. 2025), and to integrate trawl and longline surveys across British Columbia for improved groundfish distribution predictions (Thompson et al. 2022).

The general workflow for fitting these models includes:

1. building a mesh to capture spatial structure via autocorrelation matrices,
2. fitting increasingly complex models,
3. interpreting coefficients and random fields, and
4. evaluating predictions and uncertainties (Anderson et al. 2025).

The R package *sdmTMB* implements geostatistical spatial and spatiotemporal GLMMs using *TMB* (Kristensen et al. 2016) and *fmesher* (Lindgren 2026) to create stochastic partial differential equation (SPDE) matrices, a computationally efficient method for modeling spatial correlation. *sdmTMB* aims to provide a fast, flexible, and user-friendly interface, similar to *glmmTMB* (Brooks et al. 2017), but focused on spatial and spatiotemporal models using the SPDE approach. A single spatial correlation matrix was designed with the *mesh* function of the package *sdmTMB* and considered a 15 km minimum distance between two points. The same matrix was applied to model mature biomass and age-1 abundance. Spatial barriers such as Anticosti Island and the Magdalen Islands were incorporated to block spatial autocorrelation between opposite sides of the islands (see Figures 5 and 6). Models were fitted separately for the nGSL and sGSL surveys, and for mature biomass and age-1. We then used the function *sdmTMB* to model per-tow observations as a function of different explanatory covariates:

$$\text{(eq. 13) } MB_{t,y} \sim Tweedie(\mu_{t,y}, p, \phi) \text{ or } N1_{t,y} \sim NB(\mu_{t,y}, \phi)$$

$$\text{(eq. 14) } \log(\mu_{t,y}) = \mathrm{X}_{t,y}^{\mathrm{main}}\beta + O_{t,y} + \omega_t + \delta_{t,y}$$

where

- $MB_{t,y}$ is the weight of mature capelin (response data) in tow t and time y;
- $N1_{t,y}$ is the number of age-1 Capelin (response data) in tow t and time y;
- $\mu_{t,y}$ is the conditional mean on the response data scale to which a link function is applied (log);
- $\mathrm{X}_{t,y}^{\mathrm{main}}$ is the design matrix for the fixed effects representing the main covariates,
- β is a vector of fixed-effect coefficients,
- $O_{t,y}$ is an offset (swept area in km^2): a covariate with a coefficient fixed at one that enters on the linear predictor scale before the inverse log link,
- ω_t is a spatial Gaussian Markov Random Field (GMRF) component, $\omega_t \sim \mathrm{MVN}(0, \Sigma_\omega)$ with Matérn covariance built from the mesh, and
- $\delta_{t,y}$ is a spatiotemporal GMRF component, $\delta_{t,y} \sim \mathrm{MVN}(0, \Sigma_\delta)$ with Matérn covariance over space and time.

To predict the response variable ($MB_{t,y}$ or $N1_{t,y}$), we employed the Tweedie distribution (with power p and dispersion θ) for the mature biomass and the negative binomial (with dispersion θ) for age-1 numbers (with dispersion parameter θ), following previous analyses (see section 2.3.3). Space *(t)* was defined by *X* and *Y* coordinates in kilometers and time (y) corresponded to annual time steps from 1995 to 2025 in the nGSL and from 1990 to 2025 in the sGSL.

Covariates ($\mathrm{X}_{t,y}^{\mathrm{main}}$) included bottom depth and sampling time, as they are known to influence Capelin catches (Chamberland et al. 2022). Habitat type (UTH/PTH) was not considered because it captures a similar ecological effect as bottom depth. Bottom depth for each tow was obtained by intersecting tow locations with a 1x1 km² bathymetric grid, which was aggregated from a 0.5x0.5 km² grid based on the General Bathymetric Chart of the Oceans (GEBCO Compilation Group 2020; available at https://www.gebco.net). Sampling time was represented either as continuous hours or as a categorical day-night variable, with the formulation giving the best fit (lowest AIC) retained. Including sampling time accounts for nocturnal vertical migrations that reduce Capelin availability to bottom trawls at night, consistent with the 2024 assessment's recommendations (Boudreau et al. 2026). Time of day was calculated by rounding the Coordinated Universal Time (UTC) of the tow, while the day–night category was determined using location- and date-specific sunrise and sunset times via the *sunriset* function in the R package *suntools* (Bivand and Luque 2025). For depth and time (hours), we evaluated models using raw values, log-transformed values, and second-order polynomial terms applied to both scales. Future analyses will explore the use of sine–cosine transformations to model the cyclic nature of capelin vertical movement.

The identification of the most parsimonious model was carried out according to different criteria. First, a step-by-step approach using the Akaike information criterion (AIC) was performed. Candidate models were also validated with the *sanity* function of the *sdmTMB* package, which performs a suite of standard diagnostic checks on model fit, including successful convergence, a positive-definite Hessian, absence of extreme or near-zero eigenvalues, acceptable maximum gradient components (≥ 0.001), non-missing or unreasonably large fixed-effect standard errors, and acceptable estimates of range and variance parameters. The final step in model selection involved examining residual diagnostics. We used the *DHARMa* package (Hartig 2026) to assess simulated residuals for hierarchical regression models, including QQ plots, tests for overdispersion, outliers, and zero-inflation, as well as residual patterns relative to the fitted

values. Quantile residuals were also examined in relation to covariates to identify any remaining structure not captured by the model. Only once the best combination of covariates was identified did we enrich the model by adding the spatial and spatiotemporal GMRF. The latter followed an AR(1) process that defines the correlation between random field deviations from one time step to the next:

$$\text{(eq. 15) } \delta_{y=1} \sim \mathrm{MVN}(0, \Sigma_\epsilon)$$

$$\text{(eq. 16) } \delta_{y>1} = \rho\delta_{y-1} + \sqrt{1-\rho^2}\epsilon_y, \epsilon_y \sim \mathrm{MVN}(0, \Sigma_\epsilon)$$

where

- ρ represents the correlation between subsequent spatiotemporal random fields and is constrained between -1 and 1;
- $\rho\delta_{y-1} + \sqrt{1-\rho^2}\epsilon_y$ scales the spatiotemporal variance by the correlation such that it represents the steady-state marginal variance.

Next, we tested two ways of adding year as a temporal effect:

1. as a random effect, assuming year-to-year variability follows a normal distribution, and
2. as a categorical factor, estimating a separate effect for each year.

Model performance was evaluated with a 50-fold cross validation and comparing the sum of predictive log-likelihood across observations for each fold, the root mean square error (RMSE) and the mean absolute error (MAE).

Standardized indices were obtained from the selected models by predicting either mature biomass or age-1 fish abundance on the 1x1 km² depth grid. The sampling time was set to "day". The final indices from sdmTMB were then compared with the design-based model indices.

2.3.5. Absolute mature biomass

The mature biomass indices are relative and must be scaled to absolute values using plausible catchability coefficients (q) in order to approximate fishing mortality rates and to assess whether harvest levels are sustainable. During the 2021 stock assessment (Chamberland et al. 2022), values of q equal to 0.0045 and 0.00087 were applied to the sum of the nGSL and sGSL biomasses to approximate the different scales of exploitation rates (landings over available biomass). Values of q were based on catchability information of other pelagic fish in bottom trawl surveys (Harley et al. 2001; Benoît and Swain 2008). Following the 2022 stock assessment (Boudreau et al. 2023), a conservative lower limit for q of 0.1 for the sGSL and 0.01 for the nGSL surveys were deemed realistic. The difference between both regions reflects variation in habitat type coverage (surface of PTH versus UTH strata; Figure 3) and aligns with the information provided in O'Driscoll, Rose and Anderson (2002). These authors compared acoustic with trawlable Capelin densities collected during a single survey targetting Capelin (Boudreau et al. 2026).

For the 2026 assessment, only the mature biomass estimated for the nGSL with the sdmTMB approach was used to derive mature biomass trends and to approximate fishing mortality. The link between biomass estimates from the two regions remains poorly understood (e.g., relative scaling and connectivity). Because the fishery primarily targets larger capelin in 4R, it was considered precautionary to approximate mature biomass and corresponding exploitation rates using only the nGSL index. The indices therefore reflect biomass available to the fishery, rather

than total stock biomass. Based on O'Driscoll, Rose and Anderson (2002), a value of 0.01 was applied to the nGSL mature biomass index derived with the new sdmTMB approach.

2.4. FISHING MORTALITY

The annual exploitation (E_y) and fishing mortality (F_y) rates for the 4RST Capelin stock were calculated as:

$$\text{(eq. 17 and 18)}\quad E_y = \frac{L_y q}{B_{y-1}} \text{ and } F_y = -\ln\left(1 - E_y\right)$$

where;

- L_y are the annual total landings in NAFO 4RST during year y (1996-2025),
- B_{y-1} is the mature biomass index for the nGSL (1995-2024), and
- q is the catchability coefficient (0.01).

In the previous stock assessment, exploitation rates were calculated using the combined biomasses of the nGSL and sGSL. However, the same value of *q* was applied to the nGSL biomass series. The total available biomass was then reduced by a constant natural mortality rate (*M*) to account for the time lag between the surveys (late summer to early fall) and the fishery (early summer of the following year; Boudreau et al. 2023, 2026). Given the substantial uncertainties associated with *M*, no such adjustment was applied in the present assessment. Note that this only impacts the scale of the biomass series and not its trend.

The scale of F_y remains uncertain. For instance, neglecting *M* may lead to underestimation of F_y (by a factor up to about 0.6, see *M* estimate below), while precautionary biomass assumptions (e.g., *q*, NGSL-restricted biomass) may result in overestimation. Overall, estimates are more likely biased high, and are still expected to be informative in terms of overall order of magnitude.The estimated ranges and mean values of *E* and *F* were therefore compared with sustainability benchmarks reported for other small pelagic fish stocks (Patterson et al. 1992). Patterson et al. (1992) analyzed 28 stocks across 11 small pelagic species and suggested that stocks may increase under certain conditions when *F* is less than half of natural mortality, or when *E* is below 30%. To define the *F* threshold, a *M* of 0.85 was utilized, corresponding to the mean *M* estimated with the *metaM* function from the *FSA* package (Ogle et al. 2026). This estimate was based on life-history traits and environmental characteristics specific to 4RST Capelin (see Table 7 and 8 in Boudreau et al. 2026).

2.5. ASSESSING THE RELIABILITY OF CAPELIN DETECTION IN BOTTOM TRAWL SURVEYS

Unlike other major stocks, there is no directed Capelin survey in 4RST to estimate stock biomass. The index presented here is derived from opportunistically collected capelin data from two bottom trawl surveys, and therefore carries a relatively high level of uncertainty. Some of this uncertainty can be addressed by validating trawl observations against independently collected data. Two concurrently collected data sources are readily available: capelin in predator stomachs and environmental DNA (eDNA). Indeed, prey abundances in predator stomachs have already been used to estimate diet-based indices of biomass for pelagic fish (Ng et al. 2021) and are especially useful when surveys are not designed to capture forage species (Gaichas et al. 2024). Additionally, eDNA can for instance improve species distribution modelling when integrated with trawl captures (Chevrinais et al. 2025). The focus of the presented analyses is on the occurrences of capelin in both data sources, rather than on their abundance or biomass, since the number of capelin observed in predator stomachs should not

scale linearly with trawl-derived biomass, and the relationship between eDNA detections and capelin biomass also remains an area of ongoing research.

2.5.1. Predator stomach content

Capelin is considered a keystone species in the GSL ecosystem, facilitating energy transfer between lower and upper trophic levels (Savenkoff et al. 2004). It can constitute a significant element of the diet of groundfish, such as Greenland halibut and Atlantic cod. Stomachs of both these predators have been sampled regularly during the nGSL bottom trawl survey since 1993 (Ouellette-Plante et al. 2022), except for Atlantic cod between 2009 and 2014 and for Greenland halibut in 2000 and from 2009 to 2014 (Figure 7). The predator stomach sampling methodology is described in section 2.1 of Ouellette-Plante et al. 2020 and 2022. Stomach data is not uniformly spread across the survey area. To maximise spatial coverage, information from both predators (Figure 8) was pooled together for further analyses and Capelin occurrences were statistically interpolated across the area. To facilitate comparison with the mature biomass maps, we modeled the probability of capelin occurrence in the stomach contents of the two main predators with sdmTMB using the same mesh, following :

$$\text{(eq. 19) } Y_{t,y} = NB(\mu_{t,y,}\phi)$$

$$\text{(eq. 20) } logit(\mu_{t,y}) = \mathrm{X}_{t,y}^{\mathrm{main}}\beta + O_{t,y} + \omega_t$$

where

- $Y_{t,y}$ is the observed presence (1) or absence (0) of capelin in each available predator stomach in tow t and year y,
- $\mu_{t,y}$ is the expected mean probability of capelin occurrence in tow t and year y conditional on the covariates, to which a logit link function is applied, and
- $\mathrm{X}_{t,y}^{\mathrm{main}}$, β, $O_{t,y}$, ω_t are described in section 2.3.4.

A single model was fitted using capelin presence (1) or absence (0) per tow as the response, based on all stomachs sampled from each predator species across all predator length classes. The model assumed a negative binomial error distribution with a logit link. Predictor variables ($\mathrm{X}_{s,y}^{\mathrm{main}}$), including depth and sampling time (day vs. night), were similar to the mature biomass and age-1 abundance models. Predator type (Greenland halibut vs. Atlantic cod) was however also included as a covariate to account for dietary differences, as Greenland halibut have a more specialized diet focused on Capelin (DFO 2023), whereas Atlantic cod have a more generalized diet (Ouellette-Plante et al. 2020). Additionally, the two species may differ in their encounter rates with capelin. The number of stomachs sampled for each predator in a given tow was included as an offset ($O_{s,y}$), since the probability of detecting capelin increases with the number of stomachs examined. A spatial random field was included to account for spatial structure, rather than a spatiotemporal random field, consistent with common practice for modeling presence and absence data in sdmTMB (Thompson et al. 2022; Nephin et al. 2023). Model selection followed the stepwise procedure described in Section 2.3.4, using AIC, diagnostic checks, and residual analyses to identify the most parsimonious model.

The final model was used to predict and map the probability of Capelin occurrence in the stomachs of Greenland halibut and Atlantic cod across a 1x1 km² depth grid. Agreement between predicted stomach occurrence and trawl-based estimates of mature capelin biomass was assessed visually using maps and boxplots, comparing predicted stomach occurrence probabilities between tows with observed Capelin presence and absence in the bottom trawl.

2.5.2. Environmental DNA

Environmental DNA provides a complementary approach to traditional trawl surveys for inferring species presence (e.g., Chevrinais et al. 2025). Since the distribution of eDNA in the water column is heterogeneous and influenced by strong horizontal stratification, eDNA-based presence data can support species distribution modelling at spatial resolutions that may exceed those achievable with trawl captures (e.g., Jeunen et al. 2020). Such data have been used to refine historical species distribution models using sedimentary and ancient DNA, as well as contemporary models based on water-sampled eDNA (e.g., Fordham et al. 2024, Guri et al. 2025). For this study, water eDNA samples were first collected as independent efforts from 2019 to 2021 by two DFO regions (Quebec and Gulf) and then, as a joint and standardized effort since 2022. Detailed sampling and analytical methods for these datasets are described in Leung et al. (2026). In brief, samples collected in 2020, 2021, and 2022 in the nGSL, and in 2019, 2021, and 2022 in the sGSL, were used to fit the model. Model predictions were generated only for years with simultaneous sampling in both regions, namely 2021 and 2022.Sampling of eDNA was performed in the water column (most from 15 to 25 m, see Leung et al. 2026) and filtration of 1 to 2 L occurred on nylon (0.8 µm, 47 mm) or glass fiber filters (1.5 µm, 47 mm). DNA was extracted using a silicate-based column method for purification. Fish DNA was targeted for amplification of the mitochondrial 12S gene using two assays (MiFish-U, Miya et al. 2015 and the 12S160, Saunders et al. 2024). Amplification was conducted in a first qPCR followed by a second qPCR for dual indexing. Sequencing was performed on an Illumina NovaSeq6000 PE 250. Bioinformatic treatment was implemented in an in-house R pipeline (v0.2.3), available on Github (https://github.com/GenomicsMLI-DFO/MLI_metabar_pipeline) and further filtration steps were applied to increase the data quality, including standardized amplicon size selection (<130 bp for 12S160; 150–200 bp for MiFishU), removal of ESVs assigned to humans and terrestrial mammals, and retention of samples with <10% contaminant reads, <50% terrestrial mammalian taxa, and >10,000 final reads (detailed in Leung et al. 2026). Capelin presence was inferred using a detection threshold of >1000 reads to minimize false positives. This threshold was defined arbitrarily, as capelin is considered an abundant species. Moreover, only a small subset of samples with eDNA detections below this threshold (n = 13) were excluded from the analysis, which included a total of 1,039 samples. In comparison, studies on Atlantic bluefin tuna, a larger species with lower numerical abundance, have used a threshold of 100 reads (Leung et al. 2026).

Likewise to the approach used for Capelin in predator stomachs, we modelled the probability of capelin eDNA occurrence in water samples collected in the nGSL (2020-2022) and sGSL (2019, 2021 and 2022). The nGSL and sGSL data were combined as no difference in eDNA catchability was expected between regions. The prediction mesh was identical as for the predators and trawl tows, the model configurations were similar as used for the predator data (negative binomial, logit link, only sampling depth as a covariate and an offset equals to the sequencing depth of each eDNA sample to account for differences in sequencing depth and overall sampling effort among samples, and a spatial random field), and the model selection procedure was also mirrored. The probabilities of occurrence were again mapped using the 1x1 km² depth grid and visually compared with capelin catches in the bottom trawl surveys. Separate models were fitted for each vertical habitat (bottom and water column, Figure 9). Fitting a model per vertical habitat allowed to improve our understanding of Capelin available to the bottom trawl. In favourable strata (PTH), capelin were expected to be present near the bottom and available to the trawl. In less favorable habitat (UTH) on the other hand, capelin were expected to be present in the water column but unavailable to the trawl. Thus predicted eDNA occurrences at the bottom and in the water column should align with trawl observations in PTH strata, but neither should match in UTH strata.

2.6. ECOSYSTEM AND CLIMATE CHANGE CONSIDERATIONS

Capelin is a cold-water species closely associated with the cold intermediate layer (CIL) in the GSL (Chamberland et al. 2022). Reductions in CIL thickness or increases in its temperature may lower stock productivity by decreasing the availability of suitable thermal habitat. The timing of ice retreat is also important, as it influences post-winter body condition and survival (Lewis et al. 2019; Lehoux et al. 2022).

To examine thermal conditions experienced by Capelin in bottom trawl surveys, mean annual bottom temperatures were calculated from individual tows within the PTH and UTH strata of the northern and southern GSL. Broader habitat and environmental conditions were assessed using the *gslea* package (Duplisea et al. 2020), which compiles GSL ecosystem data. Indicators included CIL volume, timing of the last sea ice occurrence, and sea surface temperature (SST) from May to November across GSL ecoregions. Bottom temperatures were compared using annual averages, while CIL volume, ice timing, and SST were analyzed as standardized annual anomalies (mean = 0, variance = 1). SST and ice anomalies were multiplied by −1 to reflect their positive effects on Capelin when surface waters are colder and ice retreats earlier. Given that these variables may have a cumulative effect on capelin survival and population productivity, the sum of the annual anomalies was also calculated.

Capelin is also a keystone forage species in the GSL. Ouellette-Plante et al. (2022) analyzed stomach contents from the nGSL multispecies survey, assuming that the proportion of Capelin in predator diets may be linked to the presence and health of Capelin population in the GSL ecosystem. Atlantic Cod and Greenland Halibut were again selected as the most informative predators because they consume substantial amounts of Capelin, occur widely throughout the nGSL, and migrate vertically to feed, increasing the likelihood of detecting Capelin in their stomachs. Following Ouellette-Plante et al. (2022), the annual mean percentage (by weight) of Capelin in the stomach contents of these two predators was estimated for 1993–2024.

3. RESULTS AND DISCUSSION

3.1. COMMERCIAL LANDINGS

From 1985 to 2025, annual landings from the directed fishery and bycatch varied substantially from a minimum of 152 t in 1995 to a maximum of 12,314 t in 2011 (Table 3). During a number of years few to no landings occurred at least in part due to unfavourable market conditions and weather. The TAC was last exceeded in 2020 and 2021. Capelin have mostly been landed in NAFO Division 4R by the mobile gear fleet (small and large purse seiners) (Table 3, Figure 10). The purse seiner fleet landed most of the TAC in 4RST, although there was an increase in landings by fixed gear types since the mid 2000s, largely attributable to the arrival of the tuck seine (Figure 10B). The preliminary landings for NAFO Divisions 4R, 4S and 4T were respectively 1,773 t, 582 t and 1 t for an annual total of 2,357 t in 2024, and 1,089 t, 131 t and 4 t for a total of 1,224 t in 2025. Compared to previous years, a higher proportion of the total catch was landed by the fixed gear fleet using tuck seine and trap nets (1,671 t in 2024 and 669 t in 2025) relative to the mobile fleet composed of large and small seiners (683 t in 2024 and 489 t in 2025) (Figure 10B).

Total landings from 4R in 2024 (1,773 t) were mainly located in unit area 4Ra (1,667 t) while they were balanced between 4Ra (509 t) and 4Rc (445 t) in 2025 (1,089 t, Figure 11A, Table 4). During the 2018-2025 period, the purse and tuck seiners landed similar proportions of the TAC and landing quantities, while trap nets represented a smaller proportion of the annual catch in this Division, except for 2024 (Figure 11B). Total landings from 4R in 2024 (1,773 t) were mainly located in unit area 4Ra (1,667 t) while they were quite similar in 4Ra (509 t) and 4Rc (445 t) in

2025 (1,089 t). In 4ST, most of the landings since 2005 occurred in unit areas 4Sw (Quebec's Lower North Shore) and 4Tn (mouth of the Baie des Chaleurs) by purse seines and weirs (Figure 12). In 2024 and 2025, annual landings in 4ST were higher than the two preceding year and were located mainly in unit areas 4Sw in 2024 and in 4Sw and 4Sx in 2025. 4ST landings in 2024 and 2025 were largely attributed to purse seiners (Figure 12B).

The Capelin fishery in 4R generally occurs in June and July and the timing of the landings has varied little since detailed records have existed (Figure 13). The 4ST fishery usually starts earlier than in 4R and shows more interannual variation, likely at least in part due to the lower number of fishing trips (Figure 14). The broad spatial distribution of fishing activity and associated variability in the timing and location of the nearshore arrival of capelin may also contribute to the observed spatial patterns.

3.2. COMMERCIAL SAMPLING

The number of commercial length frequency samples and individuals measured by the DFO port-sampling program are presented in Table 5. On average, 24 samples were measured annually and were generally evenly spread among NAFO Divisions (7–8 samples per Division annually). This corresponds to an average of 5,493 individual fish measured annually and an average of about 1,200–2,000 fish per NAFO Division depending on the year. In 2024 and 2025, 19 and 6 samples were collected, comprising 3,249 and 1,179 fish, respectively. This reduced sampling effort relative to the preceding period directly reflects the lower landings observed in the last two years. The number of biological samples (subsamples of the above, as well as some opportunistic samples) analyzed are shown in Table 6. On average, a total of 515 individual fish were dissected annually for biological examination. A total of 22 samples (439 fish) were collected in 2024 but only 4 samples (141 fish) in 2025.

3.2.1. Mean total length

The time series mean total lengths (± S.D.) for females and males caught by the 4R seiner fleet were respectively 147 ± 7 mm and 165 ± 6 mm (Figure 15). From the mid-1980s to the early 1990s, lengths of both male and female Capelin were above average. This was followed by a decline in annual mean length that persisted until 2003, when these values increased to near the time series means. The historically large mean length observed for both sexes in 2014 coincided with a later-than-usual fishery (Figure 13) and reduced sampling effort (Table 5). From 2015 to 2024, capelin lengths generally fluctuated around the historic average.

3.2.2. Condition, sex ratio and GSI

The length-weight relationships of male and female Capelin caught in June by seiners are shown in Figure 16. Interannual variations in male and female body condition based on these relationships were similar in 4R, 4S and 4T (Figure 17). However, standardized body condition of Capelin in 4T was generally lower than the other two Divisions. Relative conditions were generally above average in the late 1980s for all NAFO Divisions, near the time series mean from 1990 to 2000, then above average from 2000 to 2014 for 4RS. Relative condition in 4T stayed near the time series mean during this period. Since 2015, relative condition has been near the time series mean in 4RS while slightly below the average in 4T. In 2022 and 2023, there was a reduction of Capelin body condition in 4S with values decreasing near the time series average and the condition index increased in 4R in 2023 after a slight decrease observed in 2022. A higher number of years without length data is observed in 4S (Figure 17) compared to the number of years with standardized condition index data for this Division (Figure 12), because beach seines, gillnets, traps, weirs, and other artisanal gears were excluded from the analyses.

Capelin sex ratios in the commercial fishery are generally biased towards females in samples from 4R (Figure 18), which is consistent with this commercial fishery specifically targeting ripe females. Samples taken from 4ST have higher proportions of males, which could be explained by a higher proportion of opportunistic (dip net) and fixed gear samples in these areas and males being more vulnerable to these gear types as they tend to stay in aggregations in coastal waters longer than females (Templeman 1948; Friis-Rodel and Kanneworff 2002; Maxner et al. 2016).

Female annual mean GSI ranged between 20% and 30% (Figure 19). Male gonad mass represented, on average, less than 1.5% of total mass. No major temporal trend was apparent in either time series. Female GSI was generally close to or lower than the time series average from the mid-1980s to mid-1990s then increased and remained most of the time over the average until an important reduction was observed from 2015 onwards. There were no temporal trends observed for male GSI as it remained fairly close to the average of the time series.

3.3. STOCK STATUS INDICATORS

3.3.1. Original mature biomass index

The four indicators of mature biomass fluctuated independently, although some common peaks were observed in PTH of the sGSL and nGSL, such as in 2011, 2017 and 2021 (Figure 20). The biomass of mature capelin in the nGSL-PTH varied greatly from the beginning of the time series (1995) to 2011. The index has on average remained low since. Mature biomass in the nGSL-UTH remained low throughout the time series, except for a peak period around 2010-2013. The sGSL–PTH index followed an inverse pattern to the nGSL, with below-average values prior to around 2009 and frequent high biomasses thereafter. The sGSL-UTH index was the lowest of all four and showed little variability, except for elevated values between 2008 and 2015. Standardising the relative mature biomass for a diurnal effect, whether through the inclusion of a numeric or categorical time variable, did not result in significantly different patterns and confidence intervals (Figure 20).

3.3.2. Original age-1 abundance index

The age-1 abundance indices in the nGSL-PTH and nGSL-UTH varied without trend (Figure 21). The number of age-1 Capelin in the sGSL-PTH remained stable at low values during the first 15 years, but has, on average, been higher since 2009. In the sGSL-UTH, no such trend was visible, and the time series was mostly characterized by two distinct peaks (2015 and 2023, Figure 21). Standardising the index for a diurnal effect did not result in significantly different patterns and confidence intervals (Figure 21).

3.3.3. Proposed mature biomass index

Examining the spatial distribution of high capelin catches revealed recurring concentrations around Anticosti Island and in the Strait of Belle Isle in the nGSL, as well as from the tip of the Gaspé Peninsula to Cape Breton in the sGSL (Figure 22). The persistence of spatial patterns indicate that high catches are likely biologically meaningful and should not be excluded.

Of the candidate models fitted to mature biomass observations in the nGSL, the most parsimonious included log-transformed depth, time of day as a categorical variable, and their interaction (Table 7). This model had the lowest AIC and passed the sanity check. Two alternative formulations of the temporal year effect were then evaluated: year treated as an independent factor and year modeled as a random effect. Diagnostic checks based on DHARMa residuals indicated satisfactory performance for both models (Figures 23 and 24). The

Kolmogorov–Smirnov (KS) and residual dispersion tests were nonsignificant, suggesting no major violations of model assumptions. However, the outlier test was significant for both models, reflecting the low frequency of extreme and difficult-to-model capelin catches. Quantile residuals showed no systematic patterns with respect to predictor variables (Figure 25). Results from the 50-fold cross-validation indicated slightly better predictive performance for the model with year as a random effect, which produced lower RMSE and MAE values (Table 8). This model was therefore retained for subsequent analyses.

The final nGSL model showed that mature biomass was significantly lower at greater depths and during night-time sampling (Table 9, Figure 26), with both variables having similar effect sizes. All random-effect parameters associated with the spatial and spatiotemporal fields, as well as the error distribution, were significantly different from zero and estimated with acceptable uncertainty (Table 9). Predictions of mature biomass per km² revealed recurring spatial patterns across years (Figure 27), with particularly high densities near Anticosti Island (north, northwest, and southwest), along the Quebec North Shore, and in the Strait of Belle Isle. The mature biomass index for the entire nGSL was strongly correlated ($R^2 = 0.83$) with the original index, which summed UTH and PTH biomasses without adjusting for differences in catchability (Figure 28). However, several discrepancies between the two time series highlight the sensitivity of the index to methodological choices. For example, biomass in 1999 was high under the original approach but nearly absent in the new index. These differences partly reflect the sdmTMB model weighting UTH and PTH areas by depth, whereas the original approach relied on subjective scaling assumptions. Uncertainty estimates for the new index were generally smaller and followed a different pattern, reflecting the fundamentally different methods used to estimate uncertainty. Trend analysis based on the new index indicates that, despite substantial historical fluctuations, mature biomass in the nGSL has remained consistently low since 2013.

The most parsimonious model explaining mature biomass in the sGSL included log-transformed depth (modeled as a second-degree polynomial), time of day as a categorical variable, and their interaction (Table 7, 9). Both formulations of temporal year effect performed well in DHARMa diagnostic tests (Figures 29 and 30) as well as in quantile residual diagnostics (Figure 31). Based on 50-fold cross-validation, the model with year as a categorical factor produced the lowest sum log-likelihood, RMSE, and MAE, and was therefore selected for subsequent analyses (Table 8).

Depth showed a nonlinear relationship with mature biomass (second-degree polynomial), with a positive and increasing effect up to approximately 130 m, followed by a negative effect at greater depths (Figure 32). In contrast to the nGSL, night-time sampling in the sGSL was associated with higher estimated mature biomass. However, as in the nGSL, the interaction between depth and time of day was positive, indicating that the effect of depth differed between daytime and nighttime sampling. The year effect, modeled as a categorical factor, was consistently greater than zero and remained relatively stable after an initial increase during the 1990s (Figure 33). Random-effect estimates were also similar to those in the nGSL model (Table 9).

Predicted mature biomass per km² revealed pronounced changes in spatial distribution over time (Figure 34). From 1990 to 1998, capelin were mostly observed in a limited number of hotspots across the sGSL. Beginning in 2009, elevated densities were observed over a broader area, often peaking near the Gaspé Peninsula, the central sGSL, and western Cape Breton (Figure 34). As in the nGSL, the mature biomass index derived from the sdmTMB model was strongly correlated ($R^2 = 0.95$) with the original index (Figure 35). The two relative indices differ in scale because of how depth (or UTH/PTH strata) is treated. However, the conversion from relative to absolute biomass is already highly uncertain, and this difference in scale does not

affect conclusions regarding stock status (Figure 35). Notably, uncertainty estimates are again substantially smaller for the newly proposed index.

3.3.4. Proposed age-1 abundance index

The most parsimonious age-1 abundance model for the nGSL included the same predictors as the mature biomass model for this area: log-transformed depth, time of sampling (categorical), and their interaction (Table 7). Model diagnostics of both year effect formulations were satisfactory (Figures 36, 37 and 38). As in the biomass model, the configuration with year treated as a random effect was favored based on 50-fold cross-validation (Table 8) and both fixed and random effects for this model were significant with reasonable uncertainty (Table 9). Depth and night-time sampling had significant negative effects on age-1 Capelin in the nGSL (Figure 39), while their interaction was positive. Predicted density maps showed recurring areas of high age-1 densities north of Anticosti Island, similar to the spatial patterns observed for mature biomass (Figure 40). In several years (1997, 1998, 2003, 2004, 2013, and 2022–2025), age-1 number was also elevated along the west coast of Newfoundland, sometimes concentrated near individual bays and in other cases distributed more broadly along the coast. The new and original age-1 abundance indices were again strongly correlated ($R^2 = 0.83$), which is expected given that they rely on the same underlying data (Figure 41). However, notable differences in some years, along with generally reduced uncertainty in the new index, suggest that small-amplitude variations in the time series should be interpreted cautiously.

The most parsimonious age-1 abundance model for the sGSL had the same structure as the mature biomass model for this area (Table 7) and model diagnostics were satisfactory (Figures 42, 43 and 44). Again, the model that treated year as a categorical factor was retained following the 50-folds cross-validation (Table 8). Fixed and random effects were significant with acceptable uncertainty (Table 10). The direction of the covariate effects was similar to that observed for mature biomass. Age-1 abundance tended to be higher in deeper waters and during night-time sampling. The effect of depth stabilized at approximately 100 m and deeper and was somewhat more negative during daytime and in the deeper parts of the survey area (Figure 45). Year effects increased early in the time series and then fluctuated without a clear long-term trend (Figure 46). Predicted spatial patterns of age-1 Capelin in the sGSL showed small hotspots prior to 1999 and a broader distribution in most survey years thereafter (Figure 47). From 1999 onward, high age-1 abundance was most often predicted between Chaleur Bay and the Magdalen Islands. The correlation between the original and new sGSL indices was very high ($R^2 = 0.98$; Figure 48).

It is currently unclear how informative age-1 indices are, and to what extent the signal reflects real biological change versus observation error. Potential sources of bias include estimating the proportion of age-1 fish at length using only two years of data, as well as the size selectivity of the bottom trawl gear.

3.4. SCALE OF FISHING MORTALITY

Although 4RST capelin landings varied considerably between 1998 and 2025 (Figure 10), *E* and *F* remained relatively low ($F > 0.25$) throughout most of the time series (Table 11, Figure 49). These levels are unlikely to pose a risk to a very short-lived small pelagic species such as Capelin (Patterson 1992), as *F* remained below the reference thresholds of 0.43, respectively. Furthermore, there is evidence that landings are smaller than the estimated consumption of Capelin implying that fishing mortality is considerably lower than natural mortality due to predation (Savenkoff et al. 2004, Ouellette-Plante et al. 2022). Harvest levels observed in 2025 were also considered not harmful. However, the fishing mortality index in 2024 reached the highest value in the time series (Figure 49B) and exceeded the acceptable threshold, despite

landings being significantly lower than during 2018–2021, when mature biomass in the nGSL was also low. This high value may be linked to incomplete survey coverage in 2023 (i.e., the biomass available to the fishery in 2024), particularly in the St. Lawrence Estuary and the Strait of Belle Isle, areas historically associated with high capelin densities based on sdmTMB modelling. In addition, excluding the sGSL contribution from the mature biomass used to calculate the mortality index may have contributed to this result, especially given the peak observed in 2023 (Figure 49A).

3.5. ASSESSING THE RELIABILITY OF CAPELIN DETECTION IN BOTTOM TRAWL SURVEYS

3.5.1. Predator stomach

The most parsimonious model for predicting Capelin presence in predator stomachs included log-transformed depth and predator species (Atlantic cod or Greenland halibut) as predictors (Table 12). Adding a year effect as a random effect or a categorical factor improved model fit (lower AIC). Model diagnostics (Figures 50, 51 and 52) showed no evidence of misspecification. The formulation with year modeled as a categorical factor was selected based on 50-fold cross-validation (Table 12). Both depth and predator species had significant effects, with negative first- and second-order terms for the log-transformed depth polynomial and a positive effect for Greenland halibut (Table 13; Figure 53). The random spatial effect was also significant, although its uncertainty was relatively large compared with previous models, likely reflecting the smaller number of observations in the spatial matrix. Predicted probability maps indicated that capelin were most frequently found along the Quebec North Shore (Figure 54), a pattern that remained consistent over time and aligned with predicted mature biomass from the bottom-trawl survey, which often peaked north of Anticosti Island. In contrast, the Laurentian Channel area consistently showed low probabilities in both predator and trawl datasets. Overall, capelin were more likely to occur in predator stomachs when they were also captured in bottom trawls (Figure 55). These broad-scale similarities between independent indicators suggest that bottom-trawl surveys capture large-scale spatial patterns in capelin distribution reasonably well. However, finer-scale discrepancies warrant further investigation. Trawl data reflect local biomass, whereas capelin found in predator diets may be spatially displaced due to predator movement, complicating direct comparisons. Future work could refine this comparison.

3.5.2. Environmental DNA

The models with the lowest AIC for predicting the occurrence of capelin eDNA in the water column and at the bottom across the GSL included only log-transformed bottom depth (second-degree polynomial) and year as a categorical factor (Table 14). DHARMa diagnostics (Figure 56) and residual plots relative to predictor values (Figure 57) revealed no model issues. In both models, the first-degree depth term and year had negative but nonsignificant effects, whereas the second-degree depth term was significant (Table 15, Figure 58). Random spatial fields were significant in both cases but showed greater uncertainty for the water-column eDNA model than for the bottom eDNA model. Predicted probabilities of eDNA occurrence in the GSL corresponded well with areas of high capelin catches in bottom-trawl surveys (Figure 59), consistent with predator-based results (Figure 54). Spatial patterns predicted by the water-column and bottom eDNA models were generally similar, except in the Honguedo Strait. Notably, predictions from the bottom eDNA model aligned more closely with the spatial distribution of capelin thermal habitat strata, particularly in the nGSL. As with predator data, the presence of capelin eDNA was more likely both at the bottom and in the water column when capelin were also captured in bottom trawls, although patterns varied between thermal habitat strata (Figure 60).

3.6. ECOSYSTEM AND CLIMATE CHANGE CONSIDERATIONS

Mean annual bottom temperatures recorded during the nGSL bottom-trawl survey remained relatively stable from 1990 to 2010 in the UTH strata and from 1990 to 2019 in the PTH strata (Figure 61A). After these periods, both habitat categories experienced a marked increase through 2023, followed by a decline in 2024 and 2025. The 3.3 °C threshold associated with a major shift in the cumulative frequency distribution of capelin catches (Chamberland et al. 2022) was exceeded in 2022 and 2023. In the sGSL survey, changes in mean annual bottom temperature were less pronounced (Figure 61B). Nevertheless, the PTH strata experienced an increase from 2018 to 2021, followed by a decline. The 2.2 °C threshold identified for the sGSL, corresponding to a shift in the cumulative frequency distribution of capelin catches (Chamberland et al. 2022), was exceeded in 2019 and from 2021 to 2023.

Analysis of trends in the summed annual anomalies for CIL volume, last sea-ice occurrence, and SST revealed broadly similar patterns across most ecoregions (Figure 62). The highest summed anomalies were observed in 1990–1992, and again in 2010, 2013, and 2016. Prior to 2010, anomalies were predominantly positive across ecoregions, whereas several consecutive negative years occurred afterward, notably from 2012 to 2014 and from 2021 to 2024.

The proportion of capelin in the diets of Atlantic cod and Greenland halibut showed substantial interannual variability from 1993 to 2020 (Figure 63). Despite this variability, the two predators displayed some consistency in trends. Diet composition in Capelin was generally lower in the early 2000s, followed by an increase up to the 2010 interruption of the time series. Between 2015 and 2021, Capelin represented a high proportion of the diet of both Atlantic cod and Greenland halibut in several years.

4. SOURCE OF UNCERTAINTY

Capelin are a highly migratory and widely distributed species with pronounced annual fluctuations in stock abundance and size structure. Its life-history characteristics along with the absence of a targeted survey complicates its assessment and creates several sources of uncertainty:

- Main stock status indicators
    - Stock indicators are derived from bottom trawl surveys with unspecified and potentially variable catchability of pelagic fish across space and time. Bottom trawl sample only part of the CIL where Capelin reside and shifts in vertical distribution of Capelin relative to the trawl can alter catchability. Changes in CIL thickness or temperature may also influence the observed abundance. Uncertainty could be reduced by incorporating independent but concurrent data sources such as acoustic recordings, food availability, predator diets, and environmental DNA. While the fishing mortality index uses the mature biomass index in its calculation, commercial fishing is unlikely to pose a risk to the stock, providing the assumptions underlying the absolute biomass index hold true.
- Mature biomass available to the fishery
    - Indices represent stock status in August–September, whereas the fishery begins at least six months later. Mortality between late fall and the fishing season may create discrepancies between estimated stock status and mature biomass available to the fishery. Implementing a directed capelin survey before fishing begins in key areas (4R–4Sw) would improve estimates of vulnerable biomass and understanding of spatiotemporal distribution.
- Lack of age data

- Age data are unavailable due to difficulty distinguishing true growth annuli from false annuli. This limits the ability to assess cohort contributions to mature biomass and precludes cohort analyses for the trawl surveys, thereby reducing confidence in stock status determination. Age data would help with the estimation of mortality by tracking cohorts from late summer to the fishing season.

- Incomplete coverage of trawl surveys
  - Incomplete bottom trawl survey coverage in the northern GSL in 2023, particularly in historically high-density areas, was proposed as one explanation for the elevated fishing mortality index observed in 2024. Although the spatiotemporal model used to estimate mature biomass can compensate for missing coverage, its performance in unsampled areas should be evaluated to clarify potential limitations.
- Stock structure and movements
  - 4RST capelin are managed as a single stock, although fishing is concentrated in the northeastern GSL, and the fishing mortality index is calculated using only the mature biomass index in the northern GSL. Given capelin's long-distance migrations, movement among GSL regions may influence mature biomass available to the fishery. Otolith chemistry (core and margin composition) could help identify cross-regional connectivity patterns.
- Capelin eDNA
  - Capelin occurrence inferred from eDNA metabarcoding is subject to methodological uncertainty, as this approach can be influenced by amplification bias, primer specificity, and variation in sequencing depth. Consequently, read counts may not accurately reflect true occurrence or abundance at site location. To improve quantitative inference, future work should incorporate a targeted qPCR assay specific to capelin by reanalyzing existing eDNA extracts. This approach would provide a more precise and quantitative estimate of capelin occurrence and abundance and help validate patterns observed with metabarcoding.

5. CONCLUSION

The 2024–2025 4RST capelin fisheries were characterized by landings that remained low relative to the 2018–2021 period, with less than 50% of the total allowable catch harvested. Fishing occurred predominantly off the west coast of Newfoundland and Labrador and was conducted primarily by the tuck seine and trap net fleets. The timing of fishing activity and the biological characteristics of the commercial catch, including length composition, mean length, condition, sex ratio, and gonadosomatic index, were consistent with observations from the past decade and showed no discernible temporal trends. The biomass indices developed in this assessment account for spatial and spatiotemporal autocorrelation, as well as depth and diel effects on capelin availability to bottom trawls. These revisions reduce interannual variability and uncertainty relative to previous approaches and address research recommendations from earlier assessments. Results indicate that mature biomass in the nGSL has remained persistently low since 2013, whereas the southern Gulf has exhibited higher biomass levels with episodic increases. Estimates of fishing mortality, calculated as the ratio of landings to the northern Gulf mature biomass index, have generally remained at or below 0.25. These levels are below expected natural mortality due to predation and below values considered sustainable for a short-lived species. In the absence of approved Reference Points, stock status in 2025 remains uncertain. However, given the relatively low fishing mortality and the absence of a declining biomass trend since 2013 in the northern Gulf, combined with recent increases in the

southern Gulf, harvest levels within the range observed since 2013 (1,224–11,825 t) are unlikely to pose a risk to the stock during the 2026–2027 fishing seasons.

6. ACKNOWLEDGEMENTS

The assessment of 4RST Capelin requires the collaboration and coordination of people and resources from across the Québec, Gulf, and Newfoundland-and-Labrador regions. We would like to thank everyone who participated in and contributed to the peer review, the meeting chair (Jordan Ouellette-Plante), the data management team and technical support staff at the MLI, the network of DFO port samplers, the statistics divisions of DFO, the regional DFO fisheries managers, and all the stakeholders who provided their knowledge and samples. We would also like to acknowledge the contributions made by the Canadian Coast Guard and the crew of the CCGS *Cabot* and *Cartier* (DFO's August and September multispecies bottom-trawl surveys). Finally, we are grateful to Hannah Murphy and François-Étienne Sylvain for reviewing an earlier version of this document.

7. REFERENCES CITED

Aarflot, J.M., Dalpadado, P. and Fiksen, Ø. 2020. Foraging success in planktivorous fish increases with topographic blockage of prey distributions. Mar. Ecol. Prog. Ser. 644: 129–142.

Anderson, S.C., Ward, E.J., English, P.A., Barnett, L.A.K. and Thorson, J.T. 2025. sdmTMB: an R package for fast, flexible, and user-friendly generalized linear mixed effects models with spatial and spatiotemporal random fields. Journal of Statistical Software 115, 2: 1–46.

Bailey, R.F.J., Able, K.W. and Leggett, W.C. 1977. Seasonal and Vertical Distribution and Growth of Juvenile and Adult Capelin (*Mallotus villosus*) in the St. Lawrence Estuary and Western Gulf of St. Lawrence. J. Fish. Res. Board Can. 34: 2015–2029.

Baker, K.D., Le Corre, N., Bourret, A., Parent, G., Fulton, S., Duprey, N. M., and Cox, S. 2025. Spatial stock structure of northern shrimp Pandalus borealis Krøyer, 1838 (Decapoda: Caridea: Pandalidae) in Canada's Northwest Atlantic. Journal of Crustacean Biology 45, 2

Benoît, H.P. and Swain, D.P. 2008. Impacts of environmental change and direct and indirect harvesting effects on the dynamics of a marine fish community. Can. J. Fish. Aquat. Sci. 65: 2088–2104.

Benoît, H.P., and Yin, Y. 2023. Results of Comparative Fishing Between the CCGS Teleost Fishing the Western IIA Trawl and CCGS Capt. Jacques Cartier Fishing the NEST Trawl in the Southern Gulf of St. Lawrence in 2021 and 2022. DFO Can. Sci. Advis. Sec. Res. Doc. 2023/083. xiii + 183 p.

Bill C-68: An Act to amend the Fisheries Act and other Acts in consequence. 2019. 1st Reading Feb. 6, 2018, 42nd Parliament, 2nd session. Retrieved from the Parliament of Canada website.

Bivand, R. and Luque, S. 2025. suntools: Calculate Sun Position, Sunrise, Sunset, Solar Noon and Twilight. R package version 1.1.0, https://github.com/adokter/suntools.

Boudreau, M., Chamberland, J.M., Girard, L., Boudreau, M., Benoît, H., Lehoux, C., Smith, A., Galbraith, P. and Plourde, S. 2023. Capelin in the Estuary and Gulf of St. Lawrence (NAFO Divs. 4RST) in 2021. DFO Can. Sci. Advis. Sec. Res. Doc. 2023/018. v + 51 p.

Boudreau, M., Van Beveren, E., Boudreau, M., Lévesque, L., and Plourde, S. 2026. Capelin in the Estuary and Gulf of St. Lawrence (NAFO Divisions 4RST) in 2022 and 2023. DFO Can. Sci. Advis. Sec. Res. Doc. 2026/007. v + 73 p.

Bourdages, H., Brassard, C., Desgagnés, M., Galbraith, P., Gauthier, J., Nozères, C., Scallon-Chouinard, P.-M. and Senay, C. 2019. Preliminary results from the groundfish and shrimp multidisciplinary survey in August 2018 in the Estuary and northern Gulf of St. Lawrence. DFO Can. Sci. Advis. Sec. Res. Doc. 2019/037. iv + 87 p.

Brooks, M.E., Kristensen, K., van Benthem, K.J., Magnusson, A., Berg, C.W., Nielsen, A., Skaug, H.J., Maechler, M. and Bolker, B.M. 2017. glmmTMB Balances Speed and Flexibility Among Packages for Zero-inflated Generalized Linear Mixed Modeling. The R Journal 9, 2: 378–400.

Buren, A. D., Koen-Alonso, M. and Montevecchi, W. A. 2012. Linking predator diet and prey availability: common murres and Capelin in the Northwest Atlantic. Marine Ecology Progress Series, 445: 25-35.

Burton M.P.M and Flynn, S.R. 1998. Differential postspawning mortality among male and female capelin (*Mallotus villosus* Müller) in captivity. Canadian Journal of Zoology 76, 3: 588-592.

Carscadden, J.E. 1979. Capelin (*Mallotus villosus*) in the Gulf of St. Lawrence. DFO Can. Sci. Advis. Sec. Res. Doc. 1979/24. 13 p.

Carscadden, J.E. and Misra, R.K. 1979. Multivariate Analysis of Meristic Characters of Capelin (*Mallotus villosus*) in the Northwest Atlantic. ICNAF Res. Doc. 79/II/29. Serial No. 5355.

Cayuela, H., Rougemont, Q., Laporte, M., Mérot, C., Normandeau, E., Dorant, Y., Tørresen, O.K., Hoff, S.N.K., Jentoft, S., Sirois, P., Castonguay, M., Jansen, T., Præbel, K., Clément, M. and Bernatchez, L. 2020. Shared ancestral polymorphisms and chormosonal rearrangements as potential drivers of local adaptation in a marine fish. Mol. Ecol. 29(13): 2379–2398.

Chadwick, E., Brodie, W., Colbourne, E., Clark, D., Gascon, D and Hurlbut. T. 2007. History of annual multi-species trawl surveys on the Atlantic coast of Canada. Atlantic Zonal Monitoring Program Bulletin 6: 25-42.

Chamberland, J.-M., Plourde, S. and Benoît, H.B. 2022. Biological characteristics, factors affecting catchability, and abundances indices of Capelin in the southern and northern Gulf of St Lawrence multi species bottom trawl surveys. DFO Can. Sci. Advis. Sec. Res. Doc. 2021/77. iv + 41 p.

Chamberland, J.-M., Bourdages, H., Desgagnés, M., Galbraith, P., Isabel, L., Ouellette-Plante, J., Roux, M.-J., Scallon-Chouinard, P.-M., and Senay, C. 2025. Preliminary Results from the 2024 August Ecosystemic Survey in the Estuary and Northern Gulf of St. Lawrence. DFO Can. Sci. Advis. Sec. Res. Doc. 2025/032. iv + 101 p.

Chevrinais, M., Bourret, A., Côté, G., Faille, G., Gagné, N. and Parent, G.J. 2025. Improving an endangered marine species distribution using reliable and localized environmental DNA detections combined with trawl captures. Sci Rep 15, 11926. https://doi.org/10.1038/s41598-025-95358-3

Christiansen, J. S., Præbel, K., Siikavuopio, S. I., and Carscadden, J. E. 2008. Facultative semelparity in Capelin Mallotus villosus (Osmeridae)-an experimental test of a life history phenomenon in a sub-arctic fish. Journal of Experimental Marine Biology and Ecology, 360(1): 47-55.

Courtois, R. and Dodson, J.J. 1986. Régime alimentaire et principaux facteurs influençant l'alimentation des larves de capelan (*Mallotus villosus*), d'éperlan (*Osmerus mordax*) et de hareng (*Clupea harengus harengus*) dans un estuaire partiellement mélangé. Can. J. Fish. Aquat. Sci. 43: 968–979.

Courtois, R., Simoneau, M. and Dodson, J.J. 1982. Interactions multispécifiques: répartition spatio-temporelle des larves de capelan (*Mallotus villosus*), d'éperlan (*Osmerus mordax*) et de hareng de l'Atlantique (*Clupea harengus harengus*) an sein de la communauté planctonique de l'estuaire moyen du Saint-Laurent. Can. J. Fish. Aquat. Sci. 39: 1164–1174.

Coussau, L., Van Beveren, E., Boudreau, M., and Jac, R. 2026. Preliminary results for the investigation of natal origin in capelin (*Mallotus villosus*) from the Gulf of St. Lawrence using otolith chemistry. Can. Tech. Rep. Fish. Aquat. Sci. 3762: vii + 40 p. https://doi.org/10.60825/97zm-6s40

Daigle, D., and Benoît, H.P. 2007. Procedures for commercial catch sampling of finfish and shrimp in the southern Gulf of St. Lawrence (Fisheries and Oceans Canada, Gulf Region). Can. Manuscr. Rep. Fish. Aquat. Sci. 2833: iv + 63 pp.

Dalpadado, P. and Mowbray, F. 2013. Comparative analysis of feeding ecology of Capelin from two shelf ecosystems, off Newfoundland and in the Barents Sea. Prog. Oceanogr. 114: 97–105.

Davoren, G.K. and Montevecchi, W.A. 2006. Shoal behaviour and maturity relations of spawning Capelin (*Mallotus villosus*) off Newfoundland: demersal spawning and diel vertical movement patterns. Can. J. Fish. Aquat. Sci. 63: 268–284.

de Lafontaine, Y. Demers, S. and Runge, J. 1991. Pelagic Food Web Interactions and Productivity in the Gulf of St. Lawrence: A perspective. *In* The Gulf of St. Lawrence: Small Ocean or Big Estuary? Edited by J.-C. Therriault. Can. Spec. Publ. Fish. Aquat. Sci. 113: 350 p.

DFO. 2009. A fishery decision-making framework incorporating the precautionary approach. Last updated 2009-03-23.

DFO. 2023. Assessment of the Gulf of St. Lawrence (4RST) Greenland halibut stock in 2022. DFO Can. Sci. Advis. Sec. Sci. Advis. Rep. 2023/022.

DFO. 2024. Assessment of the Estuary and Gulf of St. Lawrence (Divisions 4RST) Capelin (*Mallotus villosus*) Stock in 2022 and 2023. DFO Can. Sci. Advis. Sec. Sci. Advis. Rep. 2024/021.

DFO. 2026. Estuary and Gulf of St. Lawrence (Divisions 4RST) Capelin (*Mallotus villosus*) Stock Assessment in 2025. DFO Can. Sci. Advis. Sec. Sci. Advis. Rep. 2026/014.

Dodson, J.J., Tremblay, S., Colombani, F., Carscadden, J.E. and Lecomte, F. 2007. Trans-Arctic dispersals and the evolution of a circumpolar marine fish species complex, the Capelin (*Mallotus villosus*). Mol. Ecol. 16: 5030–5043.

Duplisea, D.E., Merette, D., Roux, M.-J., Benoît, H.P., Blais, M., Galbraith, P. and Plourde, S. 2020. gslea: the Gulf of St Lawrence ecosystem approach data matrix R-package. R package version 0.1 https://github.com/duplisea/gslea.

Flynn, S.R., Nakashima, B.S. and Burton, M.P.M. 2001. Direct assessment of post-spawning survival of female capelin, *Mallotus villosus*. Journal of the Marine Biological Association of the United Kingdom 81, 2: 307-312.

Fordham, D.A., Brown, S.C., Canteri, E., Austin, J.J., Lomolino, M.V., Haythorne, S., Armstrong, E., Bocherens, H., Manica, A., Rey-Iglesia, A., Rahbek, C., Nogués-Bravo, D. and Lorenzen, E.D. 2024. 52,000 years of woolly rhinoceros population dynamics reveal extinction mechanisms, Proc. Natl. Acad. Sci. U.S.A. 121 (24) e2316419121, https://doi.org/10.1073/pnas.2316419121

Fortier, L. and Leggett, W.C. 1983. Vertical migrations and transport of larval fish in a partially mixed estuary. Can. J. Fish. Aquat. Sci. 40: 1543–1555.

Fortier, L. and Leggett, W.C. 1985. A drift study of larval fish survival. Mar. Ecol. Prog. Ser. 25: 245–257.

Frank, K.T. and Leggett, W.C. 1981. Prediction of egg development and mortality rates in Capelin (*Mallotus villosus*) from meteorological, hydrographic, and biological factors. Can. J. Fish. Aquat. Sci. 38: 1327–1338.

Friis-Rodel, E. and Kanneworff, P. 2002. A review of capelin (*Mallotus villosus*) in Greenland waters. ICES Journal of Marine Science 59(5): 890–896.

Gaichas, S.R., Gartland, J., Smith, B.E., Wood, A.D., Ng, E.L., Celestino, M., Drew, K., Tyrell, A.S. and Thorson, J.T. 2024. Assessing small pelagic fish trends in space and time using piscivore stomach contents. Canadian Journal of Fisheries and Aquatic Sciences 81**,** 8 : 990-1012.

GEBCO Compilation Group 2020. GEBCO 2020 Grid.

Grégoire, F. and Girard, L. 2014. Abondance et distribution des œufs et des larves de poissons autres que le maquereau bleu (*Scomber scombrus L.*) récoltés dans le sud du golfe du Saint-Laurent entre 1983 et 2013. Rapp. stat. can. sci. halieut. aquat. 1256. ix + 218 p.

Grégoire, F., Girard, L., Beaulieu, J.-L., Lussier, J.-F. and Bruneau, B. 2013. Capelin (*Mallotus villosus*) in the Estuary and Gulf of St. Lawrence (NAFO Divisions 4RST) in 2012. DFO Can. Sci. Advis. Sec. Res. Doc. 2013/023. vi + 90 p.

Guri, G., Liu, O.R., Kelly, R.P., Shaffer, M.R., Parsons, K.M., Ramón-Laca, A., Nochols, K.M., Brandao-Dias, P.F.P. and Shelton, A.O. 2025. Quantitative, Multispecies Monitoring at a Continental Scale. bioRxiv, 2025-10.

Harley, S.J., Myers, R.A., Barrowman, N.J., Bowen, K., and Amiro, R. 2001. Estimation of research trawl survey catchability for biomass reconstruction of the eastern Scotian Shelf. Can. Stock Ass. Sec. Res. Doc. 2001/084. 54 p.

Hartig, F. 2026. DHARMa: Residual Diagnostics for Hierarchical (Multi-Level / Mixed) Regression Models. R package version 0.5.0, https://github.com/florianhartig/dharma.

Ingvaldsen, R.B. and Gjøsæter, H. 2013. Responses in spatial distribution of Barents Sea Capelin to changes in stock size, ocean temperature and ice cover. Mar. Biol. Res. 9(9): 867–877.

Jac, R., Coussau, L., van Beveren, E., Boudreau, M., Le Pape, O., Robert, D., Brosset, P. and Sirois, P. 2026. Multi-year stability of spatial patterns in capelin otolith-edge chemical fingerprints in the Gulf of St. Lawrence, Canada. Fisheries Research 295: 107671.

Jacquaz, B., Able, K.W. and Leggett, W.C. 1977. Seasonal distribution, abundance, and growth of larval Capelin (*Mallotus villosus*) in the St. Lawrence Estuary and Northwestern Gulf of St. Lawrence. J. Fish. Res. Board Can. 34: 2008–2014.

Jeunen, G.J., Lamare, M.D., Knapp,M., Spencer, H.G., Taylor, H.R., Stat, M., Bunce, M. and Gemmell, N.J. 2020. Water stratification in the marine biome restricts vertical environmental DNA (eDNA) signal dispersal. Environmental DNA 2, 1: 99-111.

Kenchington, E.L., Nakashima, B.S., Taggart, C.T. and Hamilton, L.C. 2015. Genetic structure of Capelin (*Mallotus villosus*) in the Northwest Atlantic Ocean. PLoS ONE. 10(3): e0122315. doi:10.1371/journal.pone.0122315

Kristensen, K, Nielsen, A, Berg, C.W., Skaug, H. and Bell, B.M. 2016. TMB: Automatic Differentiation and Laplace Approximation. Journal of Statistical Software 70,5: 1–21.

Lambert, J.-D. and Bernier, B. 1989. Observations on 4RST Capelin in the Gulf of St. Lawrence (A retrospective, 1984–1987). CAFSAC Res. Doc. 1989/008. 33 p.

Lambert, J-D. and B. Ménager. 1998. Protocoles d'échantillonnage des captures commerciales de poissons et d'invertébrés marins du golfe du Saint-Laurent. Rapp. tech. can. sci. halieut. aquat. 2208. x + 246 p.

Le Cren, E.D. 1951. The length-weight relationship and seasonal cycle in gonad weight and condition in the Perch (*Perca fluviatilis*). J. Anim. Ecol. 20(2): 201–219.

Lehoux, C., Plourde, S., Chamberland, J.-M. and Benoît, H. 2022. Linking interannual variations of Capelin abundance indices in the Gulf of St. Lawrence to environmental proxies of bottom-up regulation of cohort strength. DFO Can. Sci. Advis. Sec. Res. Doc. 2021/068. iv + 51 p.

Leung, C., Chevrinais, M., Druon, J.-N., Bowlby, H.D., Turcotte, F., Gagné, N., Parent, G.J. and Benoît, H.P. 2026. Advancing species distribution modeling with multispecies eDNA metabarcoding: the case of the Atlantic bluefin tuna (*Thunnus thynnus*) in the Gulf of St. Lawrence (Canada). Ecological Indicators 183, 114677, ISSN 1470-160X. https://doi.org/10.1016/j.ecolind.2026.114677.

Lewis, K.P., Buren, A.D., Regular, P.M., Mowbray, F.K. and Murphy, H.M. 2019. Forecasting Capelin *Mallotus villosus* biomass on the Newfoundland shelf. Mar. Ecol. Prog. Ser. 616: 171–183.

Lindgren, F. 2026. fmesher: Triangle Meshes and Related Geometry Tools. R package version 0.6.1.9006

Maxner, E., Halden, N.M. , Roth, J.D. and Davoren, G.K. 2016. Intrinsic factors influence the timing of arrival of Capelin (*Mallotus villosus*) to spawning grounds in coastal Newfoundland. Fish. Res. 179: 202–212.

McQuinn, I.H., Bourassa, M-N., Tournois, C., Grégoire, F. and Baril, D. 2012. Ecologically and biologically significant areas in the Estuary and Gulf of St. Lawrence: small pelagic fishes. DFO Can. Sci. Advis. Sec. Res. Doc. 2012/087. iii + 76 p.

Mecklenburg, C.W. and D. Steinke. 2015. Ichthyofaunal baselines in the Pacific Arctic region and RUSALCA study area. Oceanography 28(3): 158–189.

Mecklenburg, C.W., Lynghammar, A., Johannesen, E., Byrkjedal. I., Christiansen, J.S., Dolgov, A.V., Karamushko, O.V., Mecklenburg, T.A., Møller, P.R., Steinke, D. and Wienerroither, R.M. 2018. Marine Fishes of the Arctic Region. Conservation of Arctic Flora and Fauna, Akureyri, Iceland. 1. 454 p.

Miya, M., Sato, Y., Fukunaga, T., Sado, T., Poulsen, J.Y., Sato, K., Minamoto, T., Yamamoto, S., Yamanaka, H., Araki, H., Kondoh, M. and Iwasaki, W. 2015. MiFish, a set of universal PCR primers for metabarcoding environmental DNA from fishes: detection of more than 230 subtropical marine species. R Soc Open Sci. 2, 7: 150088. https://doi.org/10.1098/rsos.150088

Mowbray, F.K. 2002. Changes in the vertical distribution of Capelin (*Mallotus villosus*) off Newfoundland. ICES J. Mar. Sci. 59: 942–949.

Murphy, H. M., Adamack, A. T., Koen-Alonso, M., Lundrigan, P., and Mowbray, F. K. 2025. Running on empty: capelin diet after stock collapse. Reviews in Fish Biology and Fisheries, 35,3: 1465-1485.

Nakashima, B.S., Carscadden, J.E., and Lilly, G.R. 1982. Capelin (*Mallotus villosus*) Biology and History of the Fishery in the Northern Gulf of St. Lawrence, Div. 4RS. CAFSAC Res. Doc. 1982/029. 11 p.

Nephin, J., Thompson, P.L., Anderson, S.C., Park, A.E., Rooper, C.N., Aulthouse, B. and Watson, J. 2023. Integrating disparate survey data in species distribution models demonstrate the need for robust model evaluation. Canadian Journal of Fisheries and Aquatic Sciences 80, 12: 1869-1889.

Ng, E.L., Deroba, J.J., Essington, T.E., Grüss, A., Smith, B.E. and Thorson, J.T. 2021. Predator stomach contents can provide accurate indices of prey biomass. ICES Journal of Marine Science 78, 3: 1146-1159.

O'Boyle, R.N. and Lett, P.F.K. 1977. Status of Capelin (*Mallotus villosus*) stocks in the Gulf of St. Lawrence. CAFSAC Res. Doc. 1977/004. 18 p.

O'Driscoll, R.L., Rose, G.A. and Anderson, J.T. 2002. Counting Capelin: a comparison of acoustic density and trawl catchability. ICES Journal of Marine Science 59(5): 1062–1071.

Ogle, D.H., Doll, J.C., Wheeler, A.P. and Dinno, A. 2026. FSA: Simple Fisheries Stock Assessment Methods. doi:10.32614/CRAN.package.FSA, R package version 0.10.1, https://CRAN.R-project.org/package=FSA.

Ouellet, P. 1987. Distribution automnale des stades larvaires de capelan (*Mallotus villosus*) et de hareng (*Clupea harengus*) dans le nord du golfe Saint-Laurent en Octobre 1985. Rapp. tech. Can. sci. halieut. aquat. 1583 : 27 p.

Ouellet, P., Bui, A.O.V., Lavoie, D., Chassé, J., Lambert, N., Ménard, N. and Sirois, P. 2013. Seasonal distribution, abundance, and growth of larval Capelin (*Mallotus villosus*) and the role of the Lower Estuary (Gulf of St. Lawrence, Canada) as a nursery area. Can. J. Fish. Aquat. Sci. 70: 1508–1530.

Ouellette-Plante, J., Chabot, D., Nozères, C. and Bourdages, H. 2020. Diets of demersal fish from the CCGS Teleost ecosystemic surveys in the estuary and northern Gulf of St. Lawrence, August 2015–2017. Can. Tech. Rep. Fish. Aquat. Sci. 3383. v + 121 p.

Ouellette-Plante, J., Benoît, H., Plourde, S. and Chabot, D. 2022. Preliminary estimates of annual Capelin consumption by Atlantic Cod and Greenland Halibut. DFO Can. Sci. Advis. Sec. Res. Doc. 2022/013. iv + 48 p.

Patterson, K. 1992. Fisheries for small pelagic species: an empirical approach to management targets. Rev. Fish Biol. Fish. 2(4): 321–338.

Penton, P.M., Davoren, G.K., Montevechhi, W.A. and Andrews, D.W. 2012. Beach and demersal spawning in Capelin (*Mallotus villosus*) on the northeast Newfoundland coast: Egg developmental rates and mortality. Can. J. Zool. 90: 248-256.

Præbel K., Westgaard, J.I., Fevolden, S.E., and Christiansen, J.S. 2008. Circumpolar genetic population structure of Capelin *Mallotus villosus*. Mar. Ecol. Prog. Ser. 360: 189–199.

Purchase, C.F. 2018. Low tolerance of salt water in a marine fish: new and historical evidence for surprising local adaption in the well-studied commercially exploited Capelin. Can. J. Fish. Aquat. Sci. 75: 673–681.

Rose, G.A. 1988. Temporal and spatial variability in onshore Cod (*Gadus morhua*) migrations: Associations with atmosphere-ocean dynamics and Capelin (*Mallotus vllosus*) distributions (PhD Thesis). McGill University. Montreal, Quebec, Canada. 307 p.

Rose, G.A. 2005. Capelin (*Mallotus villosus*) distribution and climate: a sea "canary" for marine ecosystem change. ICES J. Mar. Sci. 62: 1524–1530.

Saunders, M.D., Steeves, R., MacIntyre, L.P., Knysh, K.M., Coffin, M.R.S., Boudreau, M., Pater, C.C., van den Heuvel, M.R. and Courtenay, S.C. 2024. Monitoring estuarine fish communities: environmental DNA (eDNA) metabarcoding as a complement to beach seining. Canadian Journal of Fisheries and Aquatic Sciences 81, 10: 1344-1357. https://doi.org/10.1139/cjfas-2023-0227

Savenkoff, C., Grégoire, F. and Chabot, D. 2004. Main prey and predators of Capelin (*Mallotus villosus*) in the northern and southern Gulf of St. Lawrence during the mid-1980s and mid-1990s. Can. Tech. Rep. Fish. Aquat. Sci. 2551: vi + 30 p.

Sharp, J.C., Able, K.W., Leggett, W.C. and Carscadden. J.E. 1978. The utility of meristic and morphometric characters in the identification of Capelin (*Mallotus villosus*) stocks in Canadian Atlantic waters. J. Fish. Res. Board Can. 35: 124–130.

Simard, Y., Lavoie, D. and Saucier, F.J. 2002. Channel head dynamics: Capelin (*Mallotus villosus*) aggregation in the tidally driven upwelling system of the Saguenay-St. Lawrence Marine Parks's whale feeding ground. Can. J. Fish. Aquat. Sci. 59: 197–210. doi:10.1139/F01-210

Sirois, P., Diab, G., Fortin, A.-L., Plourde, S., Gagné, J.A. and Ménard, N. 2009. Recrutement des poissons dans le fjord du Saguenay. Rev. Sci. Eau, 22(2): 341–352. doi:10.7202/037488ar

Templeman, W. 1948. The life history of the Capelin (*Mallotus villosus* O.F. Müller) in Newfoundland waters. St-John's NFLD: Newfoundland Government Laboratory. 151 p.

Thompson, P.L., Anderson, S. C., Nephin, J., Robb, C. K., Proudfoot, B., Park, A.E., Haggarty D.R. and Rubidge, E. M. 2022. Integrating trawl and longline surveys across British Columbia improves groundfish distribution predictions. Canadian Journal of Fisheries and Aquatic Sciences 80, 1: 195-210.

Vesin, J.-P. 1981. The Feeding Ecology of Capelin (*Mallotus villosus*) in the Estuary and Western Gulf of St. Lawrence (PhD Thesis). McGill University. Montreal, Quebec, Canada. 33 p.

Winters, G.H. 1970. Biological changes in coastal capelin from the over-wintering to the spawning condition. Journal of the Fisheries Board of Canada 27: 2215-2224.

TABLES

Table 1: Summary of the Estuary and Gulf of Saint Lawrence Capelin fishery quota split by NAFO Division and gear type. Capelin Fishing Areas (CFA) are indicated in parentheses (see Figure 1).

NAFO Division	Gear type	Type of quota	Allocation (%)
4R (12*–14)	Fixed	Competitive	37.82
	Mobile < 65’	Individual	24.15
	Mobile ≥ 65’	Competitive	24.15
4ST (15–16)	All	Competitive	13.88

*CFA 12 includes NAFO 3Pn and portions of 3Ps

Table 2: Coefficients of the fitted annual length (mm) weight (g) relationship equation ($Weight = a \times Length^b$) estimated from the Capelin samples in the northern (nGSL) and southern (sGSL) Gulf of St. Lawrence.

	sGSL		nGSL	
Year	**a**	**b**	**a**	**b**
1990	0.00432	3.121	-	-
1991	0.00469	3.073	-	-
1992	0.00301	3.212	-	-
1993	0.01245	2.648	-	-
1994	0.00534	2.994	-	-
1995	0.003	3.208	0.00081	3.671
1996	0.00412	3.076	-	-
1997	0.00295	3.209	0.00009	4.597
1998	0.00342	3.146	0.00145	3.467
1999	0.00341	3.157	0.00094	3.57
2000	0.00495	3.015	0.05966	2.089
2001	0.00228	3.338	0.00169	3.381
2002	0.00681	2.912	0.00358	3.089
2003	-	-	0.00182	3.31
2004	0.00354	3.158	0.00163	3.38
2005	0.0011	3.605	0.00267	3.187
2006	0.00215	3.331	0.00262	3.199
2007	0.00506	3.000	0.00173	3.342
2008	0.00301	3.206	0.00282	3.154
2009	0.00337	3.181	0.00336	3.087
2010	0.0034	3.134	0.00192	3.317
2011	0.00432	3.052	0.00216	3.253
2012	0.00319	3.202	0.00106	3.509
2013	0.00465	3.041	0.00239	3.207
2014	0.00329	3.158	0.00185	3.312
2015	0.00269	3.231	0.00040	3.676
2016	0.0032	3.176	0.00203	3.272
2017	0.00267	3.25	0.00098	3.562
2018	0.00319	3.184	0.00040	3.899
2019	0.00304	3.21	0.00123	3.461
2020	0.00156	3.479	0.0011	3.52
2021	0.0026	3.275	0.00153	3.362
2022	0.00322	3.158	0.00661	2.815
2023	0.00323	3.186	0.00253	3.214
2024	0.00444	3.082	0.00284	3.153
2025	0.0035	3.175	0.00151	3.413

Table 3: 4RST capelin commercial landings[1,2] (t) by NAFO division since 1960, including annual total landings, TACs (t), and the percentage (%) of TAC reached.

Year	Division			Total	TAC	%
	4R	4S	4T			
1960	600	46	32	**678**	-	-
1961	424	50	90	**564**	-	-
1962	514	4	143	**661**	-	-
1963	444	13	94	**551**	-	-
1964	563	33	101	**697**	-	-
1965	755	50	100	**905**	-	-
1966	735	88	43	**866**	-	-
1967	724	39	150	**913**	-	-
1968	734	30	32	**796**	-	-
1969	1,394	92	82	**1,568**	-	-
1970	339	75	42	**456**	-	-
1971	403	15	46	**464**	-	-
1972	370	41	126	**537**	-	-
1973	270	84	75	**429**	-	-
1974	180	113	128	**421**	-	-
1975	68	94	105	**267**	-	-
1976	92	48	336	**476**	-	-
1977	1,514	69	318	**1,901**	-	-
1978	8,341	37	1,323	**9,701**	-	-
1979	5,737	1,132	2,163	**9,032**	-	-
1980	1,939	15	1,566	**3,520**	-	-
1981	2,164	1	237	**2,402**	25,000	**10**
1982	156	2	235	**393**	25,000	**2**
1983	920	-	104	**1,024**	25,000	**4**
1984	1,907	-	180	**2,087**	25,000	**8**
1985	2,573	-	545	**3,118**	25,000	**12**
1986	3,721	-	226	**3,948**	25,000	**16**
1987	906	-	67	**973**	25,000	**4**
1988	4,386	129	248	**4,763**	25,000	**19**
1989	5,257	1,078	444	**6,779**	25,000	**27**
1990	6,105	164	153	**6,422**	25,000	**26**
1991	7,166	59	247	**7,472**	21,300	**35**
1992	7,851	856	56	**8,763**	5,750	**152**
1993	9,398	1,262	237	**10,897**	10,750	**101**
1994	592	208	165	**966**	11,725	**8**
1995	15	90	47	**152**	11,725	**1**
1996	6,265	461	172	**6,898**	9,850	**70**
1997	7,399	252	238	**7,889**	11,725	**67**
1998	8,749	126	776	**9,652**	11,725	**82**
1999	4,735	10	166	**4,911**	12,425	**40**
2000	5,129	-	-	**5,129**	12,425	**41**

Year	Division			Total	TAC	%
	4R	4S	4T			
2001	741	-	-	**741**	12,425	**6**
2002	3,295	77	20	**3,392**	12,425	**27**
2003	5,032	-	-	**5,032**	7,455	**68**
2004	6,521	-	-	**6,521**	7,455	**87**
2005	8,659	305	34	**8,998**	13,000	**69**
2006	9,322	2,039	518	**11,880**	13,000	**91**
2007	6,097	1,344	471	**7,911**	13,000	**61**
2008	7,846	2,126	99	**10,071**	13,000	**77**
2009	10,147	527	1,405	**12,080**	13,000	**93**
2010	-	795	1,258	**10,822**	13,000	**83**
2011	9,890	974	1,449	**12,314**	13,000	**95**
2012	8,914	478	147	**9,539**	13,000	**73**
2013	6,350	236	-	**6,587**	14,300	**46**
2014	5,683	20	-	**5,703**	14,300	**40**
2015	11,361	107	357	**11,825**	14,300	**83**
2016	9,326	78	373	**9,777**	14,300	**68**
2017	1,945	19	1	**1,965**	14,300	**14**
2018	8,141	356	6	**8,503**	9,295	**91**
2019	7,575	427	484	**8,486**	9,295	**91**
2020	7,972	1,858	547	**10,341**	9,295	**111**
2021[3]	8,013	1,841	186	**9,977**	9,295	**107**
2022[3]	4,953	117	10	**5,079**	10,225	**50**
2023[3]	1,141	12	2	**1,155**	10,225	**11**
2024[3]	1,773	582	1	**2,357**	10,225	**23**
2025[3]	1,089	131	4	**1,224**	10,225	**12**

[1]From 1960 to 1978: ICNAF Statistical Bulletins Vol. 10 to 28; from 1979 to 1984: NAFO Statistical Bulletins Vol. 29 to 34

[2]ZIFF file since 1985

[3]Preliminary data

Table 4: 4RST capelin commercial landings (t) since 1987, by NAFO unit area. NK = not known.

Year	4RA	4RB	4RC	4RD	NK	TOTAL 4R	4SI	4SS	4SV	4SW	4SX	4SY	4SZ	NK	TOTAL 4S	4TF	4TG	4TJ	4TK	4TM	4TN	4TO	4TP	4TQ	NK	TOTAL 4T
1987	624	96	146	1	40	906	-	-	-	-	-	-	-	-	-	-	-	-	-	-	-	-	67	-	-	67
1988	1,429	18	20	12	2,907	4,386	-	-	-	124	-	5	-	-	129	-	-	-	-	-	-	-	248	-	-	248
1989	1,897	47	585	76	2,652	5,257	-	-	2	1,075	-	1	-	-	1,078	-	-	-	-	-	-	-	402	7	35	444
1990	1,959	479	925	104	2,639	6,105	-	-	9	155	-	-	-	-	164	-	-	-	-	-	-	-	141	11	-	153
1991	154	82	4,907	2,023	-	7,166	-	-	-	7	-	-	51	-	59	-	-	-	-	65	-	-	160	23	-	247
1992	1,554	1,506	4,675	117	-	7,851	-	-	-	855	-	-	1	-	856	-	-	-	-	-	-	-	56	-	-	56
1993	791	1,543	5,142	1,922	-	9,398	-	-	-	1,262	-	-	-	-	1,262	-	-	-	-	-	108	-	129	-	-	237
1994	10	265	245	72	-	592	-	-	2	205	-	-	-	-	208	-	-	-	-	47	22	-	96	-	-	165
1995	15	-	-	-	-	15	-	-	-	90	-	-	-	-	90	-	-	-	-	-	-	3	39	5	-	47
1996	630	1,841	3,364	430	-	6,265	-	-	-	415	-	-	46	-	461	-	-	-	-	-	5	5	152	10	-	172
1997	734	2,480	4,171	14	-	7,399	4	-	-	202	-	30	16	-	252	2	5	-	-	7	2	2	214	5	-	238
1998	1,827	3,791	2,550	581	-	8,749	-	-	-	126	-	-	-	-	126	-	-	-	-	-	697	-	-	-	79	776
1999	29	1,675	3,031	-	-	4,735	-	-	-	10	-	-	-	-	10	-	-	-	-	70	77	-	-	-	19	166
2000	-	356	4,773	-	-	5,129	-	-	-	-	-	-	-	-	-	-	-	-	-	-	-	-	-	-	-	-
2001	-	-	605	136	-	741	-	-	-	-	-	-	-	-	-	-	-	-	-	-	-	-	-	-	-	-
2002	115	856	2,323	-	-	3,295	-	-	-	7	-	-	-	-	7	-	-	-	-	-	-	-	-	2	-	2
2003	513	1,070	3,450	-	-	5,032	-	-	-	-	-	-	-	-	-	-	-	-	-	-	-	-	-	-	-	-
2004	3,630	645	2,185	61	-	6,521	-	-	-	-	-	-	-	-	-	-	-	-	-	-	-	-	-	-	-	-
2005	5,025	1,028	2,260	346	-	8,659	-	-	-	305	-	-	-	-	305	-	-	-	-	-	-	-	34	-	-	34
2006	6,027	9	2,530	756	-	9,322	66	149	-	1,317	507	-	-	-	2,039	-	-	-	-	-	474	-	43	-	-	518
2007	5,326	6	691	73	-	6,097	-	-	-	1,344	-	-	-	-	1,344	-	-	-	-	-	430	-	41	-	-	471
2008	883	188	2,692	4,083	-	7,846	-	-	-	1,420	-	-	-	706	2,126	-	-	-	-	-	66	-	33	-	-	99
2009	2,570	2,929	4,116	531	-	10,147	-	-	-	527	-	-	-	-	527	-	-	-	-	-	1,367	-	39	-	-	1,405
2010	2,409	4,785	1,442	133	-	8,769	-	-	-	795	-	-	-	-	795	-	-	-	-	-	1,258	-	-	-	-	1,258
2011	3,378	507	4,021	1,985	-	9,890	-	-	-	974	-	-	-	-	974	24	-	-	16	-	1,409	-	-	-	-	1,449
2012	1,418	1,759	5,590	147	-	8,914	-	-	-	478	-	-	-	-	478	-	-	-	-	-	147	-	-	-	-	147
2013	5,557	344	16	378	54	6,350	-	-	-	236	-	-	-	-	236	-	-	-	-	-	-	-	-	-	-	-
2014	5,197	322	10	154	-	5,683	-	-	-	20	-	-	-	-	20	-	-	-	-	-	-	-	-	-	-	-
2015	8,048	1,746	1,309	258	-	11,361	-	-	-	107	-	-	-	-	107	-	-	-	-	-	357	-	-	-	-	357
2016	6,026	2,425	811	65	-	9,326	-	78	-	-	-	-	-	-	78	-	-	-	-	-	373	-	-	-	-	373
2017	223	1,481	240	0	-	1,945	-	-	-	19	-	-	-	-	19	-	-	-	-	-	-	-	1	-	-	1
2018	2,375	2,633	2,988	145	-	8,141	-	-	-	356	-	-	-	-	356	-	-	-	-	-	-	-	3	-	2	6
2019	3,029	2,500	1,598	442	-	7,569	-	-	-	427	-	-	-	-	427	-	-	-	-	-	480	-	10	-	-	490
2020*	2,358	2,751	2,588	179	-	7,876	-	-	-	1,856	-	1	-	-	1,858	-	-	-	-	-	490	-	53	-	4	547
2021*	2,101	2,443	3,112	357	-	8,013	-	-	-	1,688	45	-	-	-	1,733	155	-	-	-	-	-	-	33	-	-	188
2022*	3,730	565	612	28	-	4,935	-	-	-	117	-	-	-	-	117	-	-	-	-	-	-	-	10	-	-	10
2023*	1,054	-	74	-	-	1,128	-	-	-	12	-	-	-	-	12	-	-	-	-	-	-	-	2	-	-	2
2024*	1,667	36	70	-	-	1,773	-	-	-	582	-	-	-	-	582	-	-	-	-	-	-	-	1	-	-	1
2025*	509	41	445	95	-	1,090	-	-	-	52	79	-	-	-	131	-	-	-	-	-	-	-	4	-	-	4

*Preliminary data

Table 5: Number (#) of length-frequency samples collected and individual Capelin measured by port samplers in NAFO Divisions 4RST since 1984.

Year	# Samples			# Fish			Total # Samples	Total # Fish
	4R	4T	4S	4R	4T	4S	4RST	4RST
1984	6	-	1	1,193	-	351	7	1,544
1985	7	-	1	1,954	-	375	8	2,329
1986	12	5	9	3,072	1,163	2,077	26	6,312
1987	3	3	7	826	740	1,766	13	3,332
1988	17	9	17	4,484	2,078	4,405	43	10,967
1989	10	5	6	2,470	1,331	1,506	21	5,307
1990	10	17	28	2,585	4,469	7,448	55	14,502
1991	8	14	11	2,036	3,517	2,826	33	8,379
1992	9	12	10	2,302	3,130	2,555	31	7,987
1993	12	10	5	3,141	2,626	1,247	27	7,014
1994	1	10	7	256	2,616	1,657	18	4,529
1995	6	15	11	1,606	4,333	2,986	32	8,925
1996	13	15	15	3,479	6,200	3,811	43	13,490
1997	10	29	25	2,575	7,322	6,433	64	16,330
1998	9	8	5	2,245	2,080	1,359	22	5,684
1999	9	2	8	2,448	515	2,212	19	5,175
2000	6	-	3	1,553	-	553	9	2,106
2001	2	-	-	478	-	-	2	478
2002	7	-	-	1,974	-	-	7	1,974
2003	9	5	12	2,367	1,177	3,270	26	6,814
2004	8	6	4	2,070	1,524	1,015	18	4,609
2005	7	10	9	1,053	1,523	1,702	26	4,278
2006	10	3	4	1,980	542	1,019	17	3,541
2007	7	3	4	1,959	570	981	14	3,510
2008	7	4	2	1,360	770	517	13	2,647
2009	15	4	5	2,640	733	819	24	4,192
2010	6	8	17	1,032	1,317	3,261	31	5,610
2011	4	7	7	722	1,189	1,277	18	3,188
2012	10	3	9	1,941	486	1,507	22	3,934
2013	7	3	13	1,333	504	2,137	23	3,974
2014	4	4	8	783	717	1,240	16	2,740
2015	7	9	11	1,752	1,512	1,810	27	5,074
2016	6	4	19	1,047	627	3,433	29	5,107
2017	4	5	5	723	871	923	14	2,517
2018	9	19	19	1,620	3,144	3,403	47	8,167
2019	7	12	11	1,189	1,895	1,744	30	4,828
2020	-	8	5	-	1,355	780	13	2,135
2021	11	10	8	1,991	1,597	1,221	29	4,809
2022	8	9	5	1,341	1,359	788	22	3,488
2023	3	-	1	650	-	173	4	823
2024	3	10	6	546	1,704	999	19	3,249
2025	-	5	1	-	1,018	161	6	1,179

Table 6: Number (#) of biological samples collected by port samplers and individuals analysed in the laboratory since 1984.

Year	# Samples			# Fish			Total # Samples	Total # Fish
	4R	4T	4S	4R	4T	4S	4RST	4RST
1984	6	-	1	191	-	50	7	241
1985	7	-	1	235	-	31	8	266
1986	12	5	9	164	62	98	26	324
1987	3	3	7	114	80	172	13	366
1988	17	9	17	513	188	376	43	1077
1989	10	5	6	208	401	204	21	813
1990	10	17	27	177	222	207	54	606
1991	8	14	11	129	173	157	33	459
1992	9	12	10	169	85	113	31	367
1993	12	10	5	202	157	67	27	426
1994	1	10	8	17	509	306	19	832
1995	6	15	11	202	148	127	32	477
1996	13	15	15	169	162	170	43	501
1997	10	29	25	169	339	343	64	851
1998	9	8	5	139	120	52	22	311
1999	9	2	8	241	36	100	19	377
2000	8	-	3	661	-	58	11	719
2001	2	-	-	54	-	-	2	54
2002	7	-	-	204	-	-	7	204
2003	9	5	12	159	77	135	26	371
2004	8	6	4	238	107	95	18	440
2005	7	10	9	211	176	226	26	613
2006	10	3	4	302	50	94	17	446
2007	7	3	4	218	49	72	14	339
2008	7	4	2	211	60	40	13	311
2009	15	4	5	237	70	66	24	373
2010	6	8	17	157	128	243	31	528
2011	4	7	7	158	148	258	18	564
2012	10	3	9	252	52	109	22	413
2013	7	5	13	204	77	166	25	447
2014	4	6	8	170	61	90	18	321
2015	7	9	11	217	132	141	27	490
2016	6	4	20	177	60	280	30	517
2017	4	5	5	144	71	55	14	270
2018	9	19	19	238	220	365	47	823
2019	7	12	11	209	162	131	30	502
2020	-	8	5	-	134	51	13	185
2021	11	10	8	258	113	97	29	468
2022	8	5	9	245	75	119	22	439
2023	3	-	1	121	-	20	4	141
2024	3	10	6	123	13	186	19	322
2025	-	5	1	-	105	73	6	178

Table 7: Summary of the different model configurations and their associated Akaike Information Criterion (AIC) used to fit Capelin mature biomass (Biomass) and age-1 abundance with sdmTMB for the northern (nGSL) and southern (sGSL) Gulf of St. Lawrence surveys. Depth for the nGSL modeling was log transformed while it followed a second degree polynomial function of the log transformed depth for the sGSL. The dash line (-) means that the model did not converge or sanity tests weren't met. (Time.R = time in hours, Time.C = Time in categories day and night).

Model	nGSL		sGSL	
	Biomass	**Age-1**	**Biomass**	**Age-1**
	AIC	AIC	AIC	AIC
~ 1	6,504	13,971	8,549	27,790
~ Depth	6,389	13,877	8,455	27, 481
~ Depth + Time.R	-	-	8,431	27,483
~ Depth + Time.C	6,390	13,876	8,426	27,480
~ Depth + Time.C + Depth*Time.C	6,385	13,861	8,380	27,424

Table 8: Sum log-likelihood (LL), root mean square error (RMSE) and mean absolute error (MAE) estimated with the 50-folds cross-validation for the different model configurations used to fit mature biomass (Biomass) and age-1 Capelin numbers and considering year effect as an categorical factor (FC) or as a random effect drawn from a normal distribution (RE) and following an autoregressive order 1 (AR(1)) process. (FE = Combination of fixed-effects predictive variables selected from the lowest AIC in Table 7).

	nGSL			sGSL		
Model	**LL**	**RMSE**	**MAE**	**LL**	**RMSE**	**MAE**
Biomass ~ FE + RE + AR(1)	-22,336	55.43	3.90	-17,209	86.23	4.21
Biomass ~ FE + FC + AR(1)	-23,189	62.48	4.12	-16,884	77.18	3.78
Age-1 ~ FE + RE + AR(1)	-35,406	993.78	55.73	-25,712	1,584.16	241.14
Age-1 ~ FE + FC + AR(1)	-35,786	992.87	55.34	-25,895	1,549.38	236.54

Table 9: Fixed and random effects and distribution parameters coefficients with their uncertainties [95% confidence interval]of the selected mature biomass (Biomass) and age-1 abundance (Age-1) sdmTMB models for the northern Gulf of St. Lawrence survey (nGSL). Time is categorical (day/night). The dash line (-) means that the model did not converge or sanity tests weren't met.

Fixed parameters		**Definition**	**Biomass**	**Age-1**
Main effects ($\boldsymbol{\beta}$)	β_0	intercept	9.66 [8.01; 11.32]	15.29 [12.78; 17.81]
	β_1	log(depth)	-1.77 [-2.06; -1.48]	-2.59 [-3.06; -2.13]
	β_2	time	-1.68 [-3.04; -0.32]	-5.08 [-7.37; -2.80]
	β_3	depth*time	0.31 [0.06; 0.57]	0.93 [0.50; 1.37]
Distribution parameters (tweedie)	ϕ	dispersion parameter	0.82 [0.76; 0.89]	0.37 [0.33; 0.42]
	p	power of the Tweedie distribution	1.61 [1.60; 1.63]	-
Parameters controlling the spatial ($\boldsymbol{\omega_t}$) and spatiotemporal ($\boldsymbol{\delta_{t,y}}$) random fields	κ	matérn range parameter shared between $\omega_t$and $\delta_{t,y}$	93.20 [83.81; 103.64]	121.80 [106.16; 139.72]
	σ_ω^2	marginal variance of the sparse precision matrix of ω_t	35.14 [27.65; 44.66]	42.81 [32.09; 57.11]
	σ_δ^2	marginal variance of the sparse precision matrix of $\delta_{t,y}$	40.66 [34.98; 47.26]	52.12 [43.60; 62.30]
	ρ	correlation between subsequent spatiotemporal random fields $\delta_{t,y}$	0.41 [0.31; 0.50]	0.47 [0.35; 0.57]

Table 10: Fixed and random effects and distribution parameters coefficients with their uncertainties [95% confidence interval] of the selected mature biomass (Biomass) and age-1 abundance (Age-1) sdmTMB models for the southern Gulf of St. Lawrence survey (sGSL). Time is categorical (day/night). The dash line (-) means that the model did not converge or sanity tests weren't met. Coefficient estimates of the fixed effect of the year as factor are presented in Figures 34 and 47 for the mature biomass and age-1 Capelin respectively.

Fixed parameters		**Definition**	**Biomass**	**Age-1**
Main effects (β)	β_0	intercept	-8.74 [-11.03; -6.45]	-5.15 [-7.85; -2.46]
	β_1	poly(log(depth,1))	101.09 [76.20; 125.97]	104.60 [74.33; 134.88]
	β_2	poly(log(depth,2))	-80.49 [-99.87; -61.11]	-108.70 [-131.67; -85.74]
	β_3	time	0.35 [0.15; 0.55]	-0.25 [-0.49; 0]
	β_4	poly(log(depth,1))*time	34.28 [17.63; 50.93]	53.61 [33.14; 74.07]
	β_4	poly(log(depth,2))*time	20.23 [3.97; 36.49]	31.88 [11.26; 52.50]
Distribution parameters (tweedie)	ϕ	dispersion parameter	1.16 [1.06; 1.28]	0.31 [0.28; 0.33]
	p	power of the Tweedie distribution	1.61 [1.60; 1.63]	-
Parameters controlling the spatial (ω_t) and spatiotemporal ($\delta_{t,y}$) random fields	κ	matérn range parameter shared between $\omega_t$and $\delta_{t,y}$	67.54 [60.03; 76.00]	86.70 [76.69; 98.03]
	σ_ω^2	marginal variance of the sparse precision matrix of ω_t	21.62 [16.99; 27.53]	34.09 [26.36; 44.08]
	σ_δ^2	marginal variance of the sparse precision matrix of $\delta_{t,y}$	29.97 [25.84; 34.76]	37.04 [31.50; 43.56]
	ρ	correlation between subsequent spatiotemporal random fields $\delta_{t,y}$	0.44 [0.35; 0.52]	0.43 [0.32; 0.54]

Table 11: Summary of values for the harvest level indicators estimated from 1996 to 2023 (mean, minimum, and maximum) and in 2024 and 2025. (CI = confidence interval).

Indicator	Mean [CI 95%]	Minimum	Maximum	2024	2025
Exploitation rate	0.068 [0.046; 0.091]	0.003	0.219	0.783	0.031
Fishing mortality	0.073 [0.048; 0.099]	0.003	0.248	1.529	0.031

Table 12: Summary of the different model configurations, their associated Akaike Information Criterion (AIC) and results of the 50-folds cross-validation used to fit the presence and absence (PA) of Capelin in Greenland halibut and Atlantic cod stomachs combined in the northern Gulf of St. Lawrence. The variable Depth followed a second degree polynomial function of the log-transformed bottom depth. The dash line (-) means that no cross-validation was performed. (Pred = Cod or Greenland halibut as factor, RE = year as a random effect, FC = year as a factor, LL = Sum log-likelihood, RMSE = root mean square error, MAE = mean absolute error (MAE).

Model	AIC	LL	RMSE	MAE
PA ~ 1	3,384	-	-	-
PA ~ Depth	3,354	-	-	-
PA ~ Depth + Pred	3,349	-	-	-
PA ~ Depth + Pred + RE	3,198	-1,546	0,345	0,236
PA ~ Depth + Pred + FC	3,157	-1,563	0,345	0,234

Table 13: Fixed and random effects coefficients with their uncertainties [95% confidence interval] of the model configuration selected to fit to presence and absence of Capelin in Greenland halibut and Atlantic cod stomachs combined in the northern Gulf of St. Lawrence.

Fixed parameters		Definition	Estimates
Main effects ($\boldsymbol{\beta}$)	β_0	intercept	-2.36 [-3.22; -1.50]
	β_1	poly(log(depth,1))	-33.53 [-44.99; -22.08]
	β_2	poly(log(depth,2))	-25.96 [-34.65; -17.26]
	β_3	predator(Greenland halibut)	0.40 [0.17;0.64]
Parameters controlling the spatial ($\boldsymbol{\omega_t}$) random fields	κ	matérn range parameter shared between ω_t	178.29 [95.60; 332.52]
	σ_ω^2	marginal variance of the sparse precision matrix of ω_t	32.02 [13.92; 73.67]

Table 14: Summary of the different model configurations and their associated Akaike Information Criterion (AIC) used to fit the presence and absence (PA) of Capelin environmental DNA in the water column (eDNA-WC) and at the bottom (eDNA-BD) for the northern and southern Gulf of St. Lawrence combined. The variable Depth followed a second degree polynomial function of the log-transformed bottom depth. The dash line (-) means that the model did not converge or sanity tests weren't met. (Loci = 12s160 or MiFishU as factor, RE = year as a random effect, FC = year as a factor).

Model	eDNA-WC	eDNA-BD
	AIC	AIC
PA ~ 1	547	562
PA ~ Depth	546	529
PA ~ Depth + Loci	549	531
PA ~ Depth + RE	539	-
PA ~ Depth + FC	536	531

Table 15: Fixed and random effects coefficients with their uncertainties [95% confidence interval] of the model configuration selected to fit to the presence and absence of Capelin eDNA in the water column (eDNA-WC) and at the bottom (eDNA-BD) for the northern and southern Gulf of St. Lawrence combined.

Fixed parameters		Definition	eDNA-WC	eDNA-BD
Main effects ($\boldsymbol{\beta}$)	β_0	intercept	0.34 [-1.37; 2.05]	-1.02 [-2.31; 0.26]
	β_1	poly(log(depth,1))	-2.35 [-10.67; 5.97]	-8.45 [-22.09; 5.19]
	β_2	poly(log(depth,2))	-7.22 [-13.70; -0.75]	-33.24 [-44.77; -21.72]
	β_3	year(2020)	-0.34 [-1.40; 0.71]	0.24 [-0.97; 1.46]
	β_4	year(2021)	-0.58 [-1.54; 0.39]	0.20 [-0.90; 1.31]
	β_5	year(2022)	-1,29 [-2.19; -0.38]	-0.29 [-1.27; 0.68]
Parameters controlling the spatial (ω_t) and spatiotemporal ($\delta_{t,y}$) random fields	κ	matérn range parameter shared between $\omega_t$and $\delta_{t,y}$	542.49 [169.9; 1732.12]	125.85 [66.76; 237.25]
	σ_ω^2	marginal variance of the sparse precision matrix of ω_t	80.18 [21,13; 7304,24]	1.75 [1.18; 2.60]

FIGURES

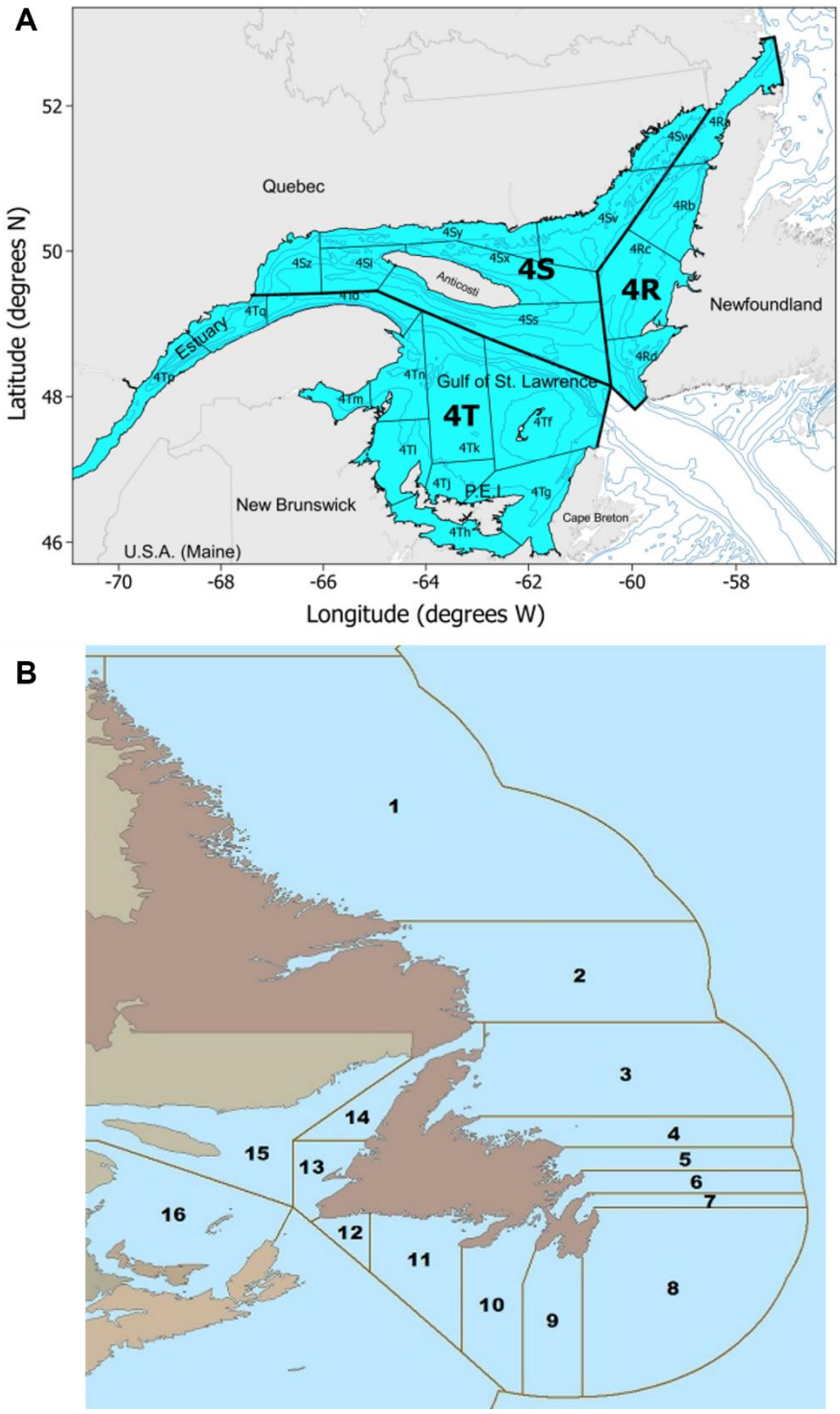


Figure 1: Maps of NAFO Divisions and unit areas of the Estuary and Gulf of St. Lawrence (A). Capelin fishing areas defined by DFO are shown in B.

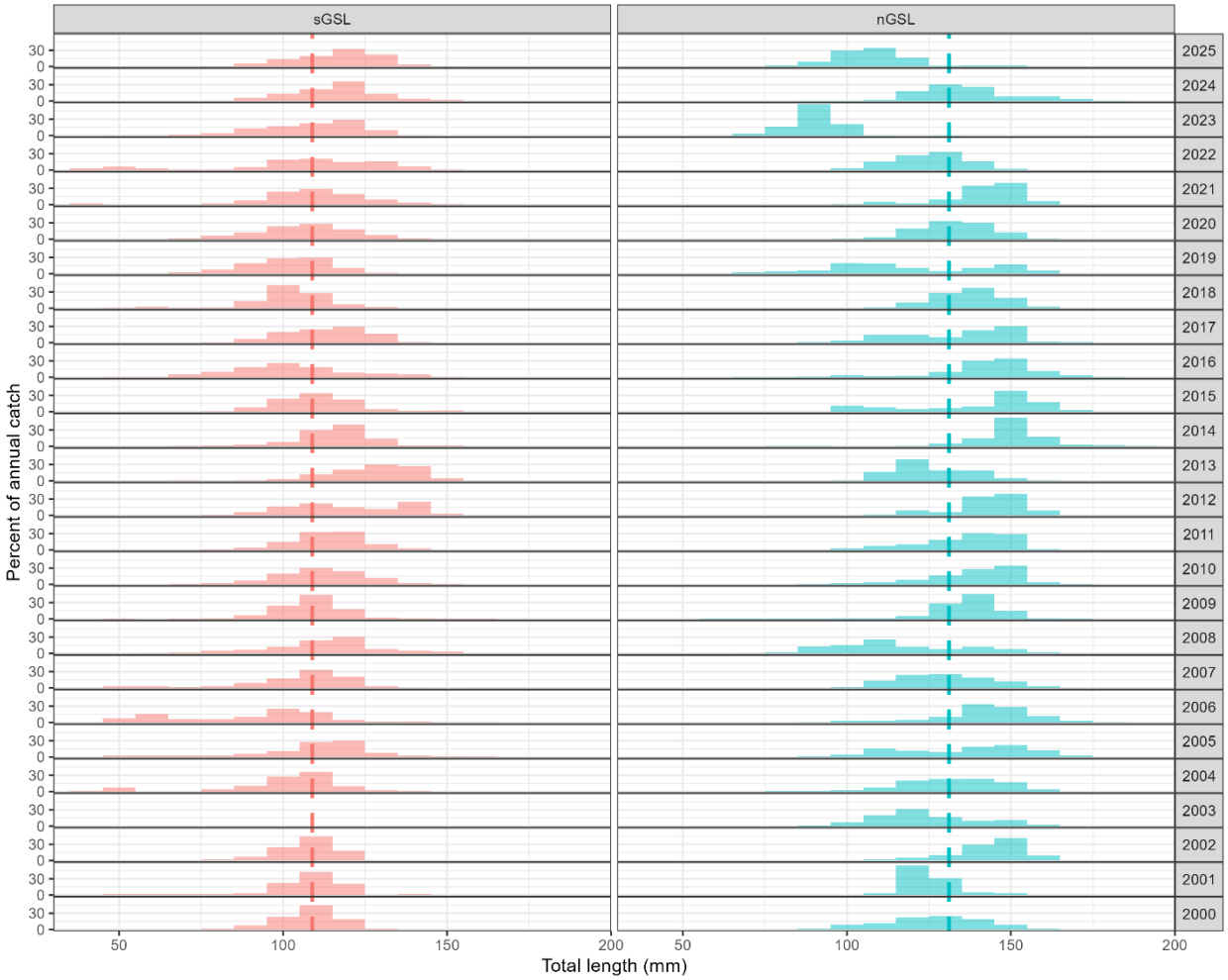


Figure 2: Comparison of annual relative length frequency distributions from the northern and southern Gulf of St. Lawrence bottom trawl surveys from 2000 to 2025. Vertical dashed line represents the 2000-2025 mean length.

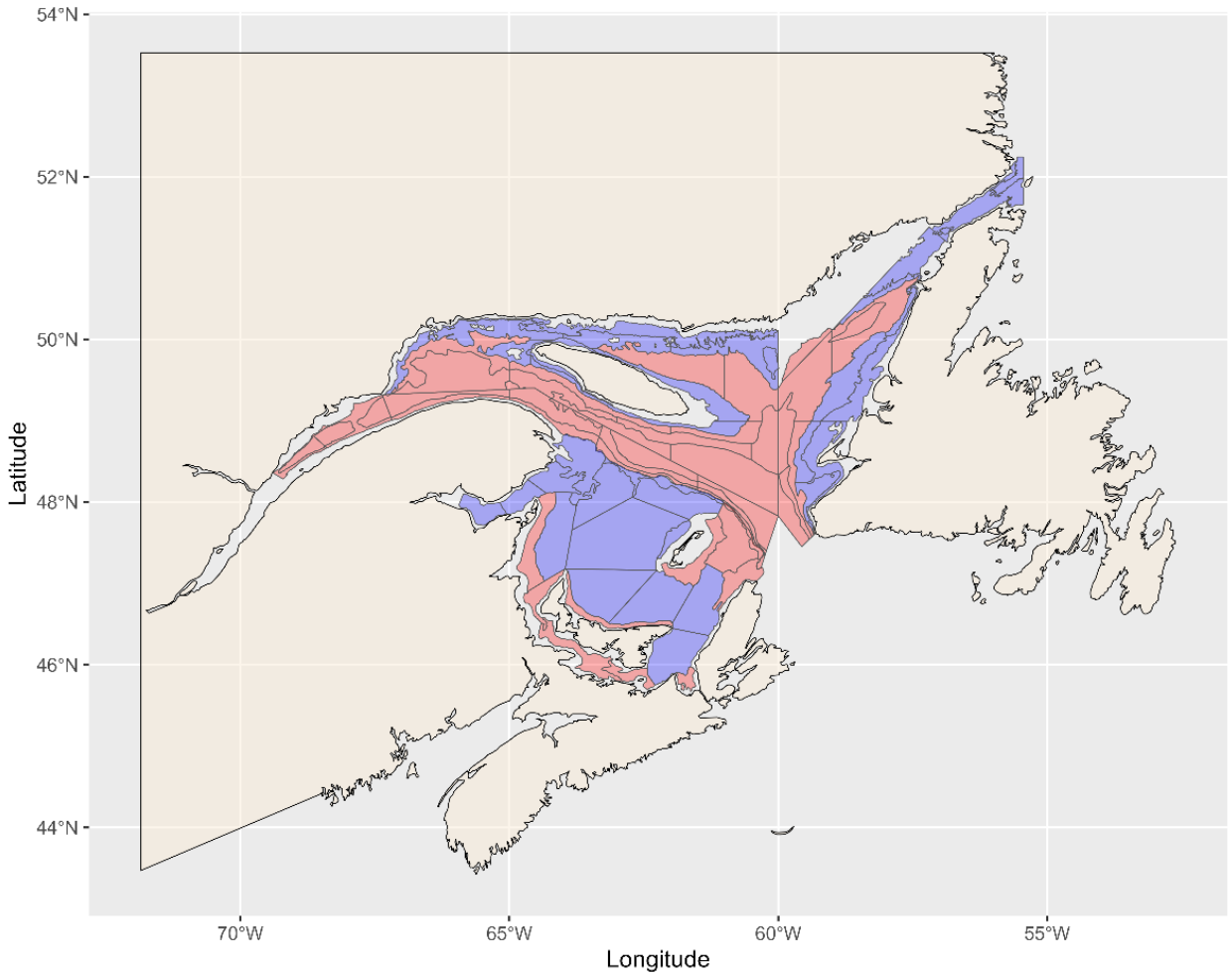


Figure 3: Map of the northern and southern Gulf of St. Lawrence strata identified as preferred (blue) and unfavourable (red) thermal habitat for Capelin.

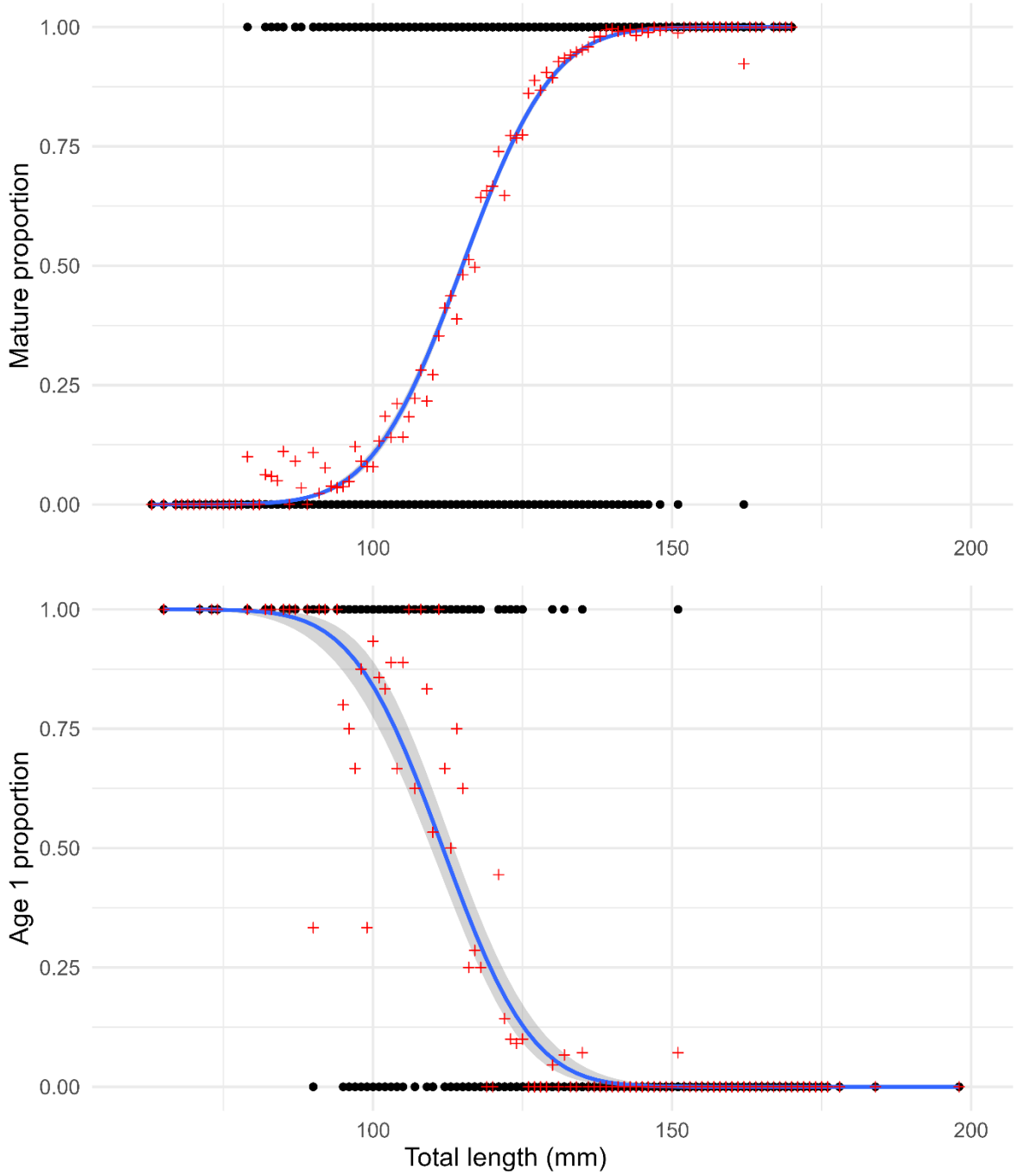


Figure 4: Estimated (blue lines) and observed (black dots) proportions at length of mature (upper panel) and age-1 (lower panel) Capelin sampled in the northern and southern Gulf of St. Lawrence bottom trawl surveys (2018-2025). The black dots represent either a mature (1) or immature (0) Capelin (upper panel) or an age-1 (1) or not (0) Capelin (lower panel). Red crosses represent the mean proportion at length of mature or age-1 Capelin for a given length category in mm.

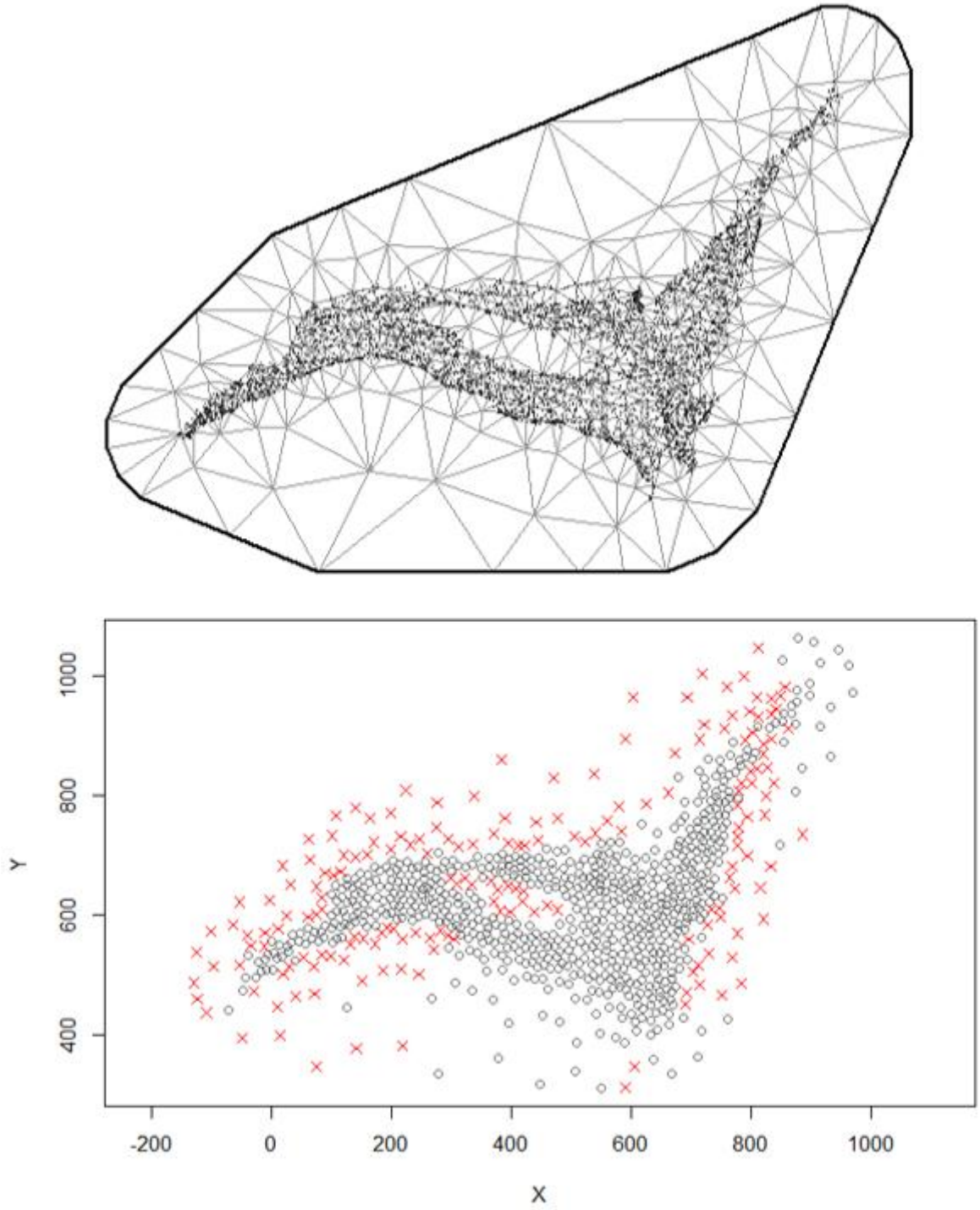


Figure 5: Triangulated grid constituted of vertices (lines) used to represent the continuous spatial process of Capelin catches with the nGSL bottom trawl surveys considering a minimum vertex length of 15 km (upper panel) and intersection of vertices (lower panel) that are connected (point) or not (red cross).

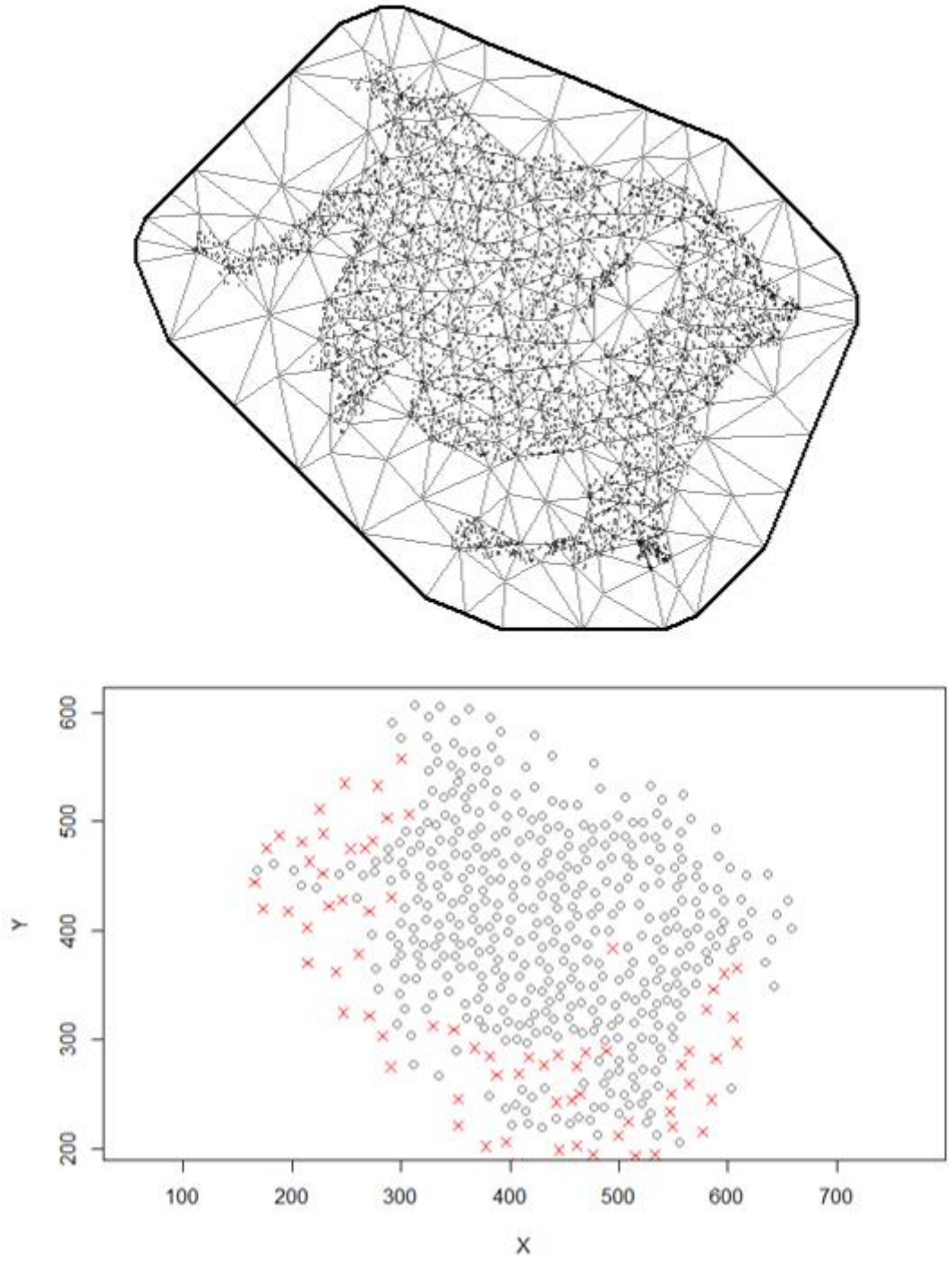


Figure 6: Triangulated grid constituted of vertices (lines) used to represent the continuous spatial process of Capelin catches with the sGSL bottom trawl surveys considering a minimum vertex length of 15 km (upper panel) and intersection of vertices (lower panel) that are connected (point) or not (red cross).

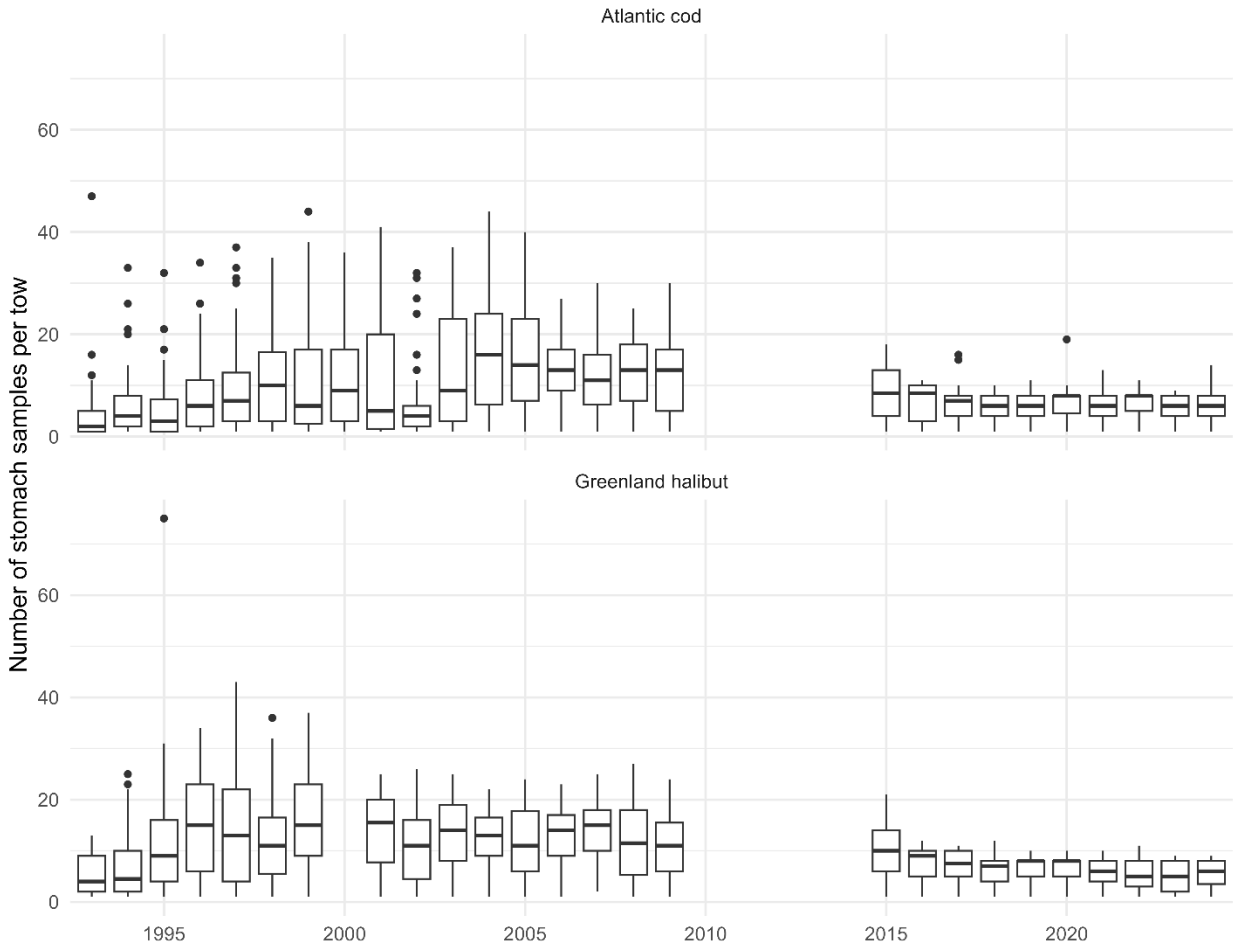


Figure 7: Boxplots of the number of Greenland halibut and Atlantic cod stomachs per tow collected during bottom trawl surveys in the northern Gulf of St. Lawrence.

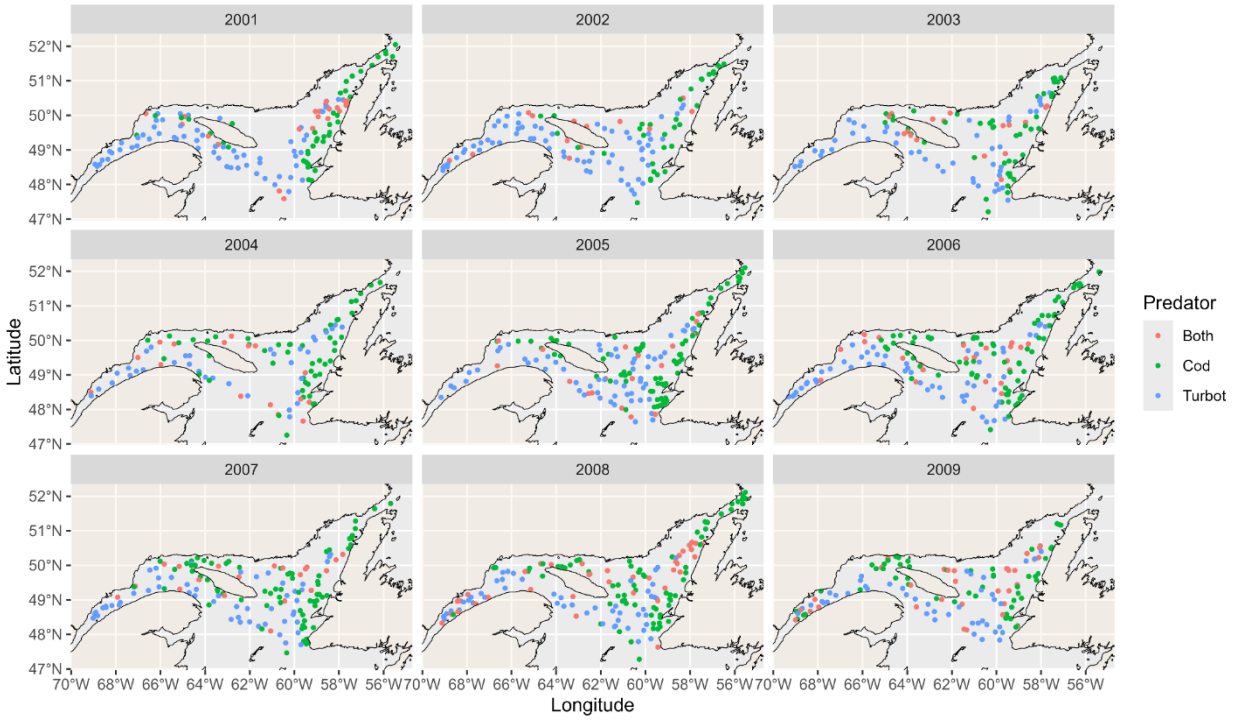


Figure 8: Maps of bottom trawl tows from the northern Gulf of St. Lawrence survey where stomachs of Greenland halibut, Atlantic cod, or both were collected from 2001 to 2009.

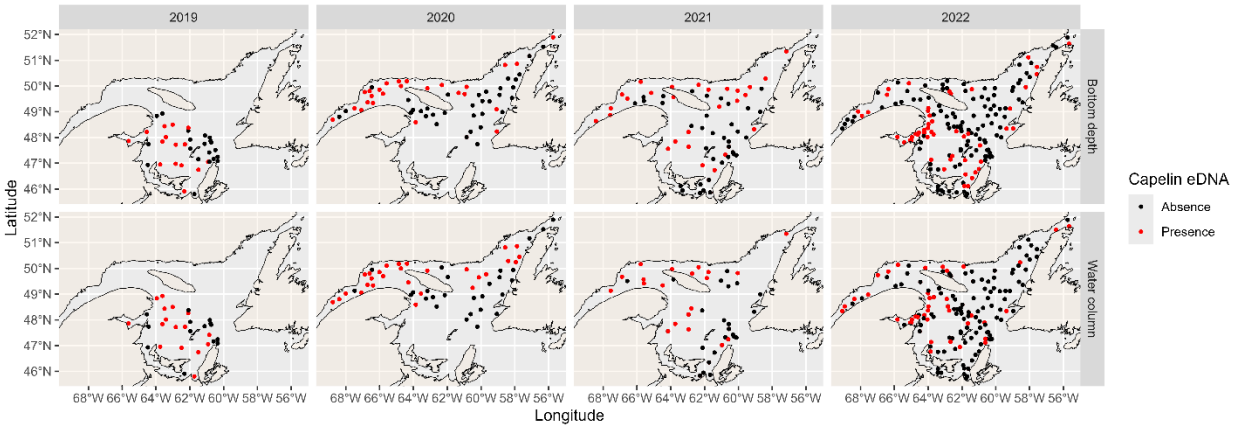


Figure 9: Maps showing the presence or absence of capelin environmental DNA in water samples collected in the northern and southern Gulf of St. Lawrence, at the bottom and within the water column.

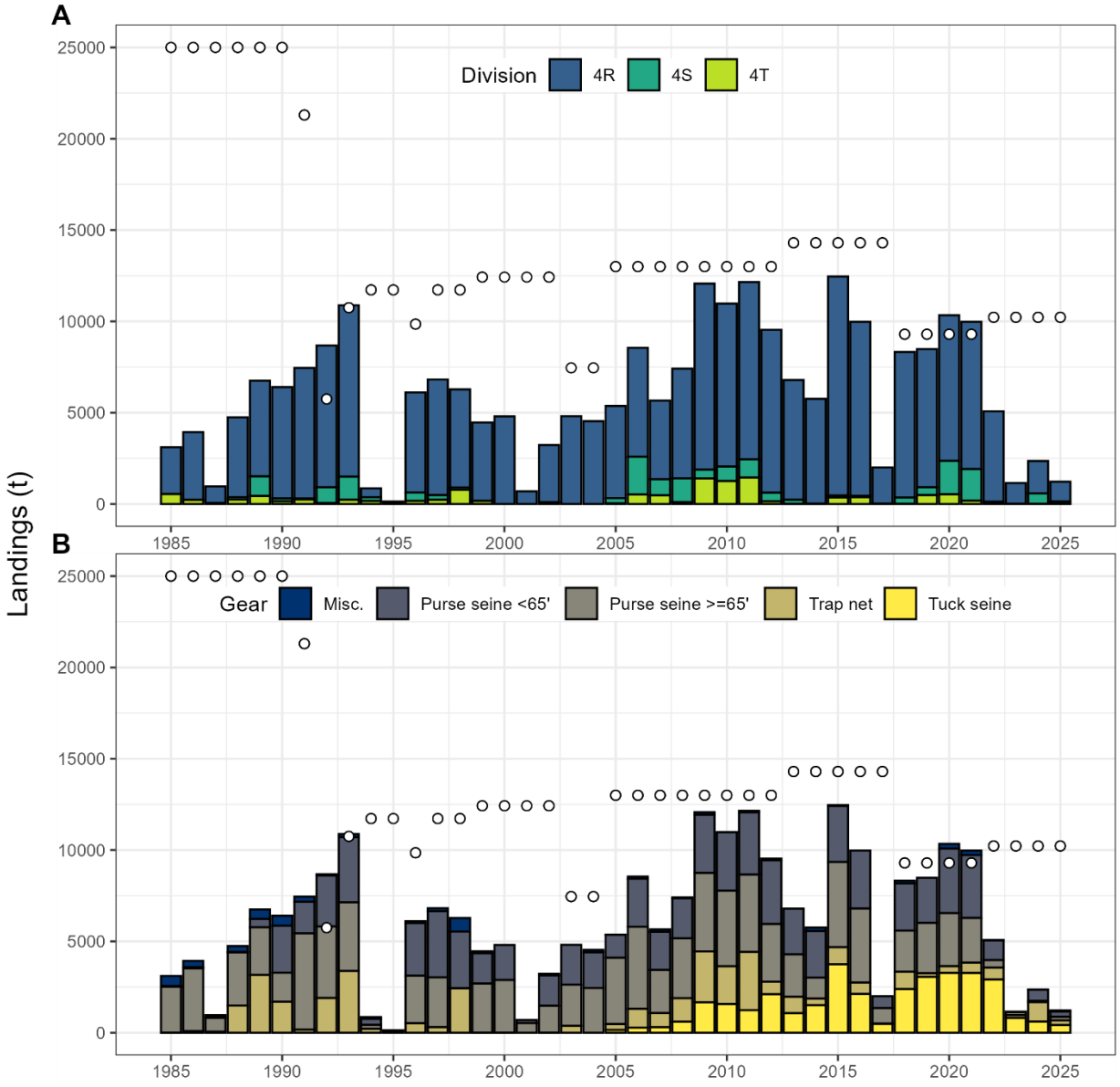


Figure 10: 4RST Capelin landings (t) by A) NAFO and B) main fishing gears for the 1985–2025 period. The white circles represent the annual TACs. Landings for 2021 to 2025 are preliminary. Misc. = Miscellaneous gear types and unknown.



Figure 11: Annual commercial landings (t) of Capelin in NAFO Division 4R for the 1985–2025 period. A) Landings by NAFO unit area. B) Landings by major fishing gear type. C) Landings by existing allocations. Landings for 2021 to 2025 are preliminary. Unit area 4Ru corresponds to landings recorded in Division 4R, but for which the exact unit area is unknown. Misc. = Miscellaneous and unknown.

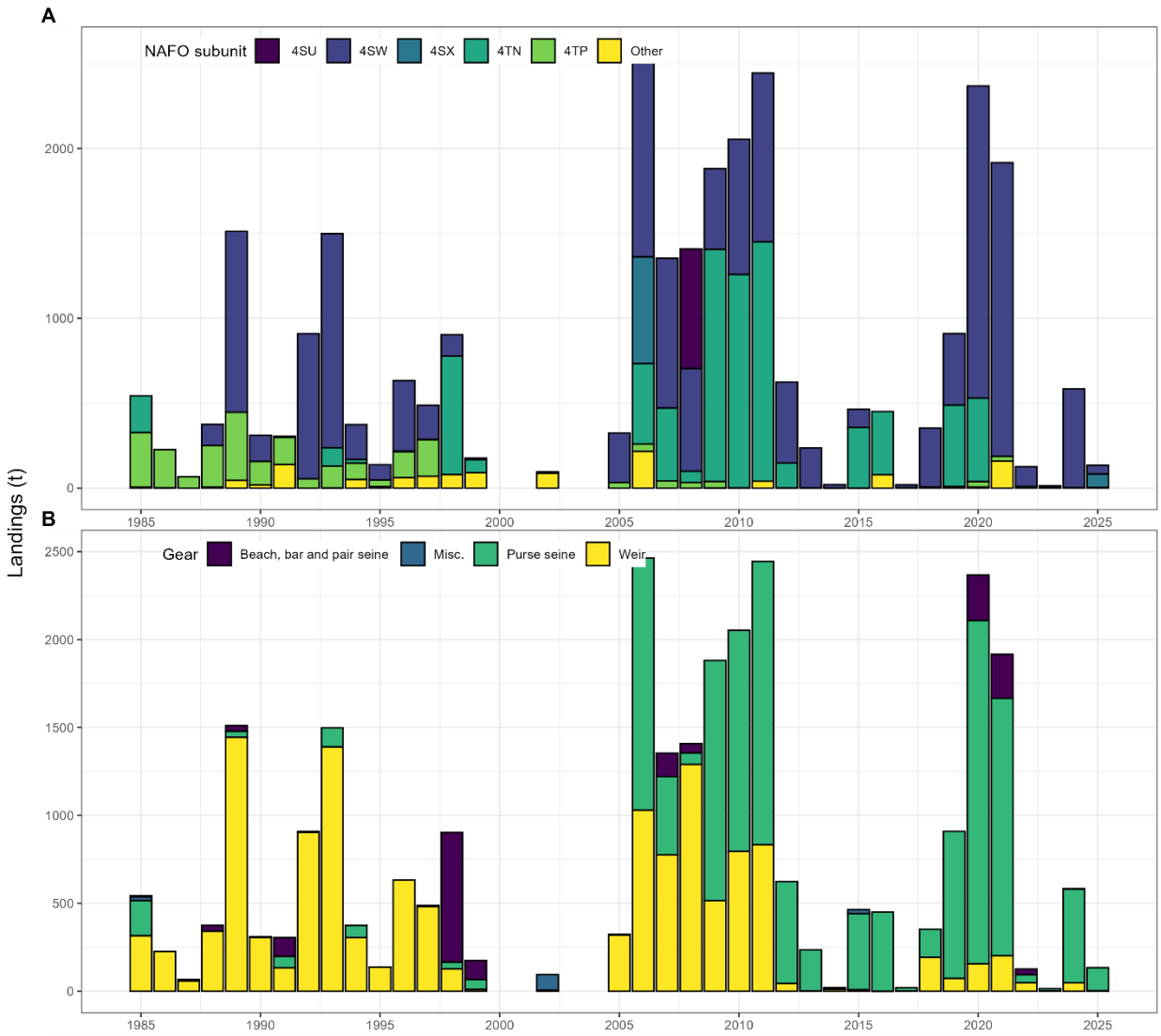


Figure 12: Annual commercial landings (t) of Capelin within NAFO Divisions 4ST for the 1985–2025 period. A) Landings by NAFO unit area. B) Landings by major fishing gear type. Landings for 2021 to 2025 are preliminary. Unit area 4Su corresponds to landings recorded in Division 4R, but for which the exact unit area is unknown.

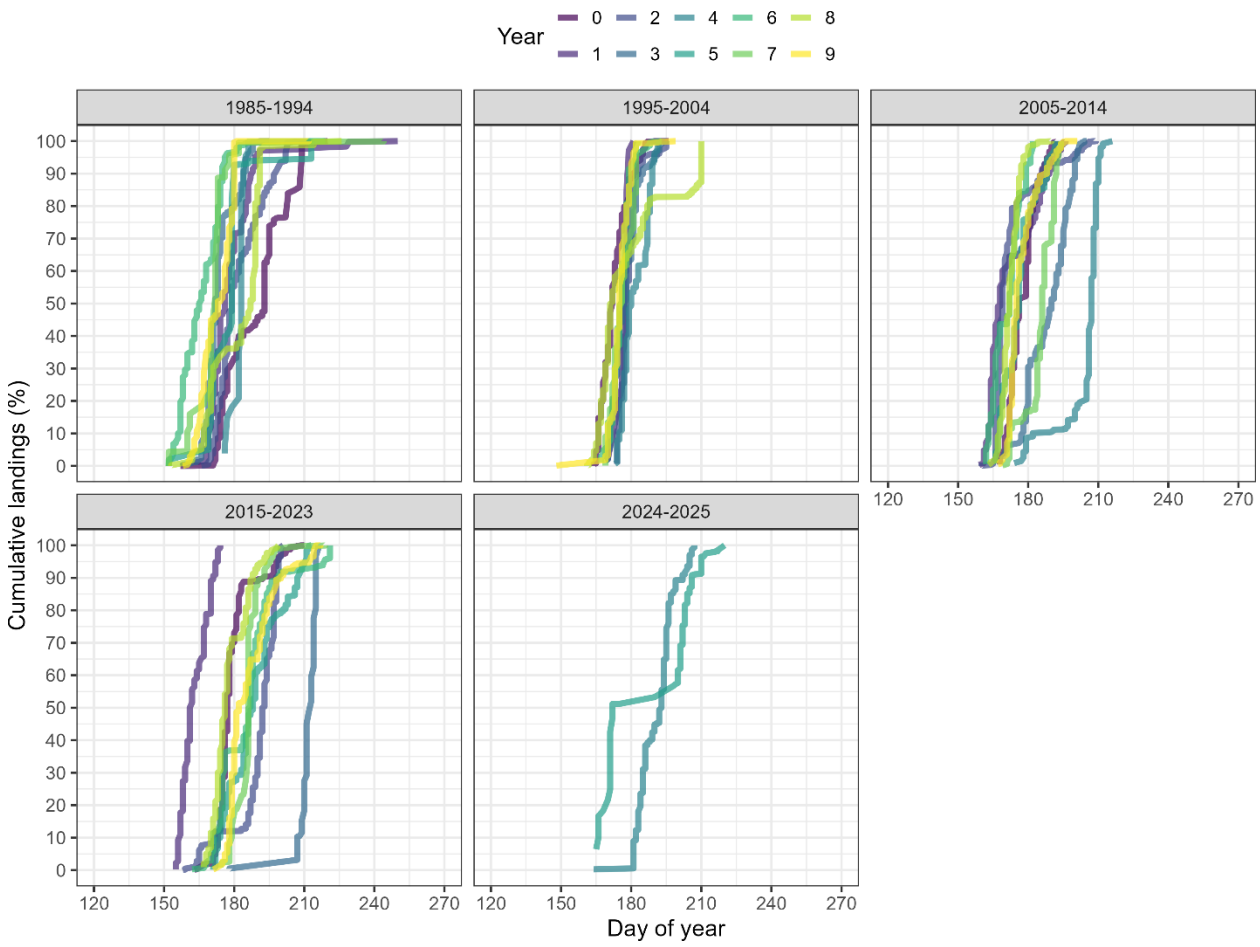


Figure 13: Cumulative distribution functions of Capelin landings (%) in relation to day of the year, for NAFO Division 4R. Line colours progress from violet to yellow based upon the last digit of the year (0–9).

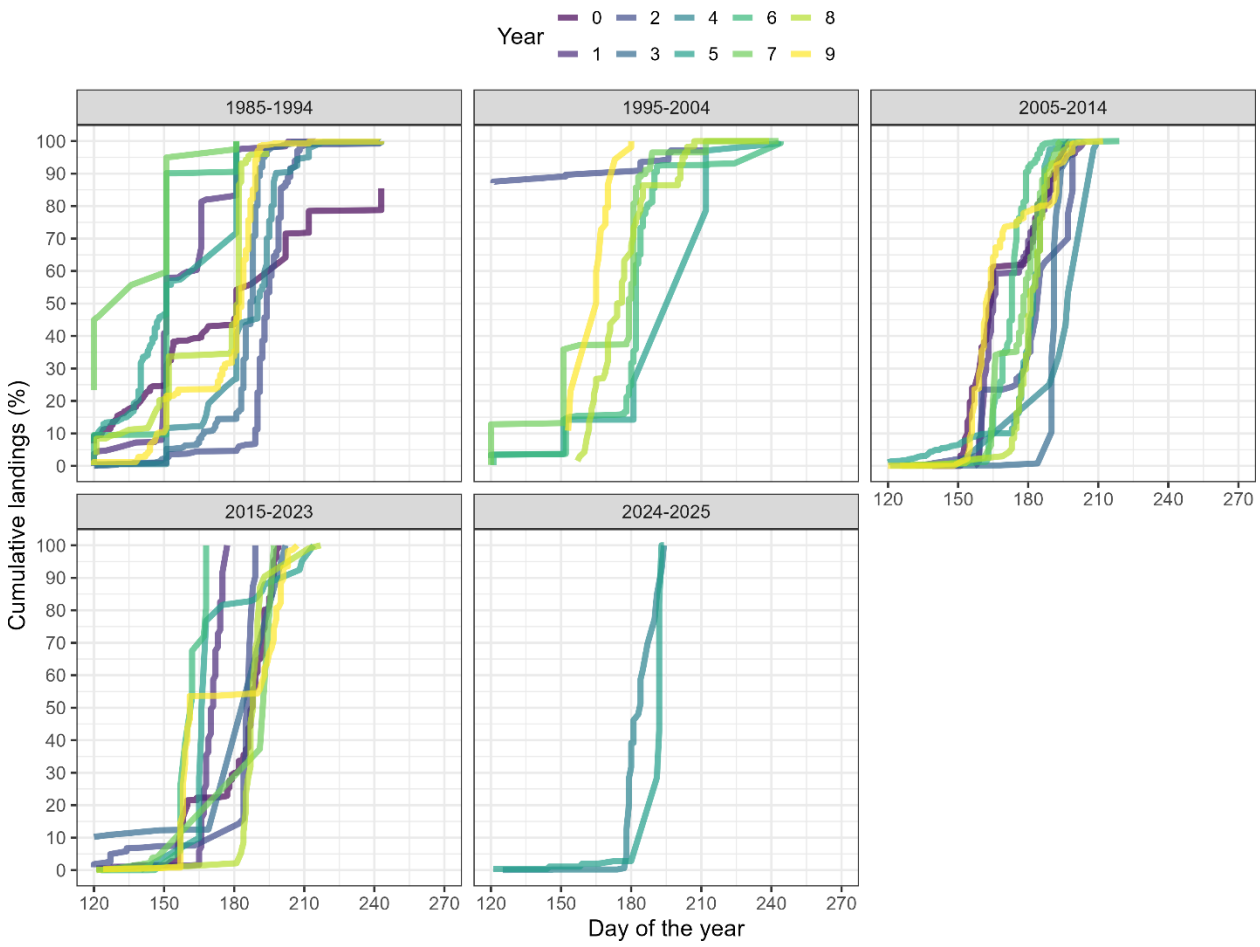


Figure 14: Cumulative distribution functions of Capelin landings (%) in relation to day of the year, for NAFO Divisions 4ST. Line colours progress from violet to yellow based upon the last digit of the year (0–9).

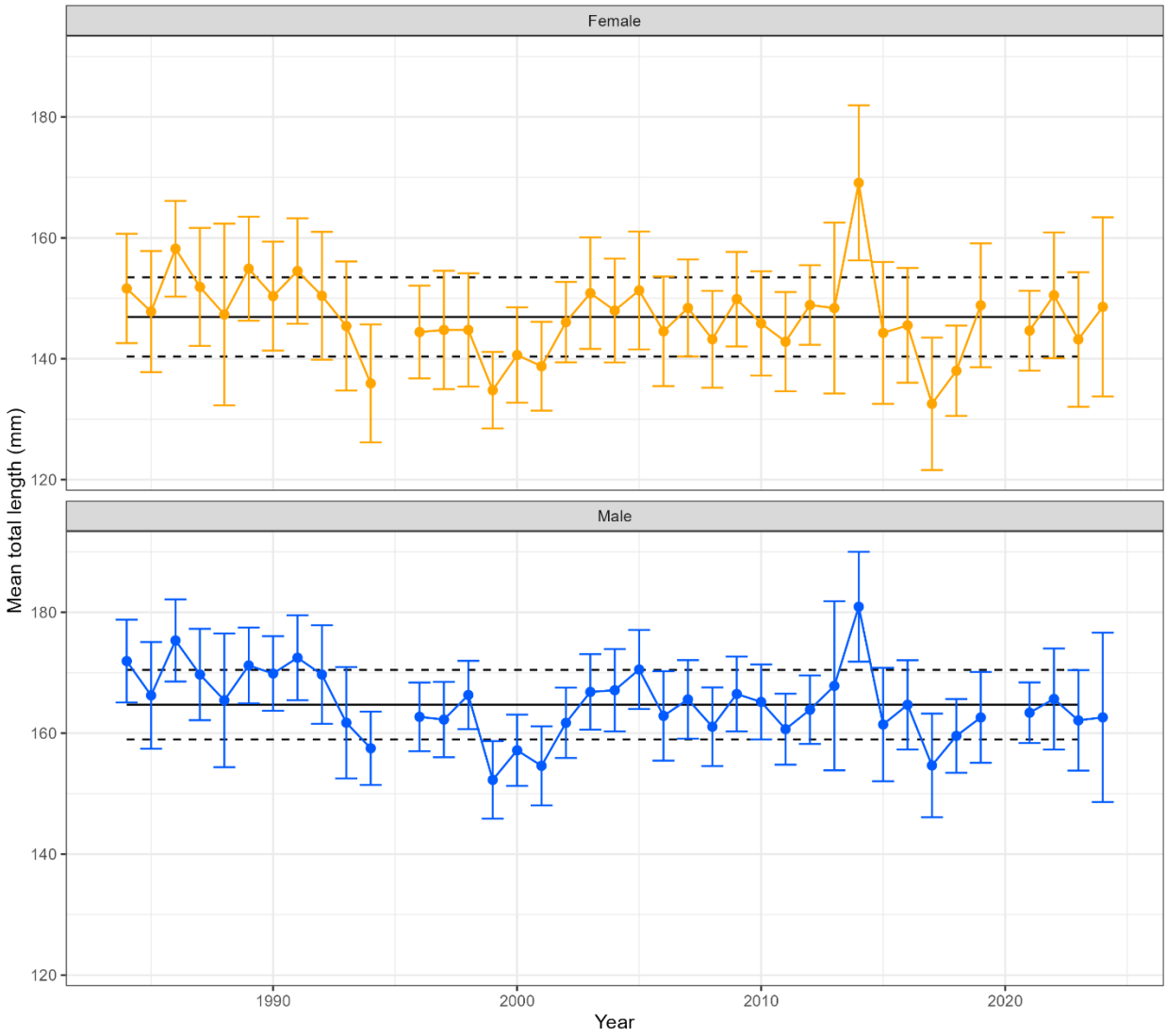


Figure 15: Annual mean total lengths (mm) of female and male Capelin sampled with purse and tuck seines in NAFO Division 4R since 1984 by DFO's port sampling program. The horizontal lines represent the 1984–2024 mean ± 1 S.D. Error bars represent the annual S.D. No sample was collected from 4R in 2025.

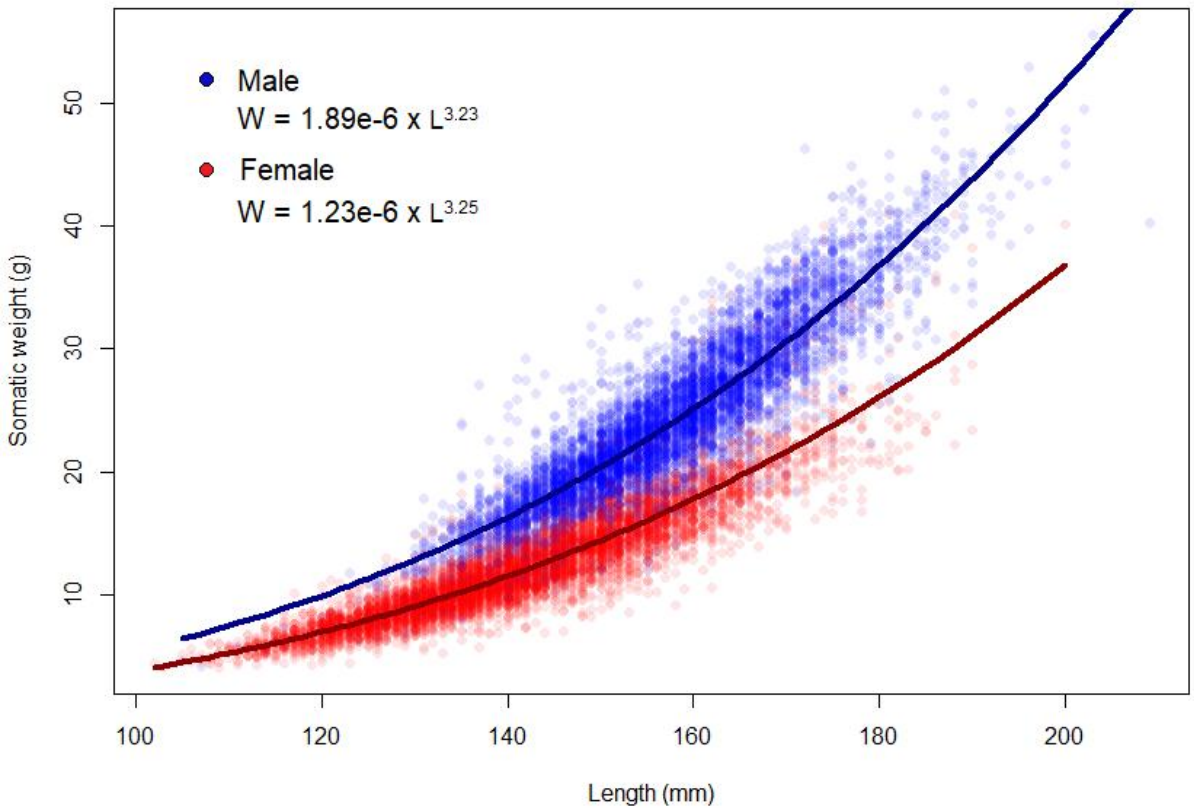


Figure 16: Length-weight relationships of male and female Capelin caught in the commercial fisheries of NAFO Divisions 4RST from 1984 to 2025. Each point corresponds to a specimen for which all three measures (sex, length and weight) were recorded.

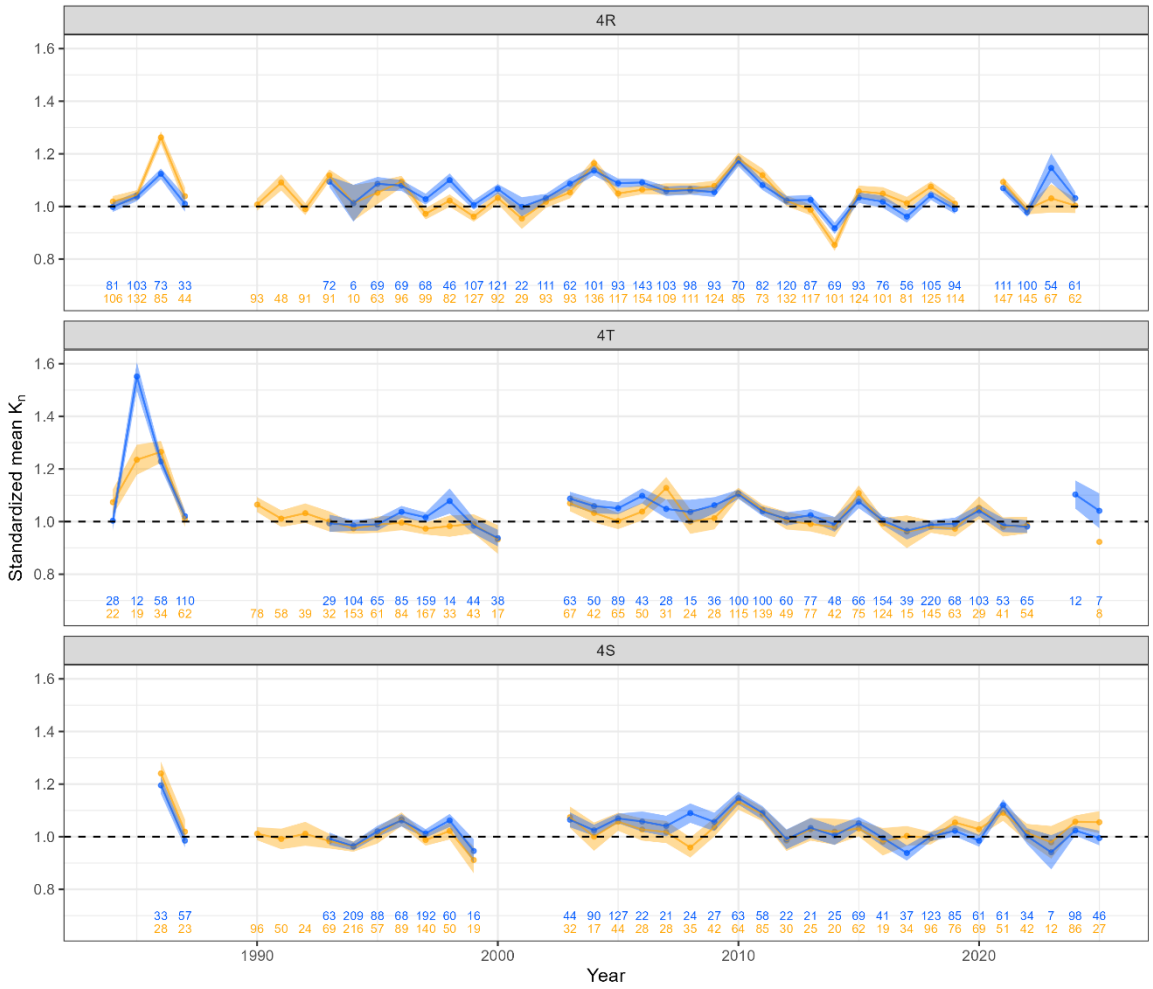


Figure 17: Annual relative body condition (K_n) of male (blue) and female (yellow) Capelin per NAFO Division from biological commercial fishery samples. K_n was standardized for gear (seine, all types) and month (June). The shaded areas represent the 95% confidence intervals. The numbers of fish per sex used in the analysis are indicated on the x-axis.

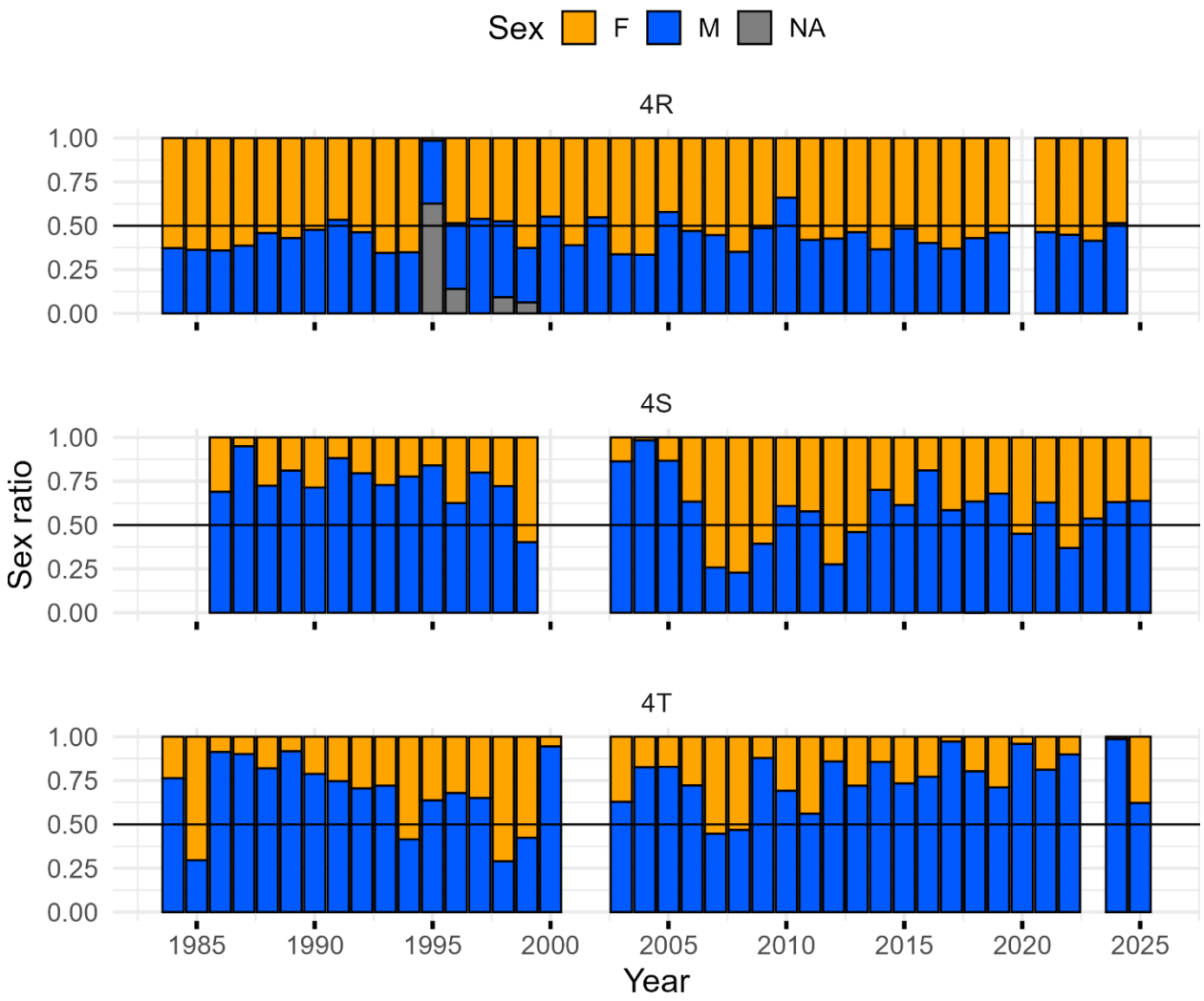


Figure 18: Annual sex ratios of Capelin in the commercial fishery, by NAFO Division. (NA : undetermined sex).

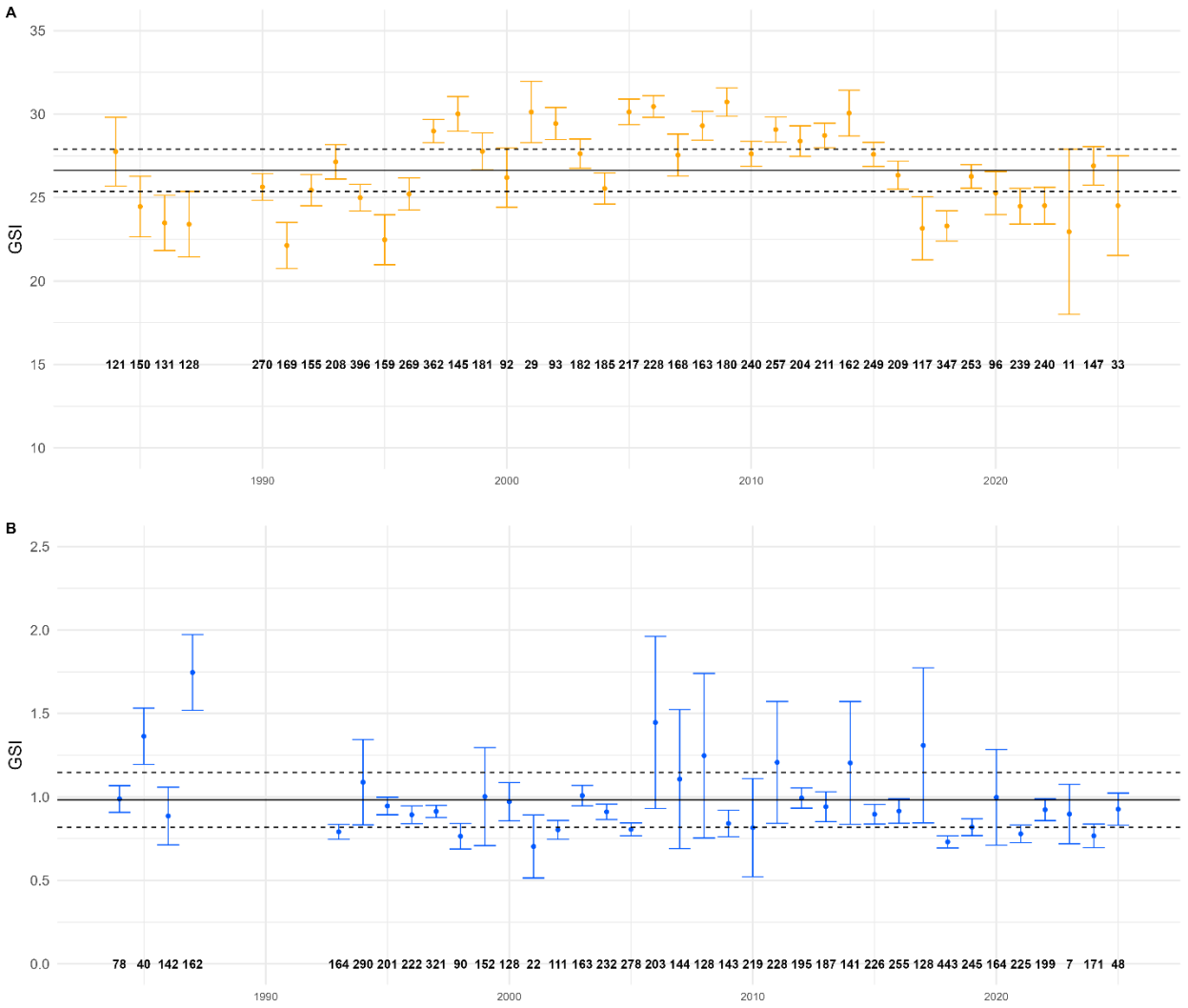


Figure 19: Annual mean (± 95% confidence intervals) gonadosomatic indices (GSI) of female (A) and male (B) Capelin. The horizontal plain and dashed lines represent the 1984-2025 mean and 95% confidence interval respectively.

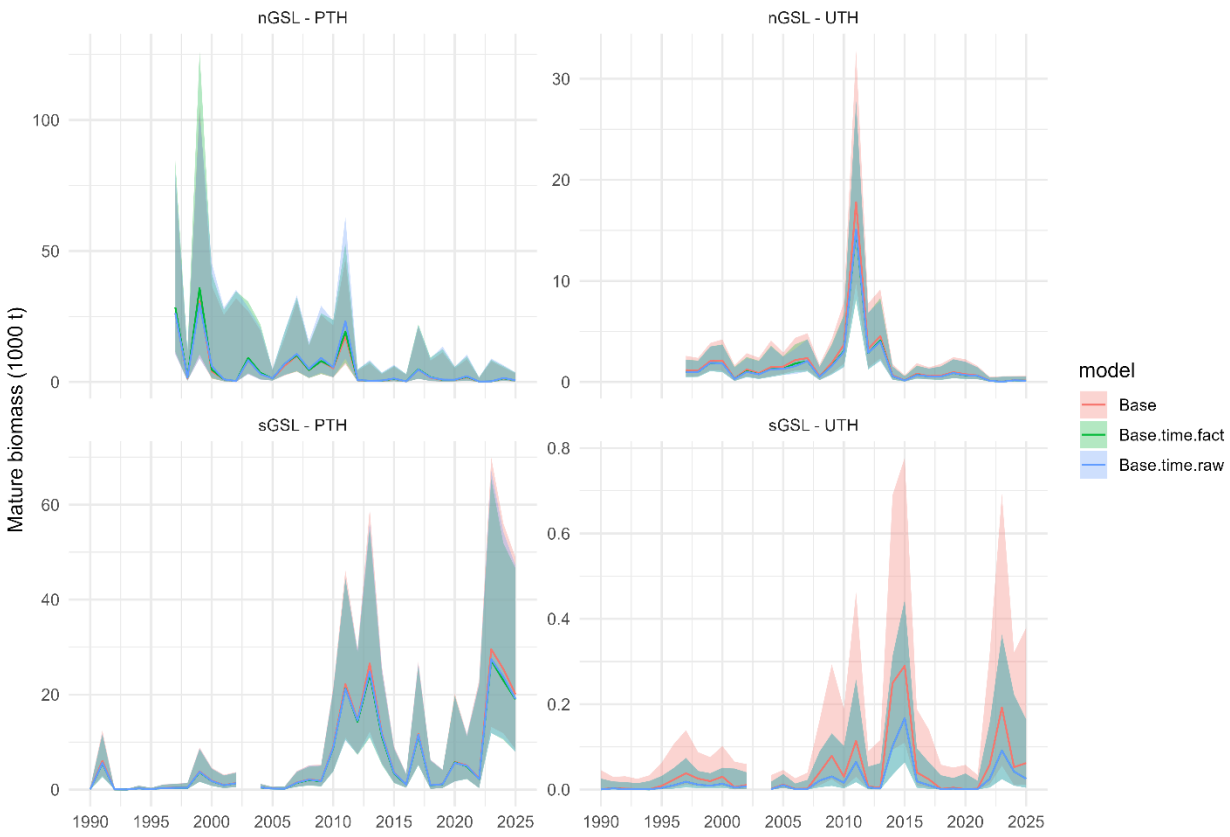


Figure 20: Mature capelin biomass estimated with the design-based approach in the preferred thermal habitat (PTH) and the unfavorable thermal habitat (UTH) in the northern (nGSL) and southern (sGSL) Gulf of St. Lawrence using the initial model configuration (Base) described in Chamberland et al. (2022), and standardizing the catches for the time of the day at 10 AM (Base.time.raw) and the category "day" (Base.time.fact). The shaded areas represent the 95% confidence intervals.

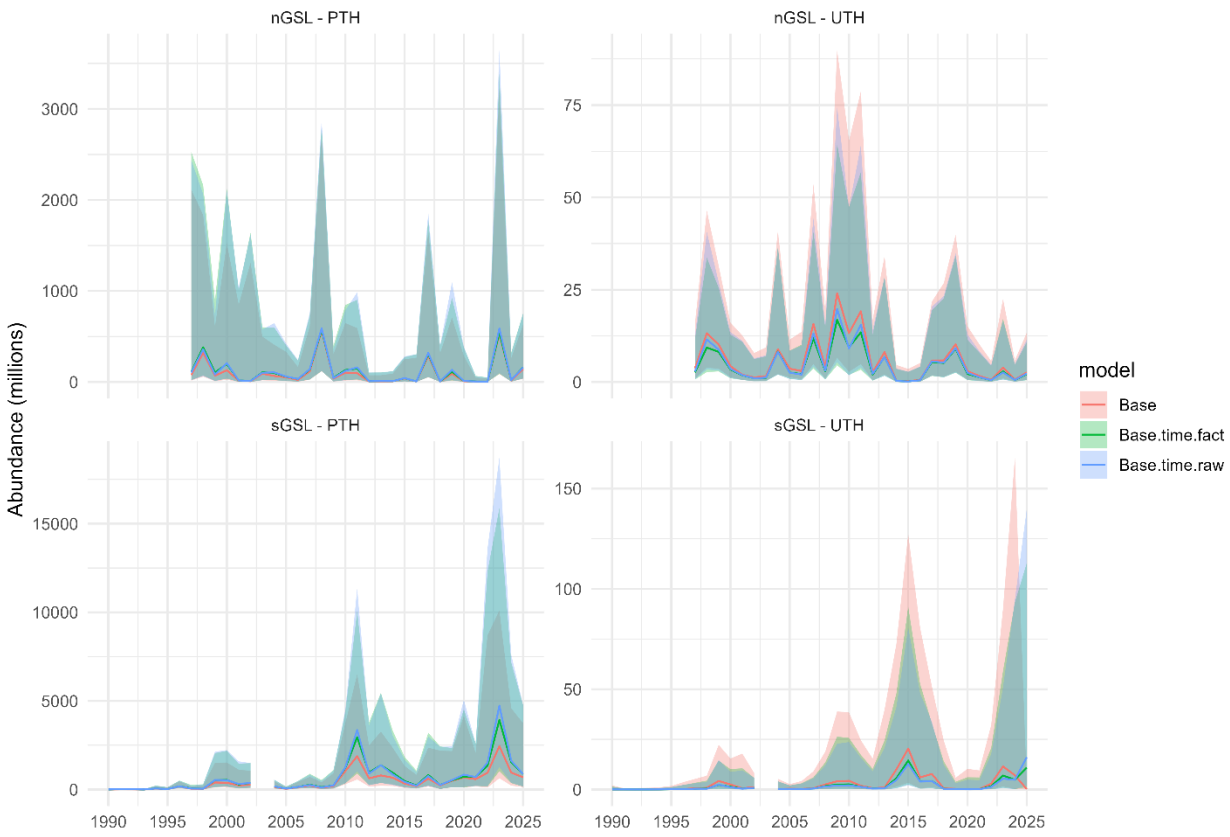


Figure 21: Age-1 Capelin abundance estimated with the design-based approach in the preferred thermal habitat (PTH) and the unfavorable thermal habitat (UTH) in the northern (nGSL) and southern (sGSL) Gulf of St. Lawrence using the initial model configuration (Base) described in Chamberland et al. (2022), and standardizing the catches for the time of the day at 10 AM (Base.time.raw) and the category "day" (Base.time.fact). The shaded areas represent the 95% confidence intervals.

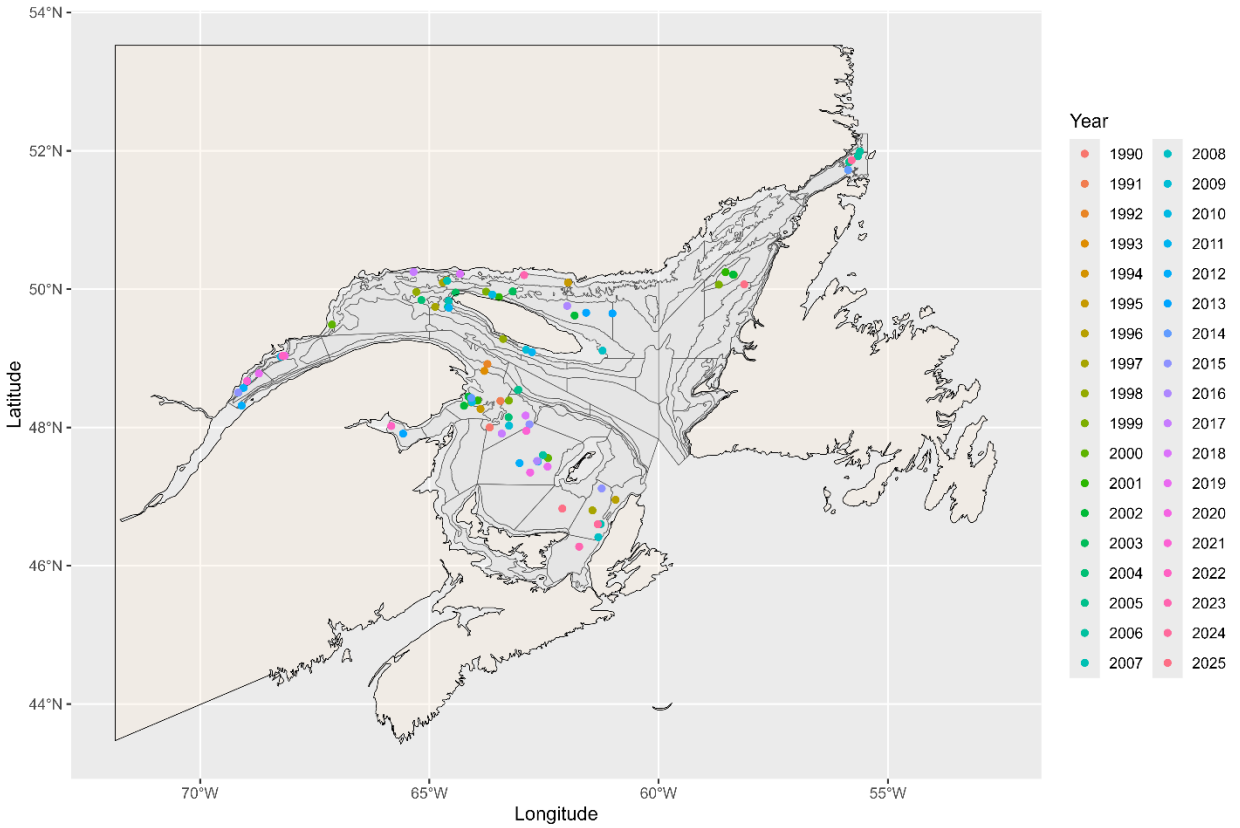


Figure 22: Location of mature Capelin catch weight greater than the 99 percentile of annual positive catch in the northern and southern Gulf of St. Lawrence bottom trawl surveys. The polygons delineated by solid black lines represent the different strata sampled during the bottom trawl surveys in the northern and southern Gulf of St. Lawrence.

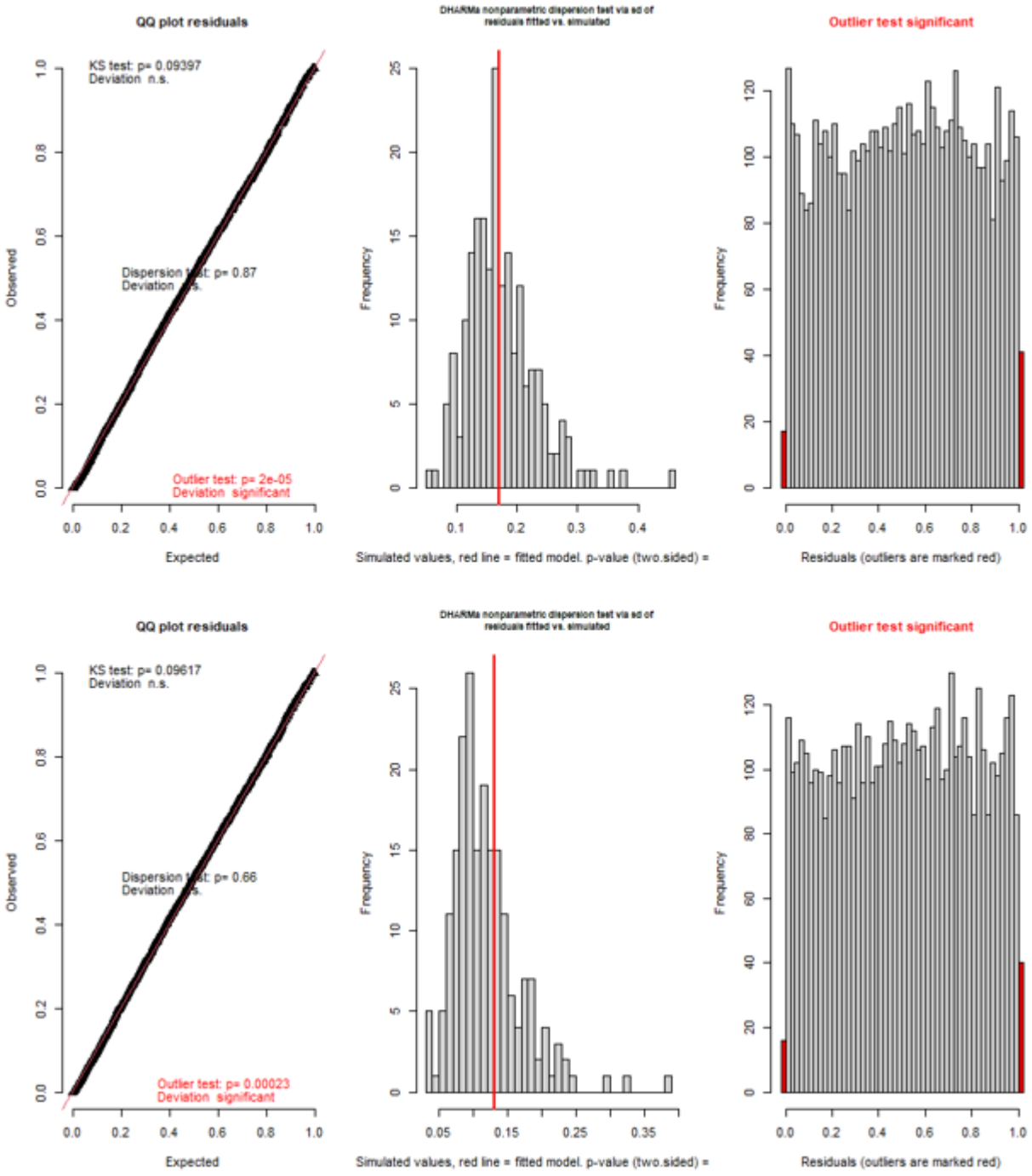


Figure 23: DHARMa diagnostic plots for the models used to fit the Capelin mature biomass in the northern Gulf of St. Lawrence and considering temporal effect of year as a random effect drawn from a normal distribution (upper panels) or as an independent factor (lower panels).

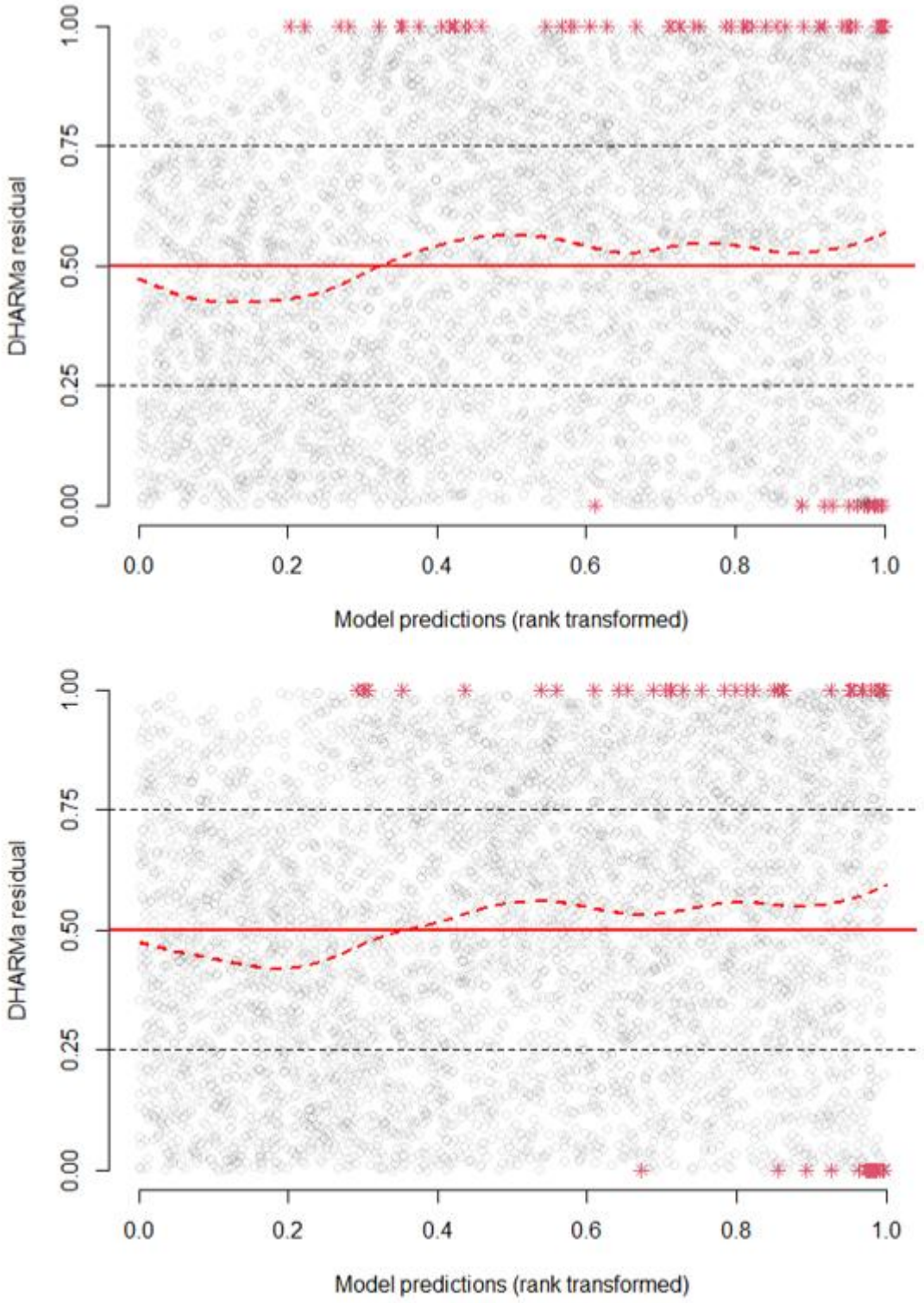


Figure 24: DHARMa residual plots for the models used to fit the Capelin mature biomass in the northern Gulf of St. Lawrence and considering temporal effect of year as a random effect drawn from a normal distribution (upper panel) or as a categorical factor (lower panel).

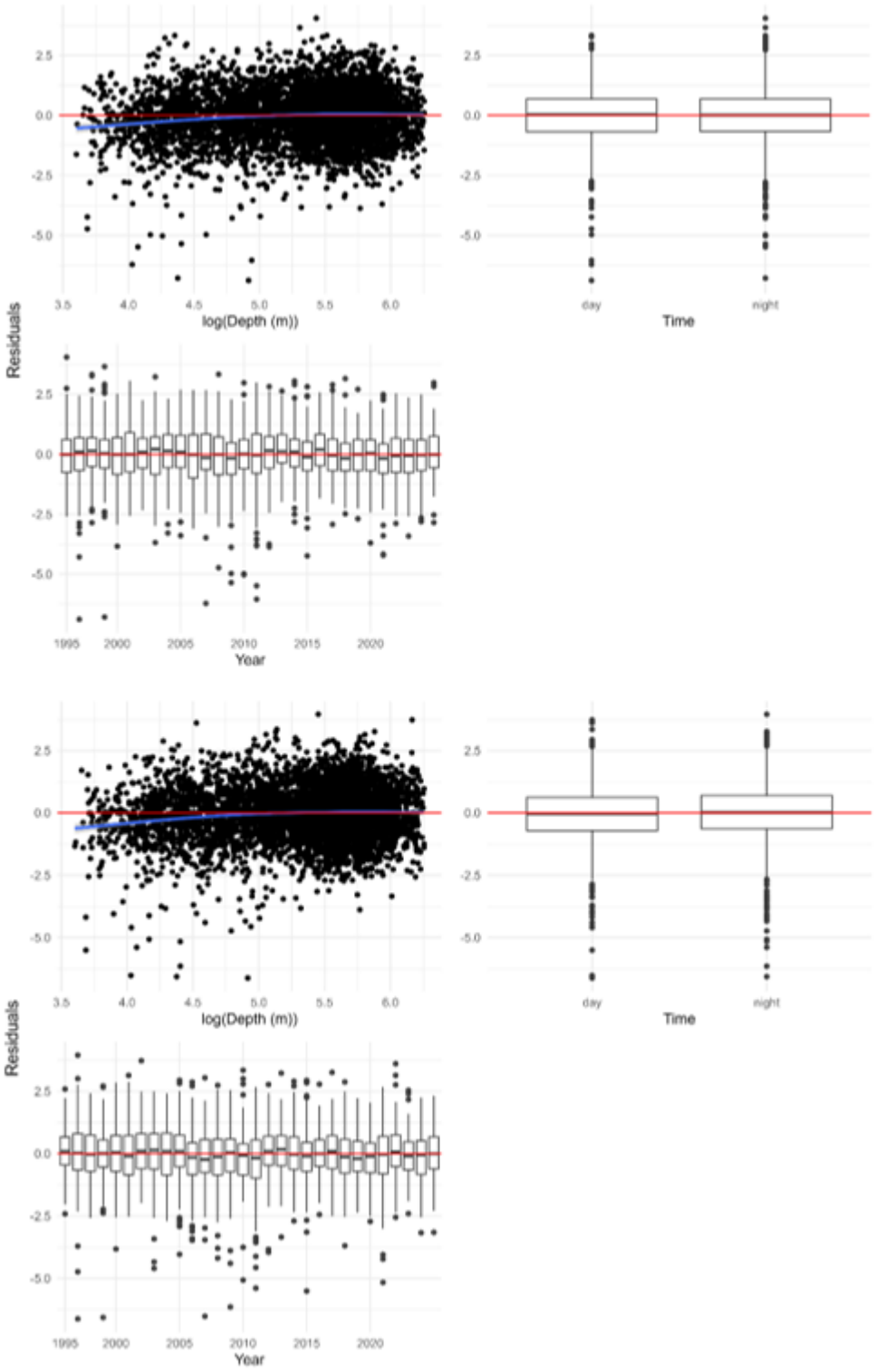


Figure 25: Quantile residuals in relation to the different predictive variables (log transformed depth, time of the day in categories and year) used to fit mature capelin biomass in northern Gulf of St. Lawrence considering temporal effect of year as a random effect drawn from a normal distribution (upper panels) or as a categorical factor (lower panels). The horizontal red line indicates a value of 0, and the blue line represents a smoother distribution of residual values.

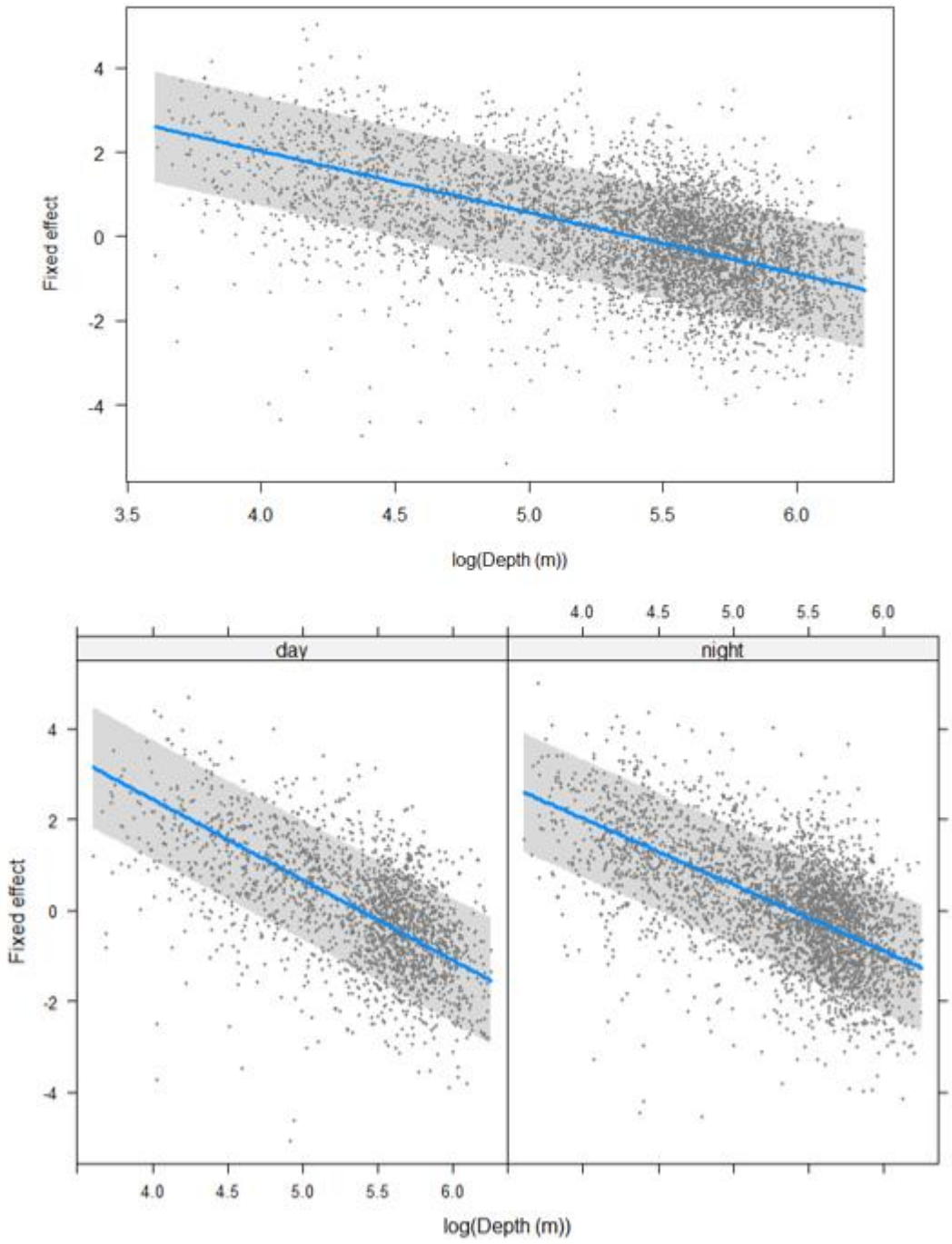


Figure 26: Conditional mean (blue line) and 95% confidence interval (shaded area) of the log-transformed depth (upper panel) and the interaction of the log-transformed depth and the time of the day (lower panels) effects on the mature Capelin weight caught in the northern Gulf of St. Lawrence bottom trawl survey estimated with the sdmTMB selected model.

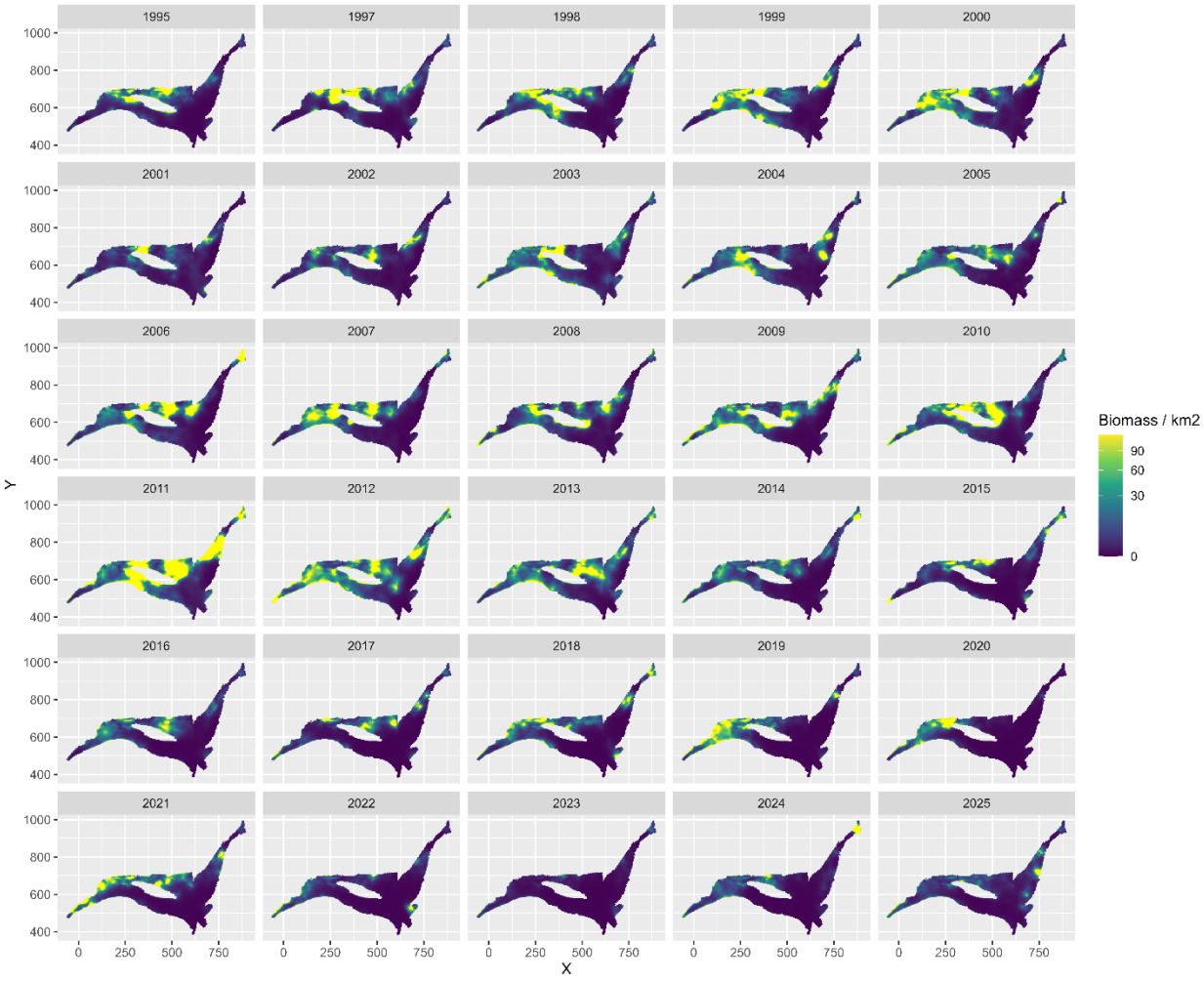


Figure 27: Annual maps of mature capelin biomass (kg) in the northern Gulf of St. Lawrence predicted with the selected sdmTMB model.

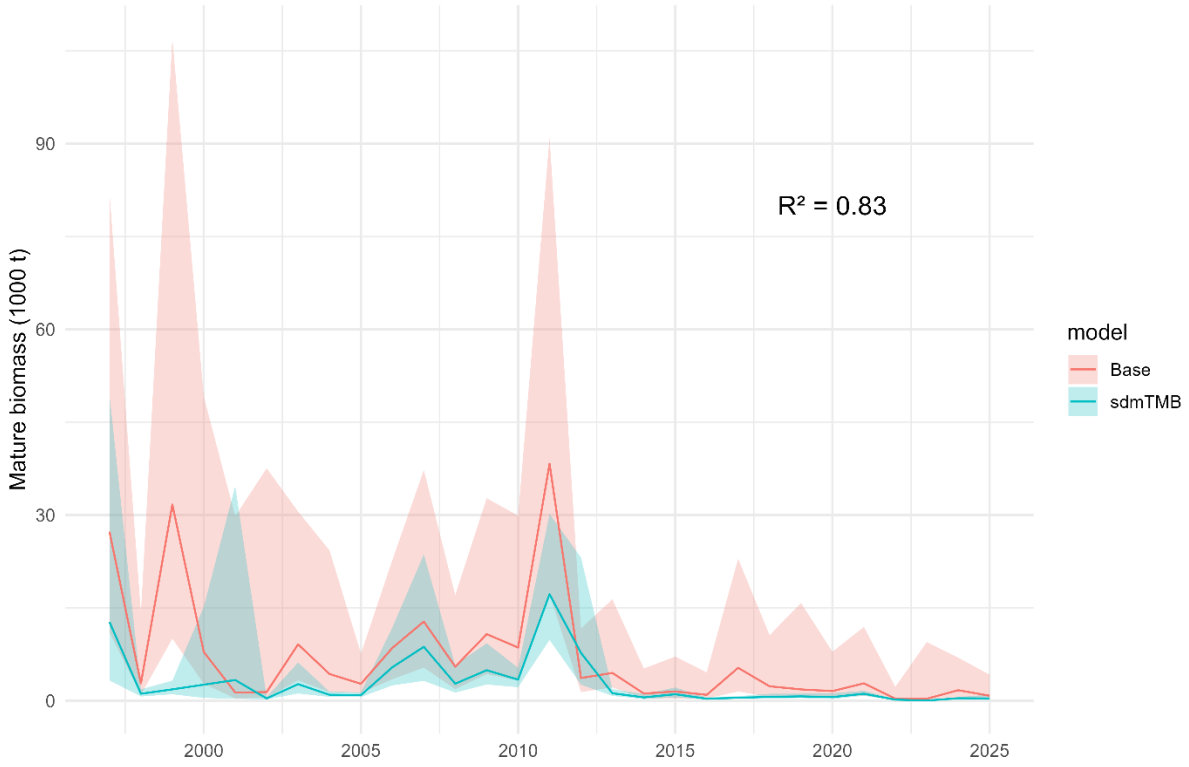


Figure 28: Mature capelin biomass estimated using design-based (red) and sdmTMB (blue) approaches in the northern Gulf of St. Lawrence, with R² values from Pearson correlations based on annual comparisons. Shaded areas represent 95% confidence intervals.

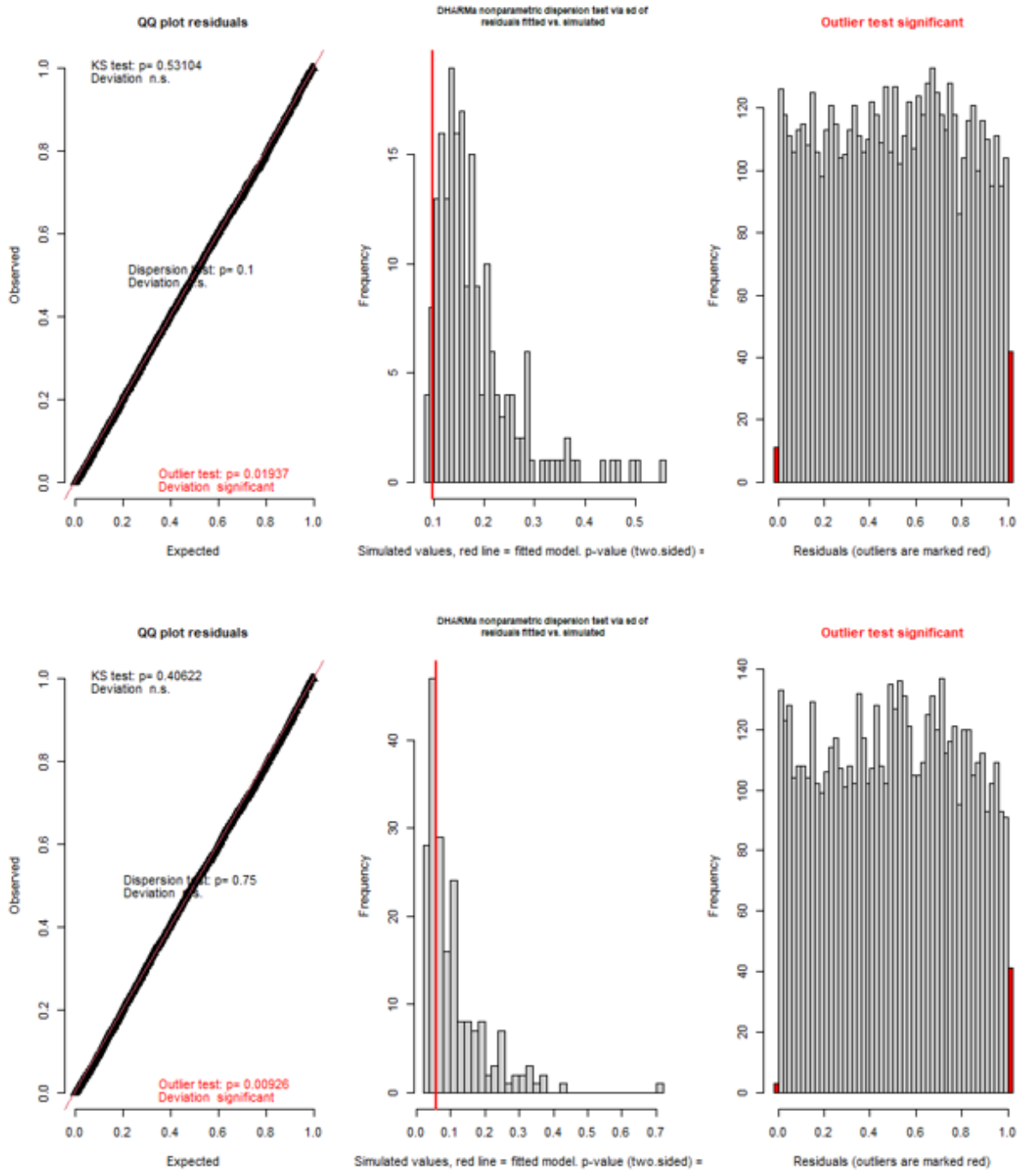


Figure 29: DHARMa diagnostic plots for the models used to fit the Capelin mature biomass in the southern Gulf of St. Lawrence and considering temporal effect of year as a random effect drawn from a normal distribution (upper panels) or as a categorical factor (lower panels).

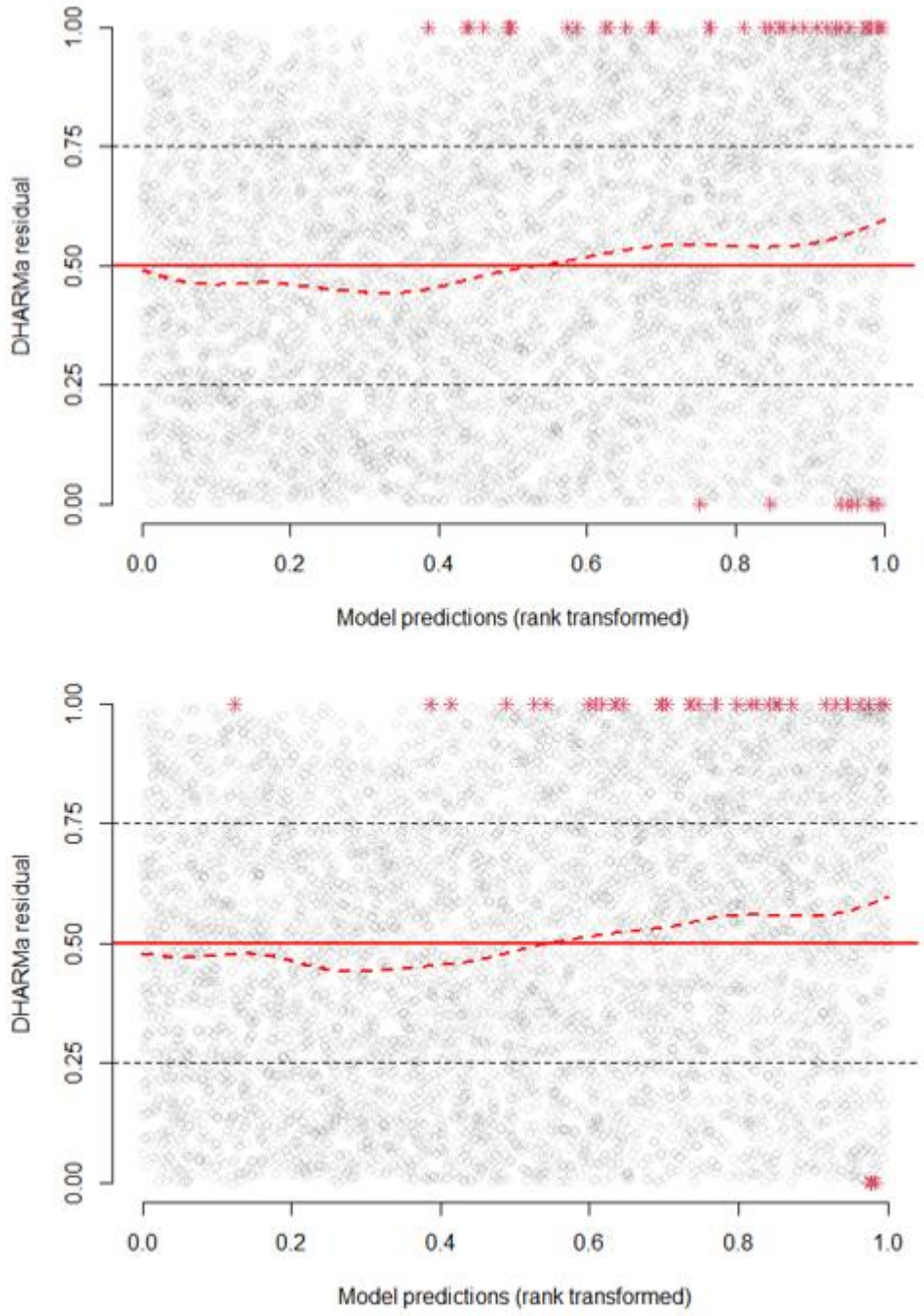


Figure 30: DHARMa residual plots for the models used to fit the Capelin mature biomass in the southern Gulf of St. Lawrence and considering temporal effect of year as a random effect drawn from a normal distribution (upper panel) or as a categorical factor (lower panel).

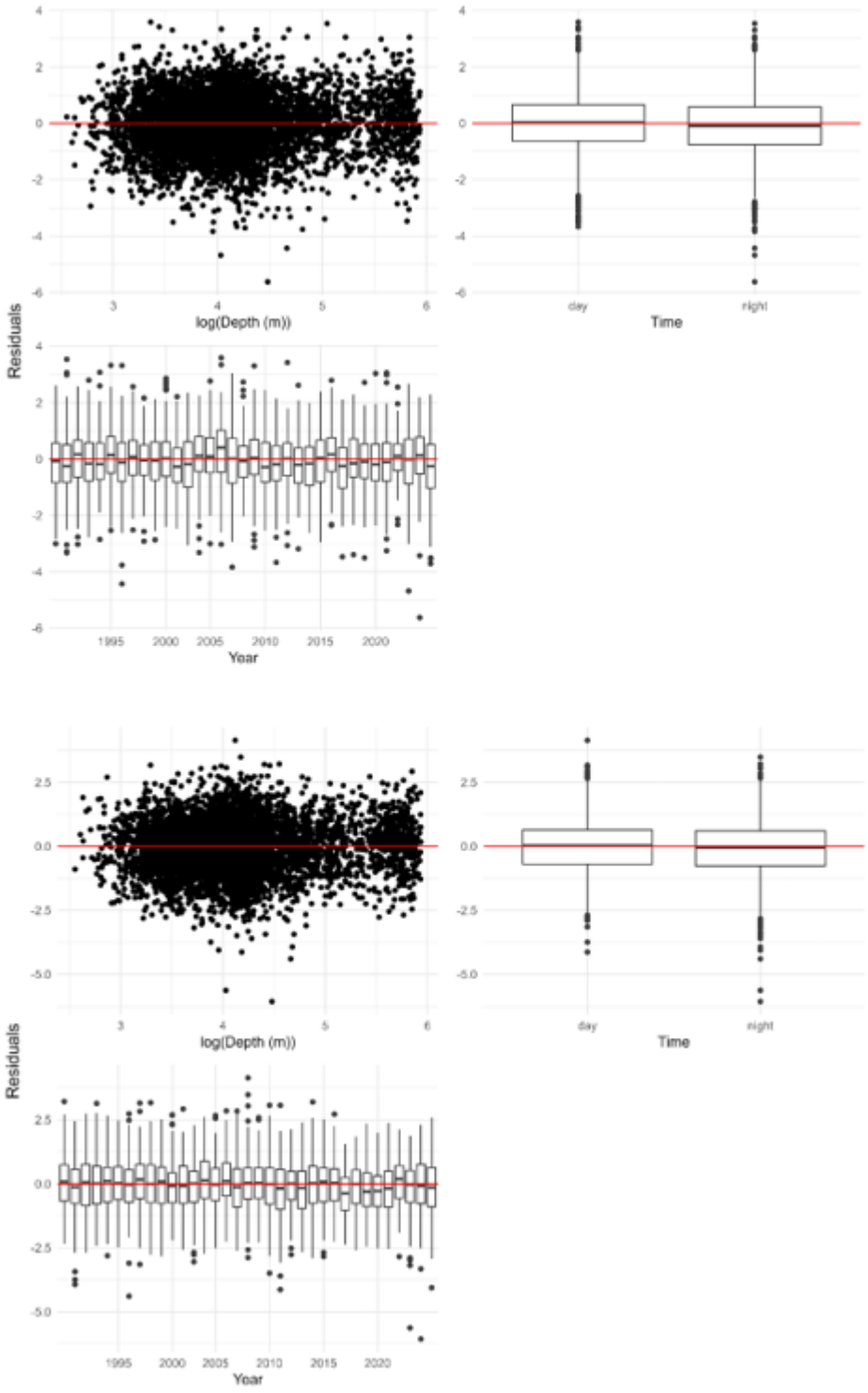


Figure 31: Quantile residuals in relation to the different predictive variables (log transformed depth, time of the day in categories and year) used to fit mature capelin biomass in southern Gulf of St. Lawrence considering temporal effect of year as a random effect drawn from a normal distribution (upper panels) and as a categorical factor (lower panels). The horizontal red line indicates a value of 0, and the blue line represents a smoother distribution of residual values.

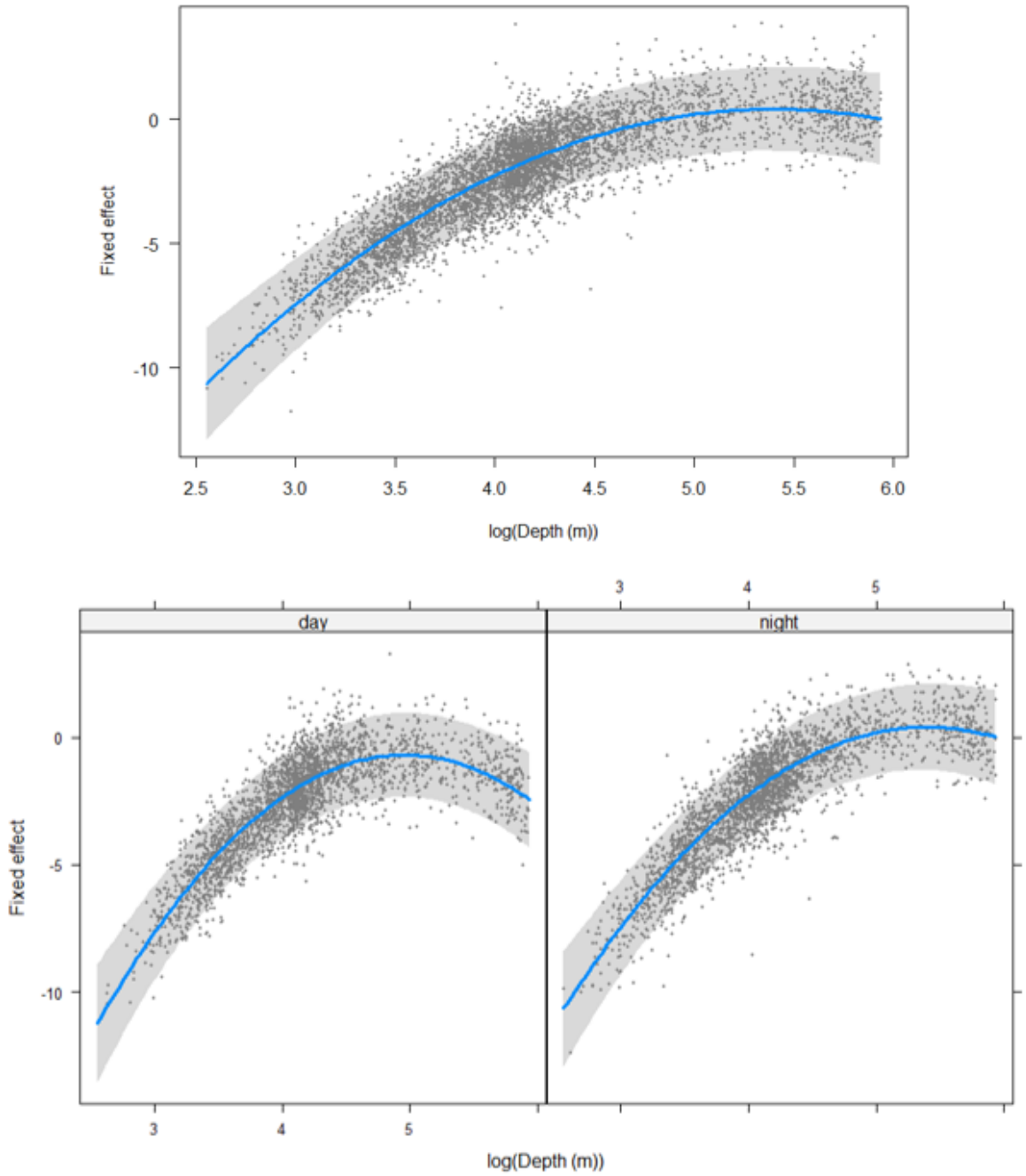


Figure 32: Conditional mean (blue line) and 95% confidence interval (shaded area) of the log-transformed depth (upper panel) and the interaction of the log-transformed depth and the time of the day (lower panels) effects on the mature Capelin weight caught in the southern Gulf of St. Lawrence bottom trawl survey estimated with the sdmTMB selected model.

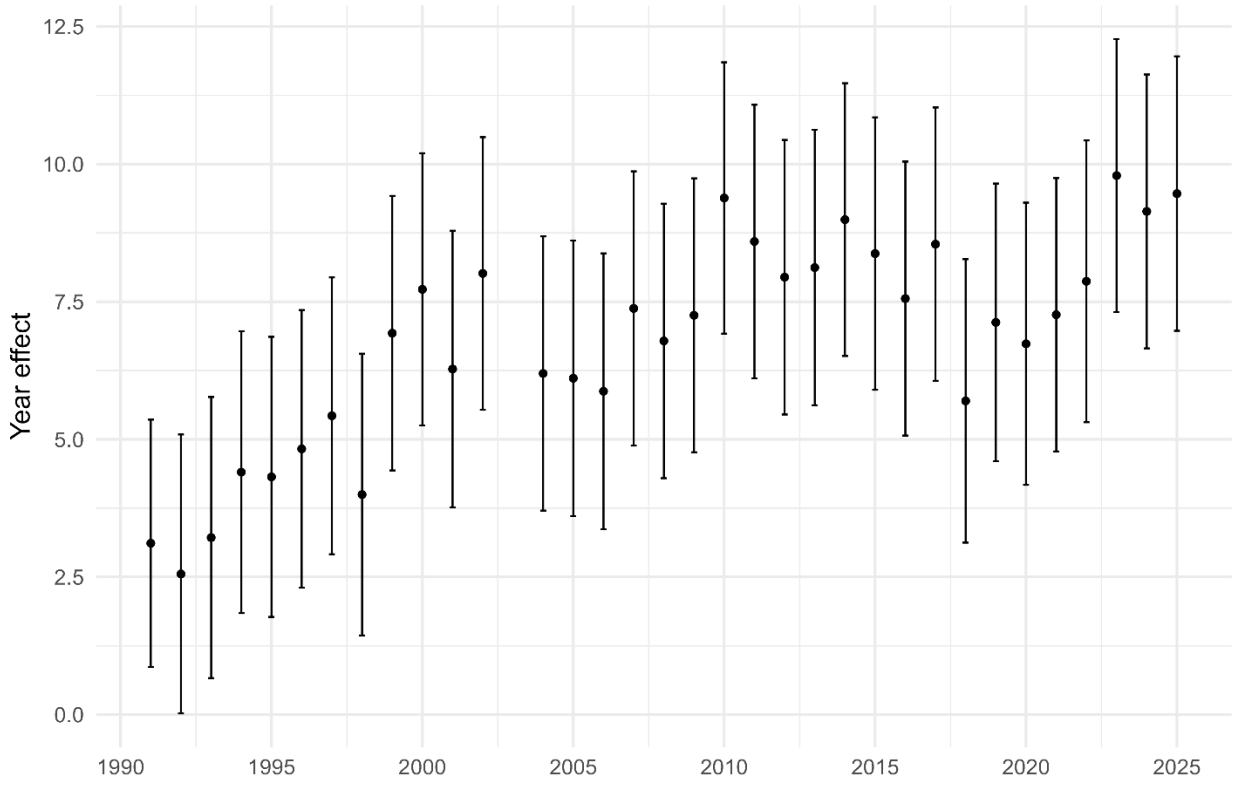


Figure 33: Coefficients (points) and confidence intervals (vertical lines) of temporal effect of year as a categorical factor from the selected model used to fit mature Capelin biomass in the southern Gulf of St. Lawrence.



Figure 34 : Annual maps of mature capelin biomass values predicted with the sdmTMB selected model and 1x1 km² depth grid in the southern Gulf of St. Lawrence.

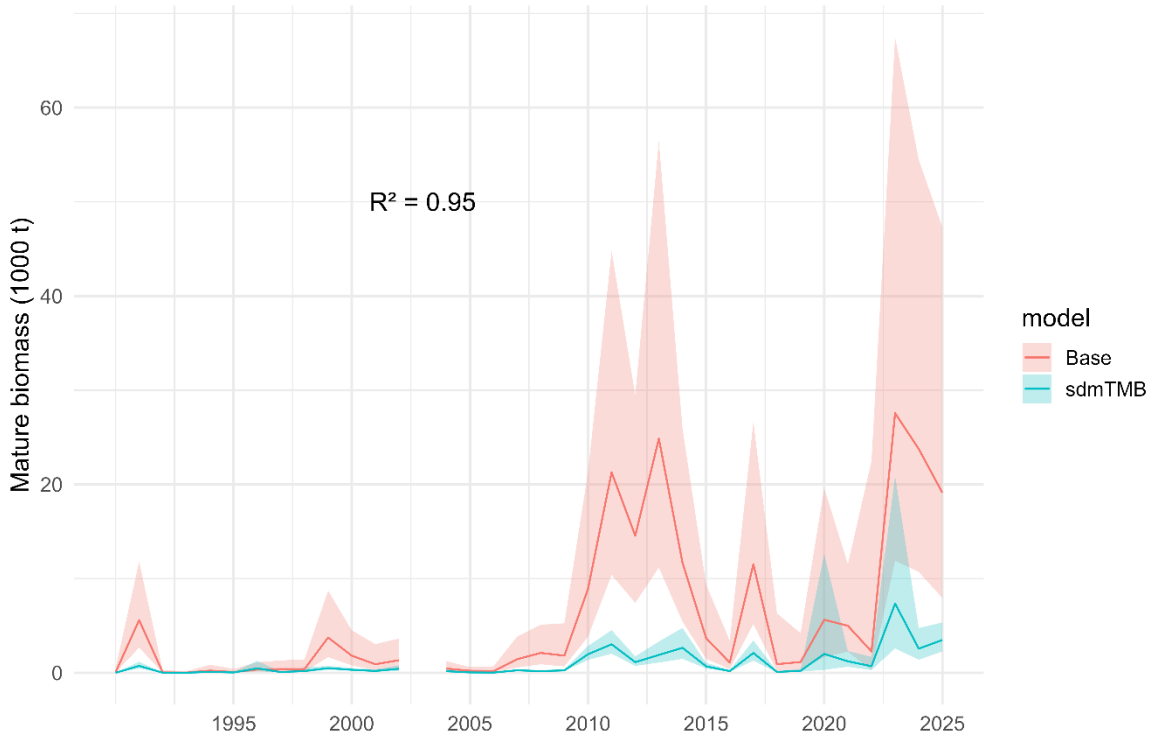


Figure 35: Mature capelin biomass estimated using design-based (red) and sdmTMB (blue) approaches in the southern Gulf of St. Lawrence, with R² values from Pearson correlations based on annual comparisons. Shaded areas represent 95% confidence intervals.

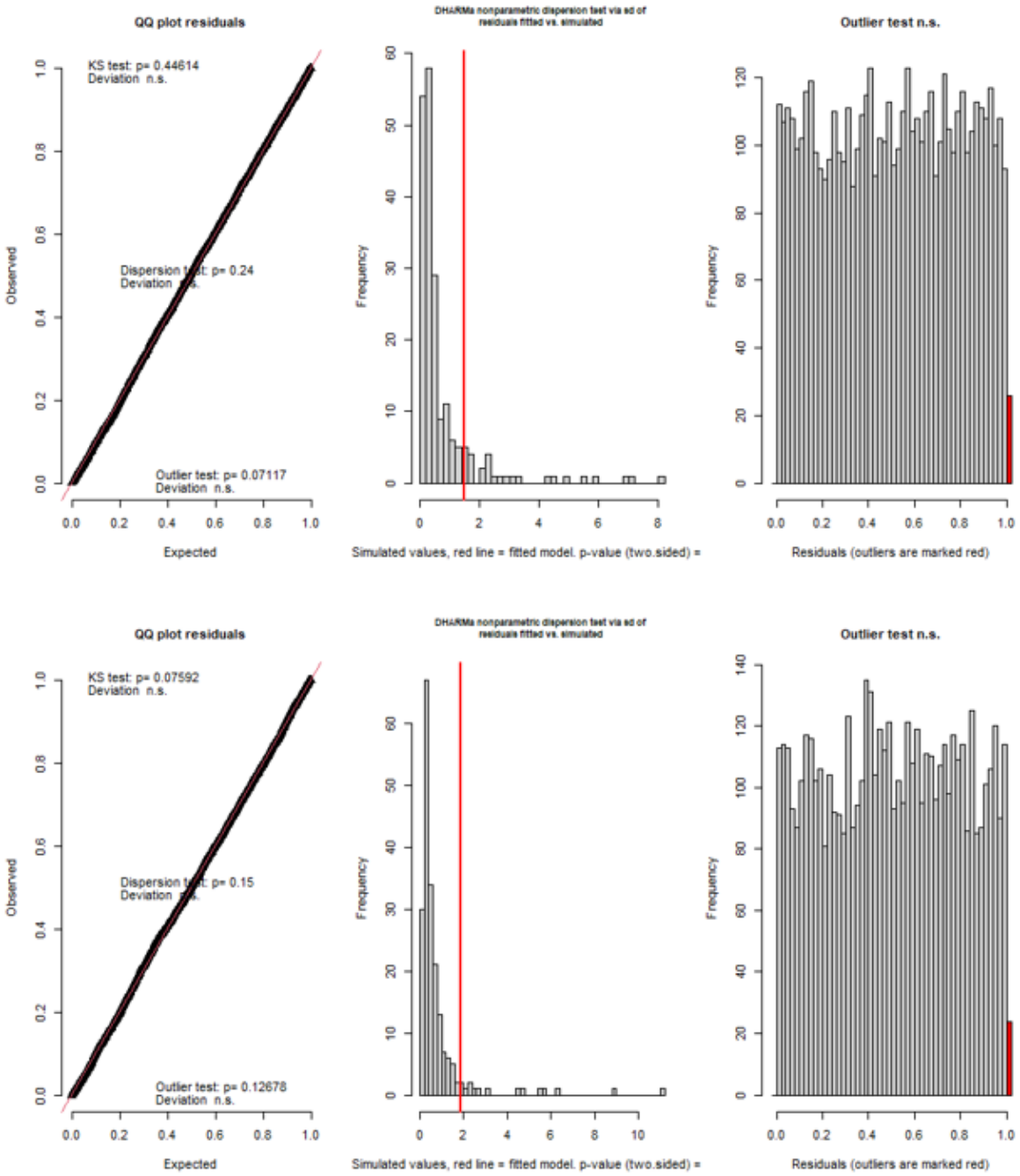


Figure 36: DHARMa diagnostic plots for the models used to fit age-1 Capelin in the northern Gulf of St. Lawrence and considering temporal effect of year as a random effect drawn from a normal distribution (upper panels) or as a categorical factor (lower panels).

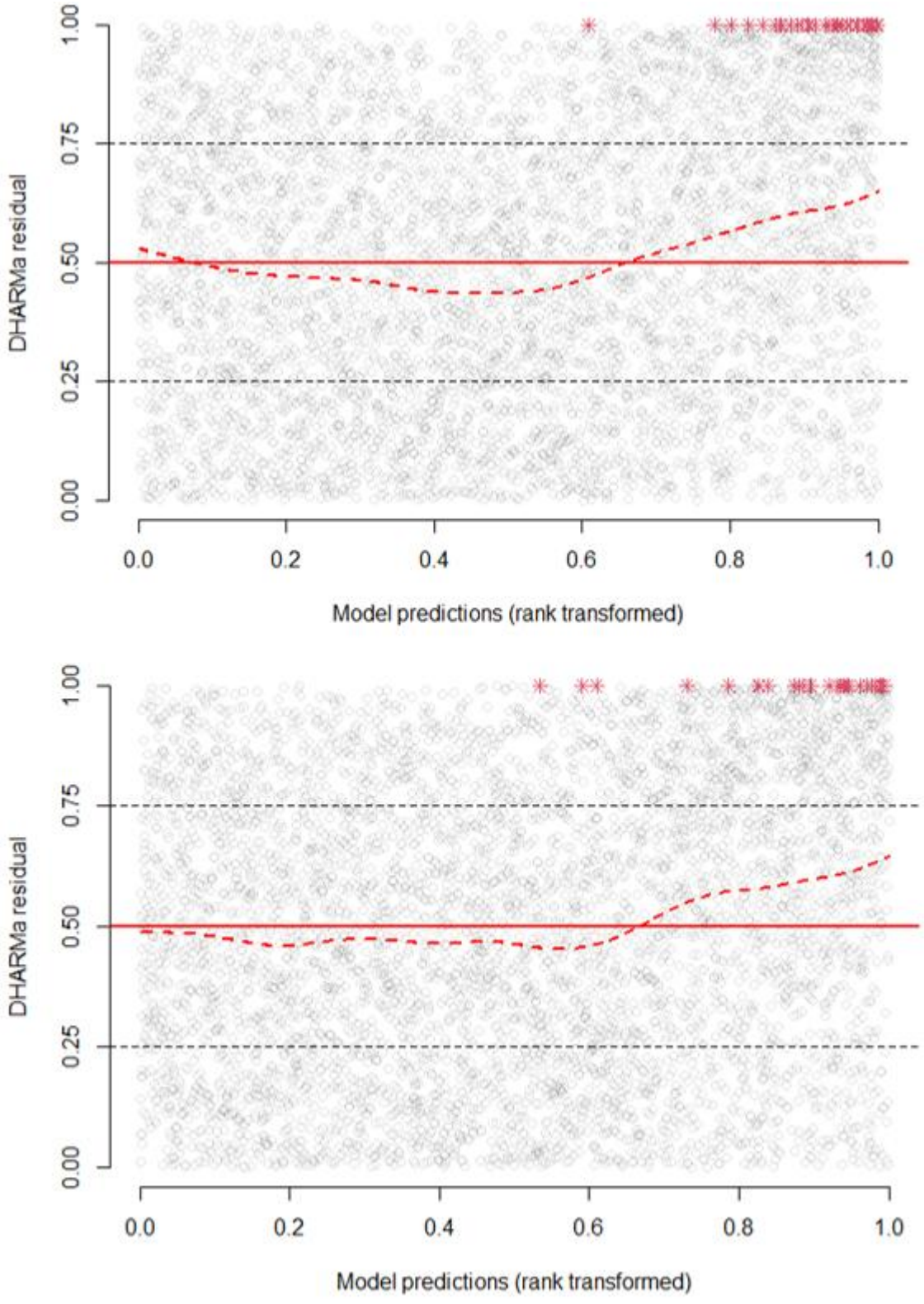


Figure 37: DHARMa residual plots for the models used to fit age-1 Capelin in the northern Gulf of St. Lawrence and considering temporal effect of year as a random effect drawn from a normal distribution (upper panel) or as a categorical factor (lower panel).

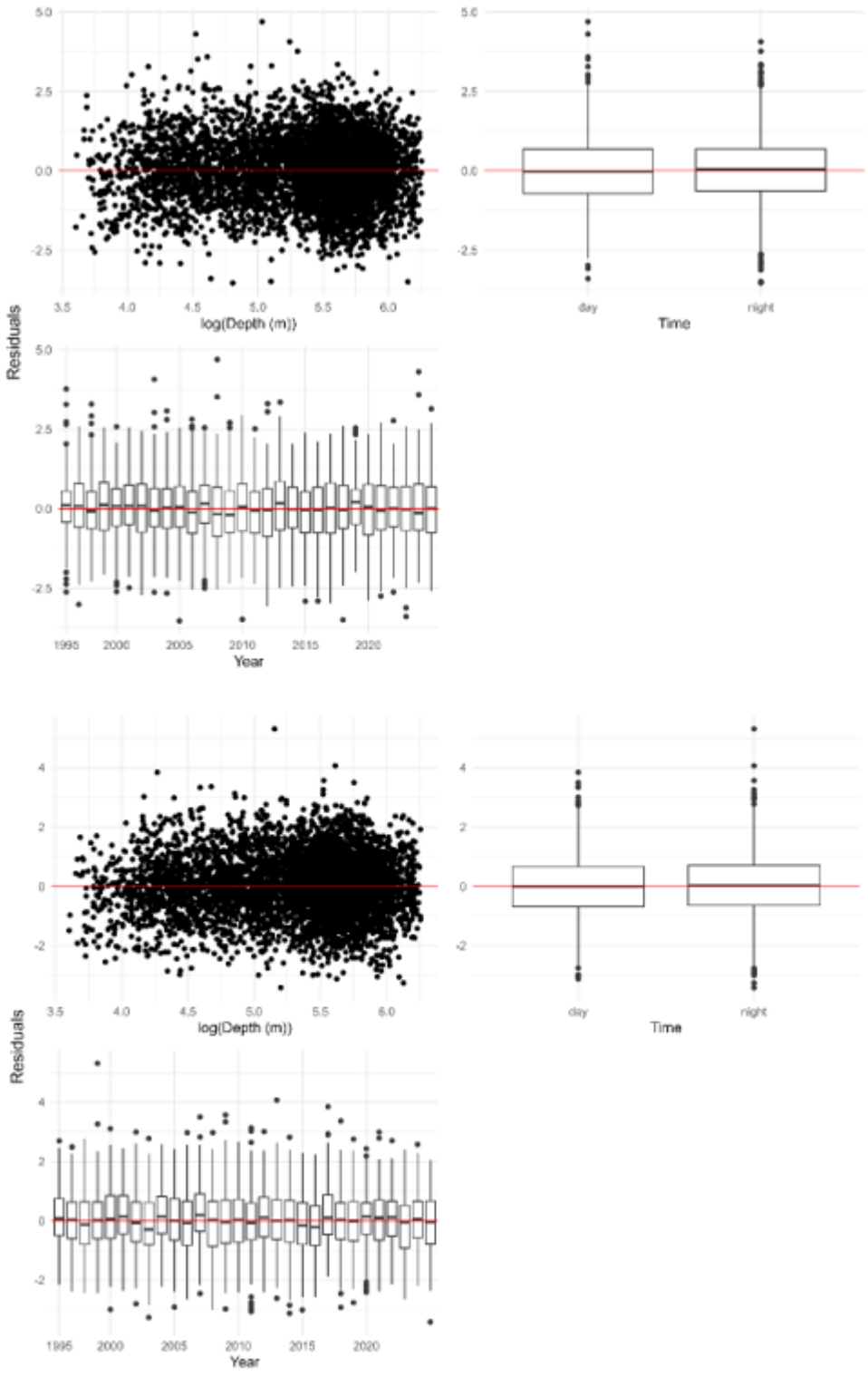


Figure 38: Quantile residuals in relation to the different predictive variables (log transformed depth, time of the day in categories and year) used to fit age-1 Capelin in the northern Gulf of St. Lawrence considering temporal effect of year as a random effect drawn from a normal distribution (upper panels) and as a categorical factor (lower panels). The horizontal red line indicates a value of 0, and the blue line represents a smoother distribution of residual values.

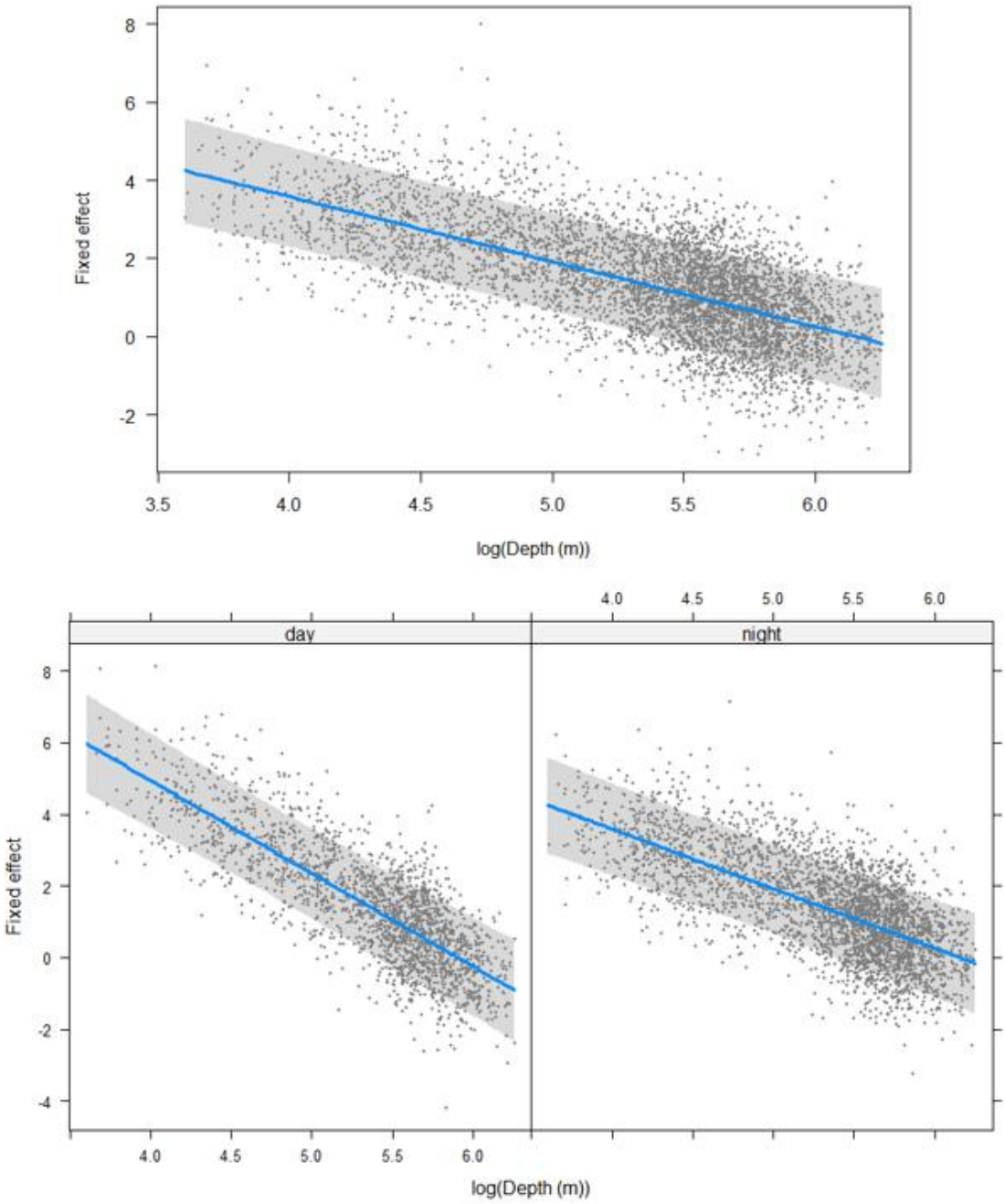


Figure 39: Conditional mean (blue line) and 95% confidence interval (shaded area) of the log-transformed depth (upper panel) and the interaction of the log-transformed depth and the time of the day (lower panels) effects on the age-1 Capelin number caught in the northern Gulf of St. Lawrence bottom trawl survey estimated with the sdmTMB selected model.

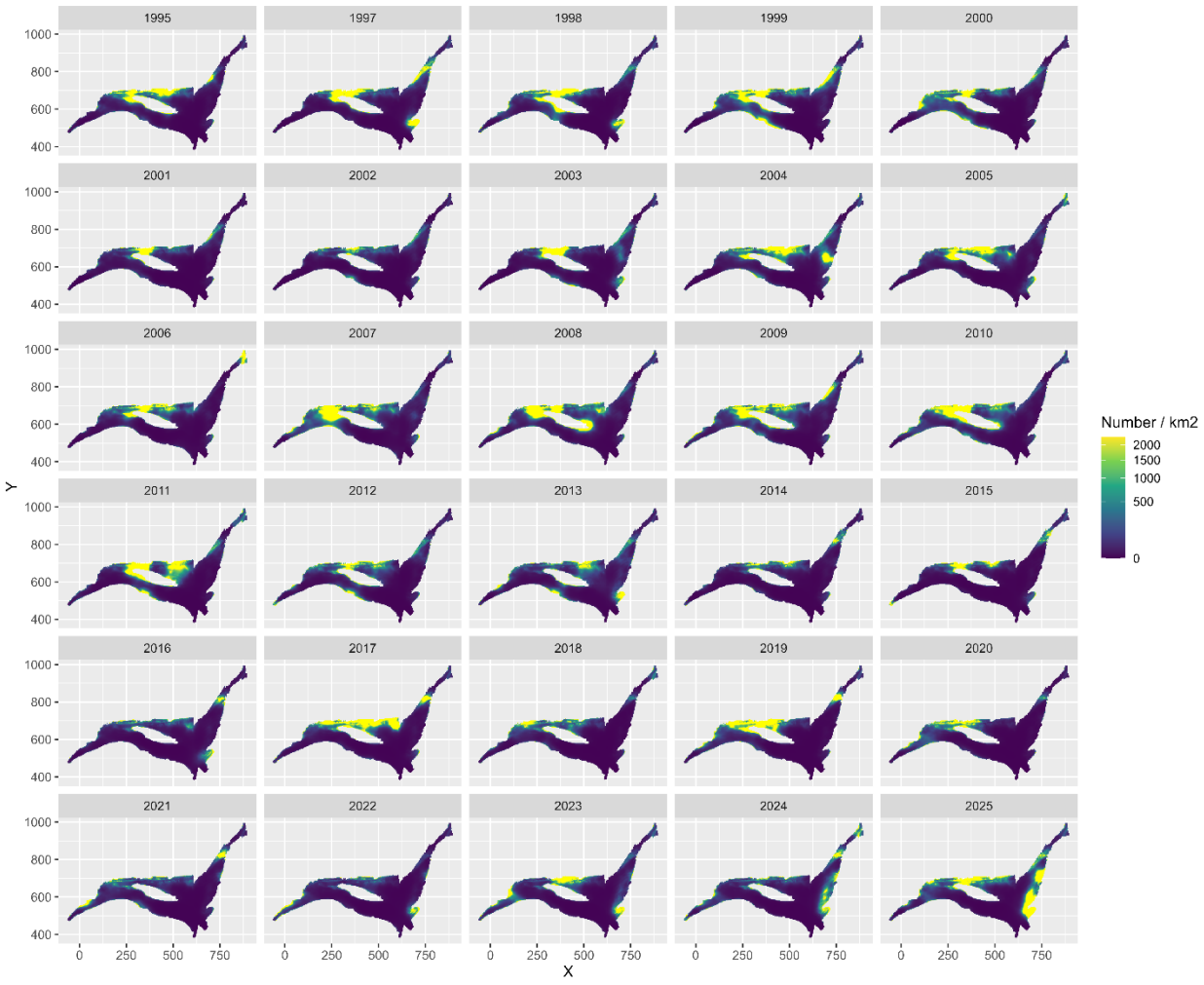


Figure 40: Annual maps of age-1 Capelin numbers predicted with the sdmTMB selected model and 1x1 km² depth grid in the northern Gulf of St. Lawrence.

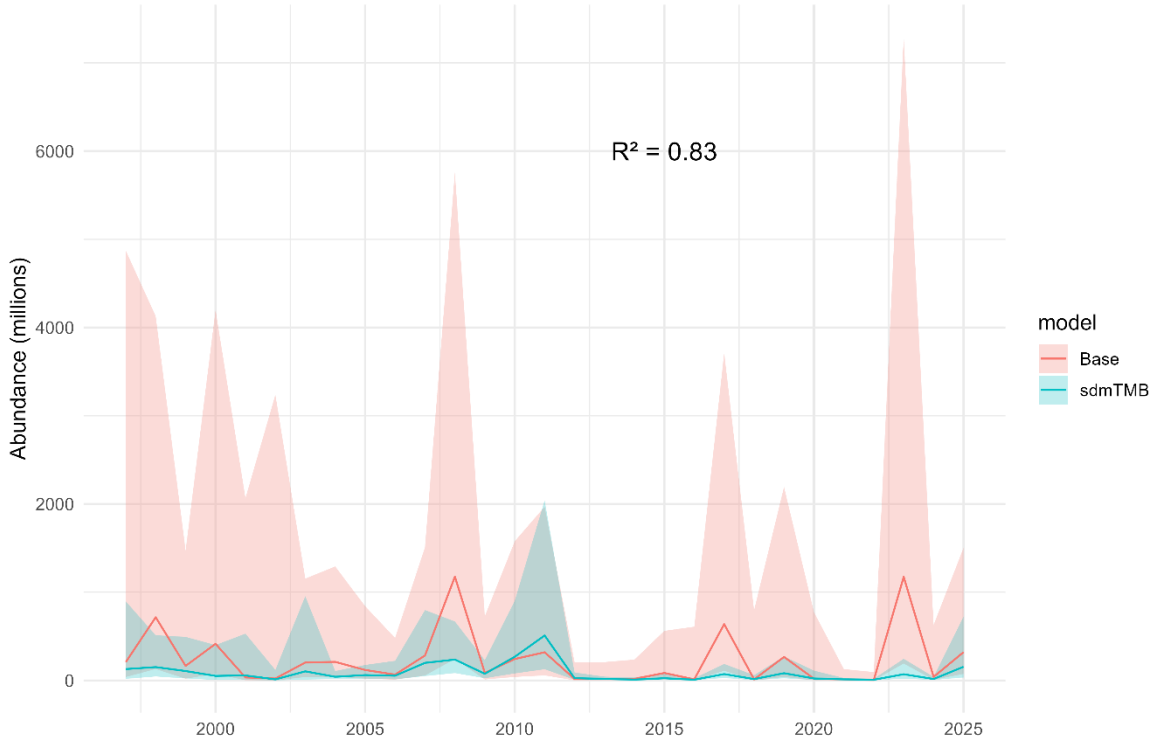


Figure 41: Abundance of age-1 Capelin estimated using design-based (red) and sdmTMB (blue) approaches in the northern Gulf of St. Lawrence, with R² values from Pearson correlations based on annual comparisons. Shaded areas represent 95% confidence intervals.

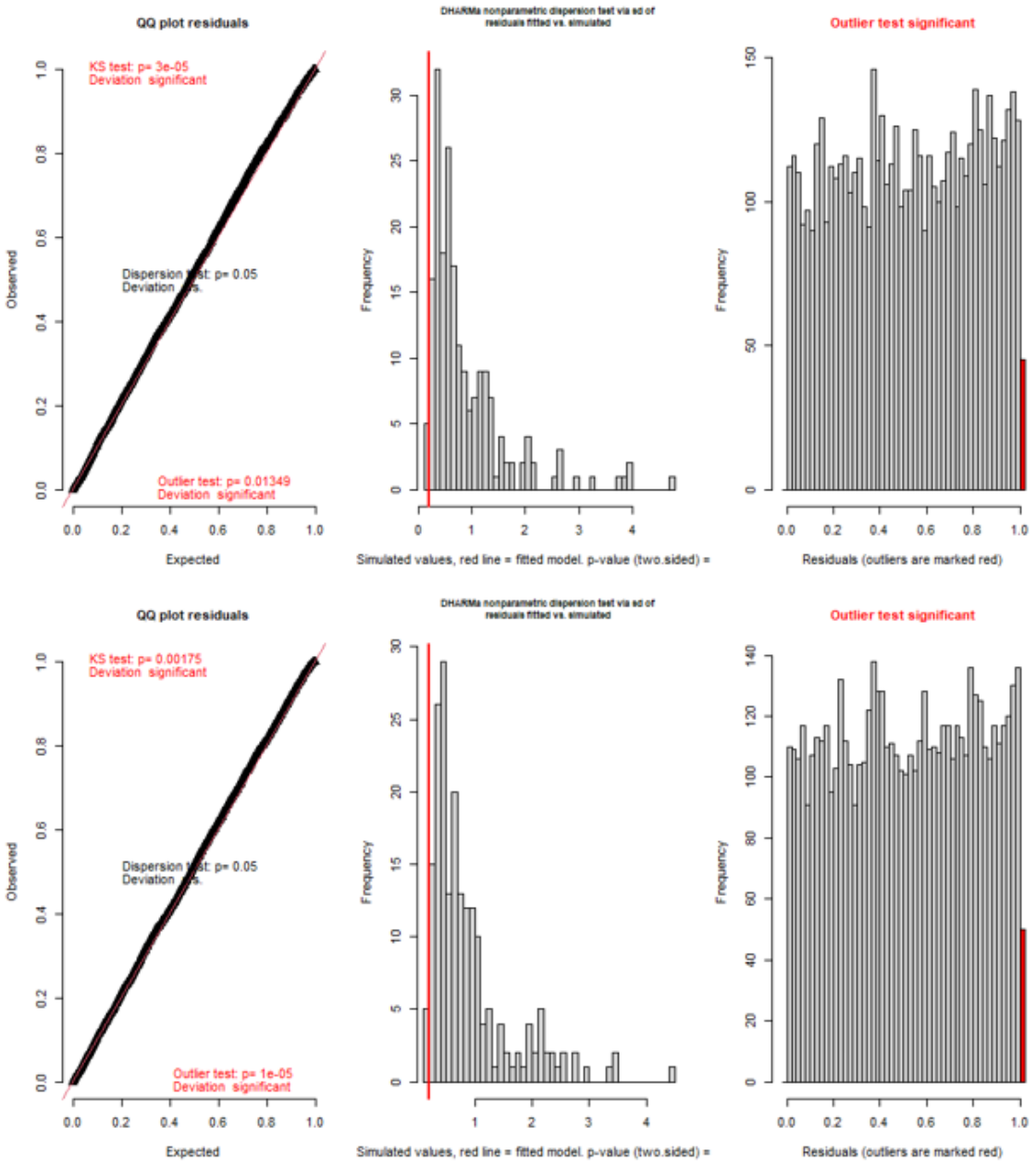


Figure 42: DHARMa diagnostic plots for the models used to fit age-1 Capelin in the southern Gulf of St. Lawrence and considering temporal effect of year as a random effect drawn from a normal distribution (upper panels) or as a categorical factor (lower panels).

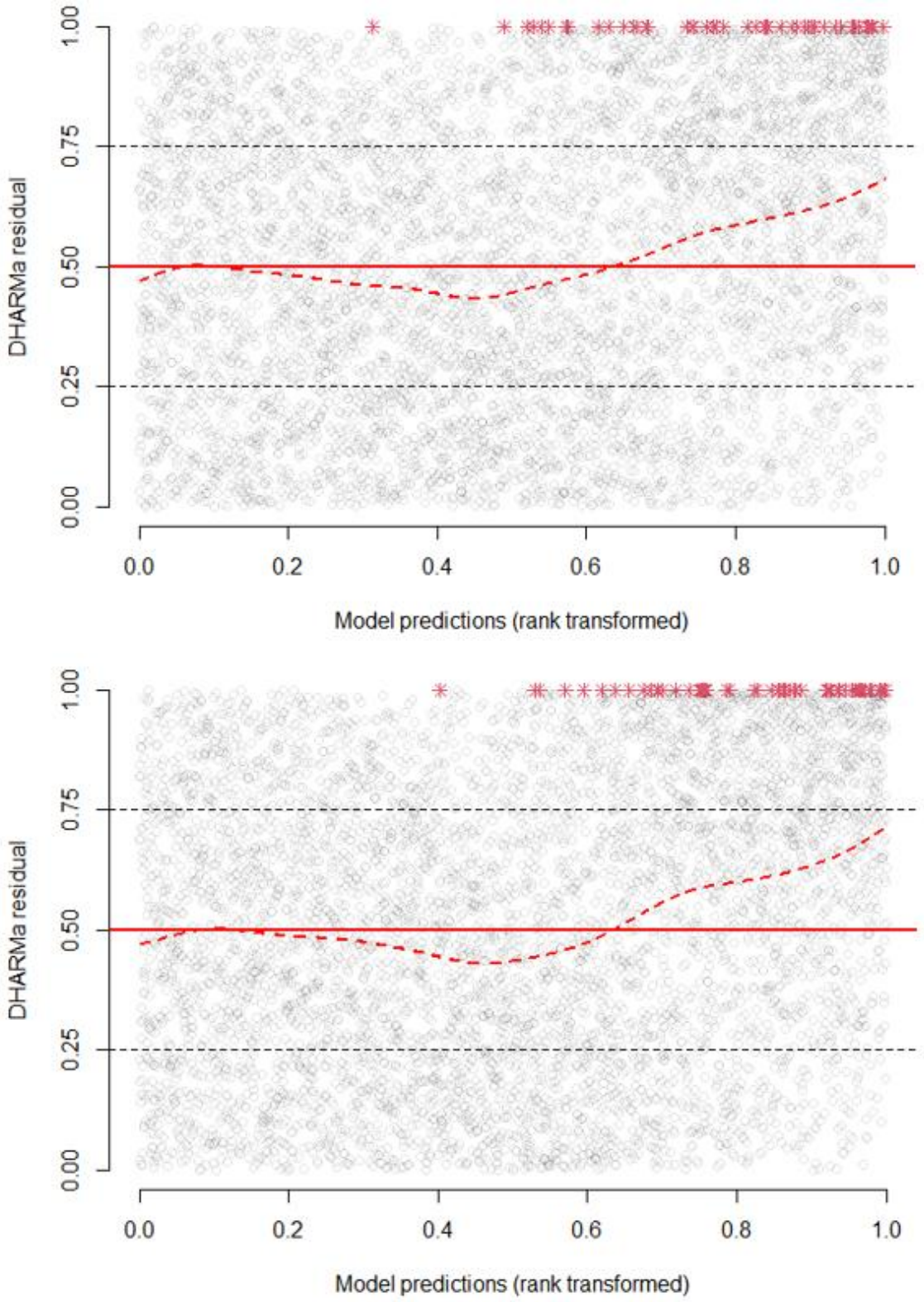


Figure 43: DHARMa residual plots for the models used to fit age-1 Capelin in the southern Gulf of St. Lawrence and considering temporal effect of year as a random effect drawn from a normal distribution (upper panel) or as a categorical factor (lower panel).

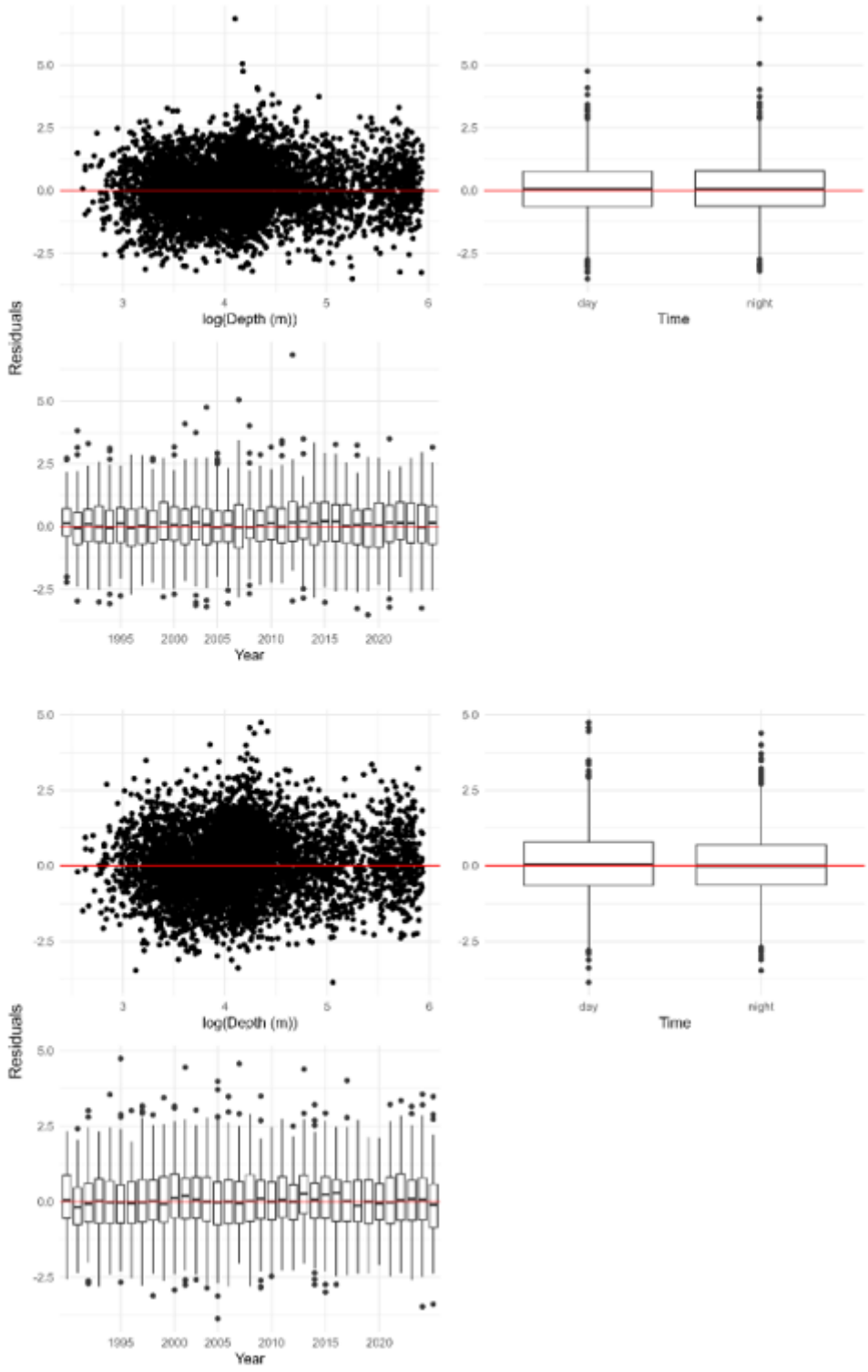


Figure 44: Quantile residuals in relation to the different predictive variables (log transformed depth, time of the day in categories and year) used to fit age-1 Capelin in the southern Gulf of St. Lawrence considering temporal effect of year as a random effect drawn from a normal distribution (upper panels) and as a categorical factor (lower panels). The horizontal red line indicates a value of 0, and the blue line represents a smoother distribution of residual values.

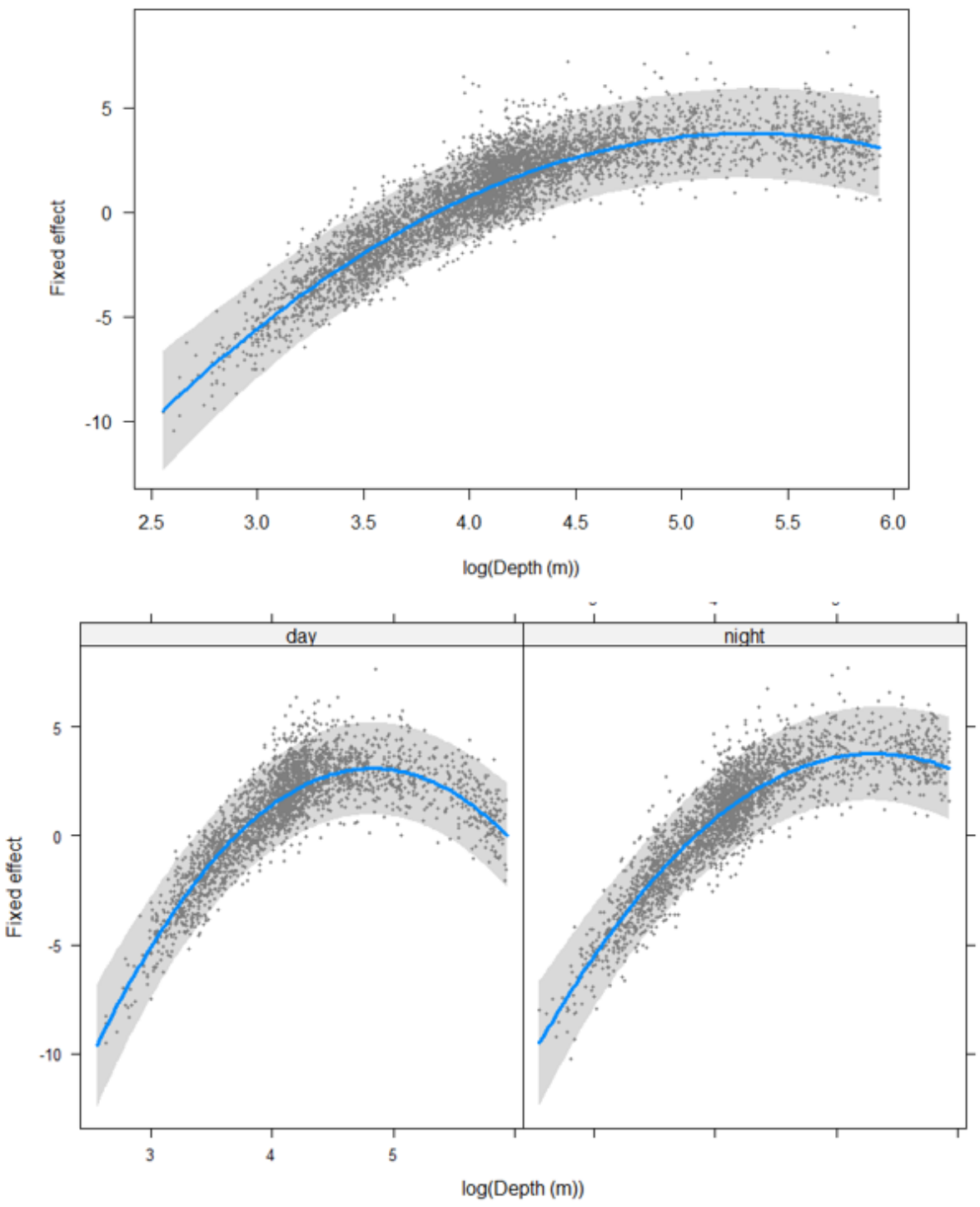


Figure 45: Conditional mean (blue line) and 95% confidence interval (shaded area) of the log-transformed depth (upper panel) and the interaction of the log-transformed depth and the time of the day (lower panels) effects on the age-1 Capelin number caught in the southern Gulf of St. Lawrence bottom trawl survey estimated with the sdmTMB selected model.

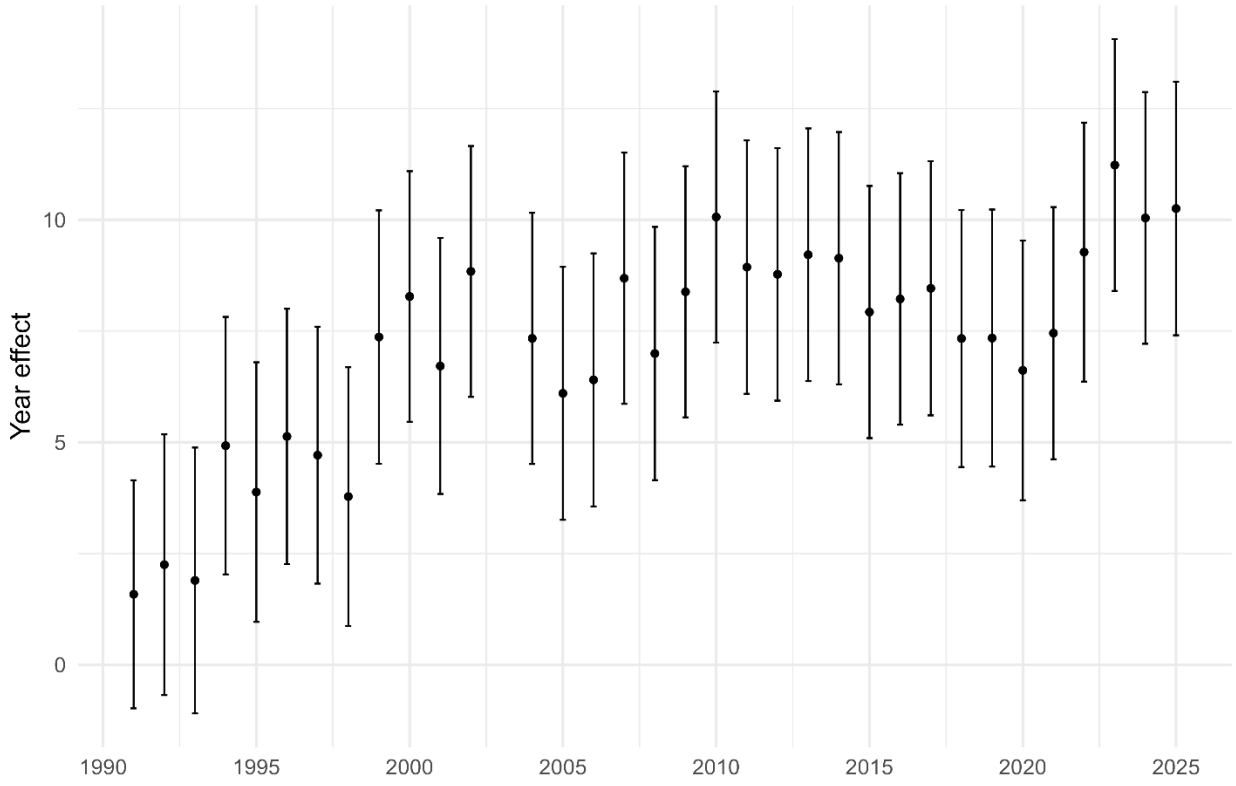


Figure 46: Coefficients (points) and confidence intervals (vertical lines) of temporal effect of year as a categorical factor from the selected model used to fit age-1 Capelin abundance in the southern Gulf of St. Lawrence.



Figure 47: Annual maps of age-1 Capelin numbers predicted with the sdmTMB selected model and 1x1 km² depth grid in the southern Gulf of St. Lawrence.

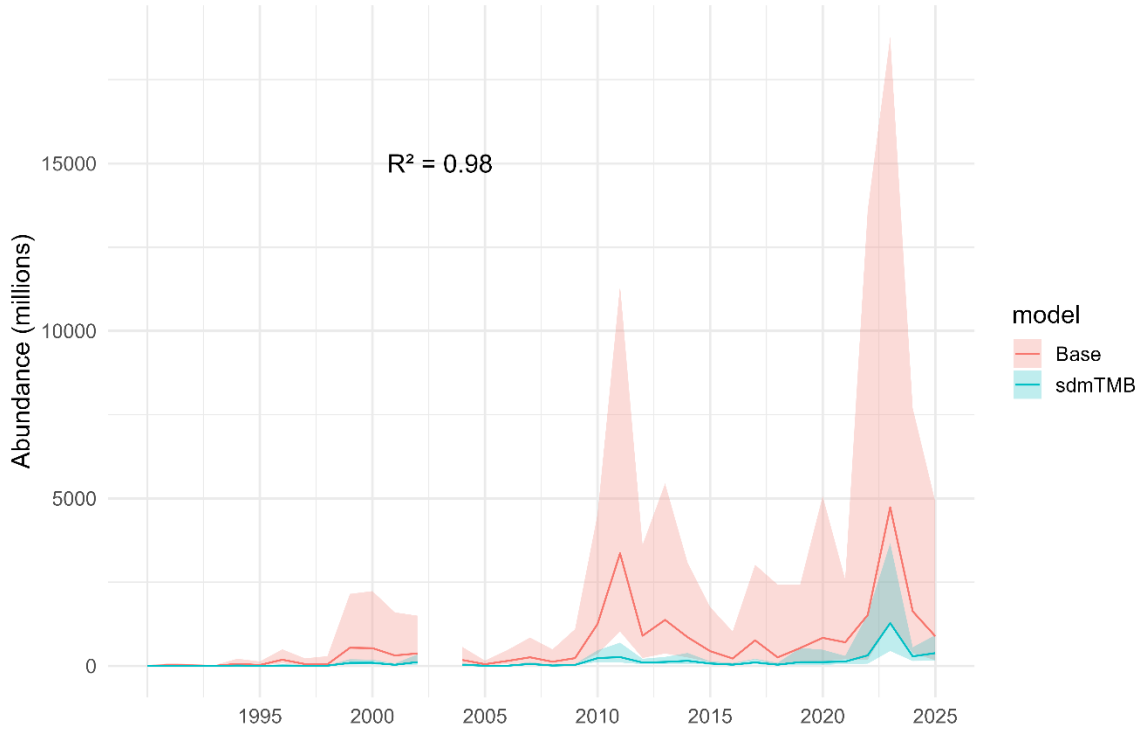


Figure 48: Abundance of age-1 Capelin estimated using design-based (red) and sdmTMB (blue) approaches in the southern Gulf of St. Lawrence, with R² values from Pearson correlations based on annual comparisons. Shaded areas represent 95% confidence intervals.

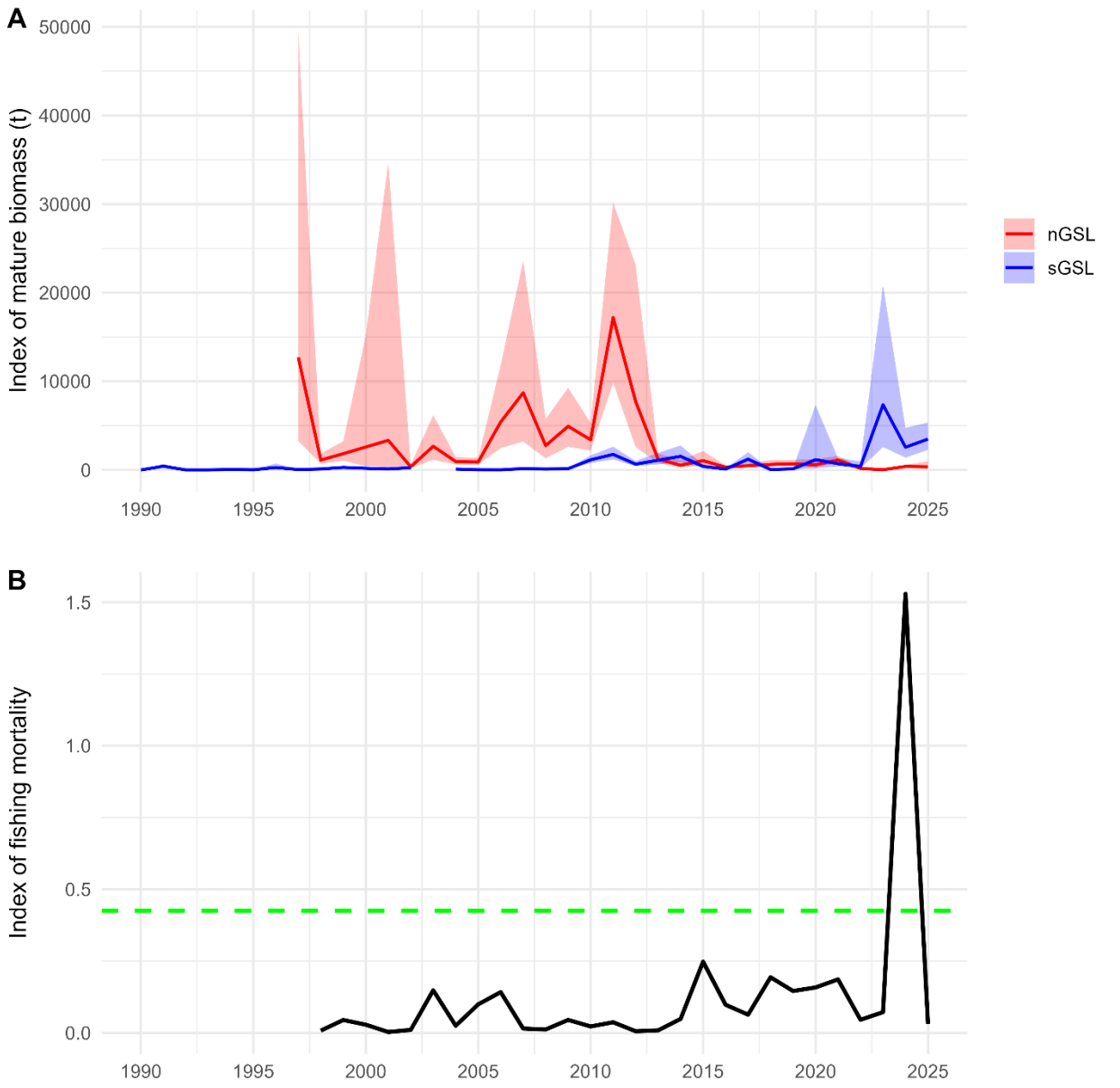


Figure 49: Time-series of (A) the mature biomass indices estimated with sdmTMB in the northern (nGSL) and southern (sGSL) Gulf of St. Lawrence and (B) the index of fishing mortality estimated with the ratio of total landings over the scaled mature biomass in the nGSL of the preceding year. The shaded areas in the upper panel represent the 95% confidence intervals. The horizontal dashed line in the lower panel represents levels over which harvest are causing serious harm to small pelagics according to Patterson 1992 (i.e. fishing mortality = ½ of natural mortality).

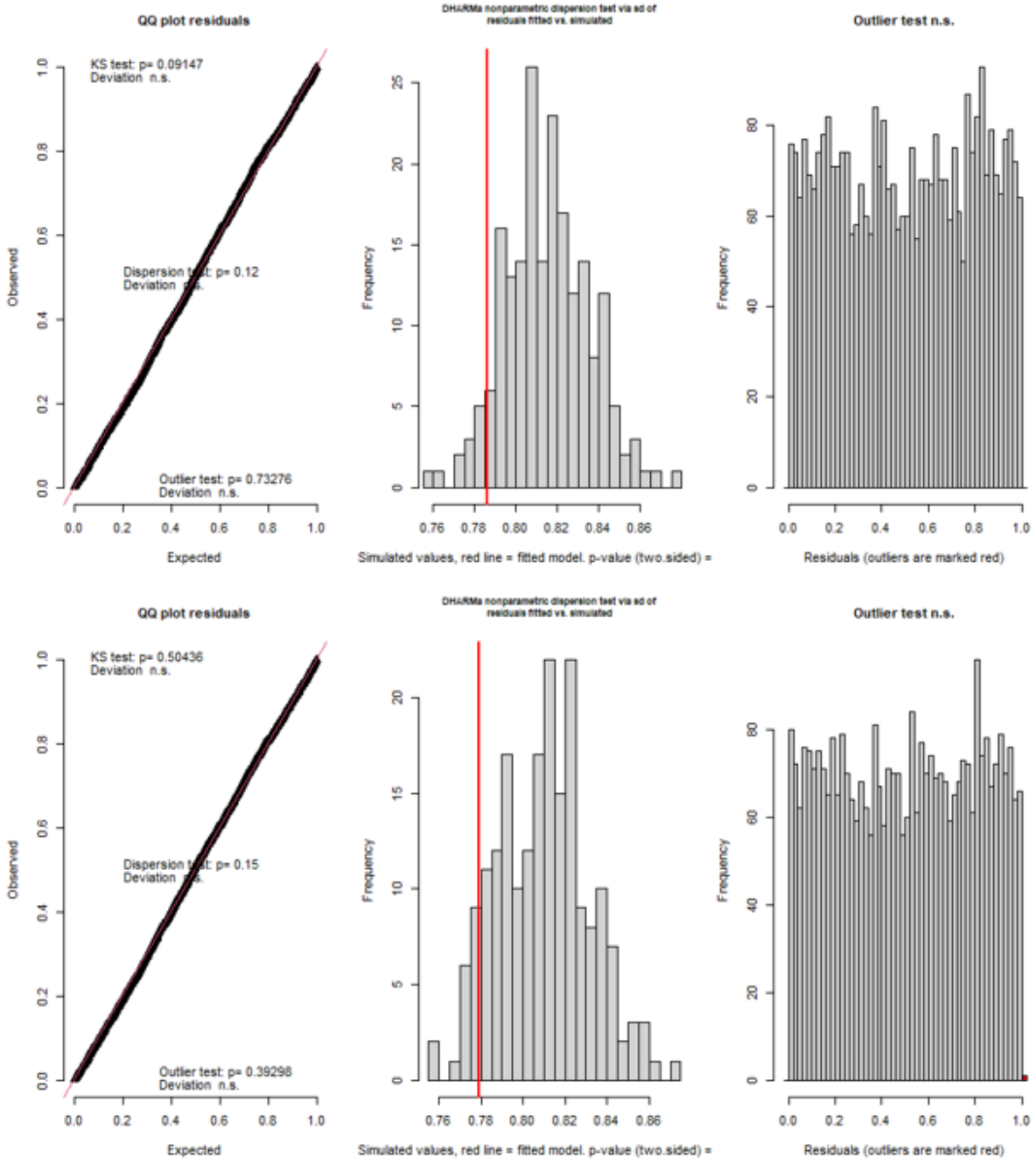


Figure 50: DHARMa diagnostic plots for the models used to fit the presence and absence of Capelin in Greenland halibut and Atlantic cod stomachs in the northern Gulf of St. Lawrence and considering temporal effect of year as a random effect drawn from a normal distribution (upper panels) or as a categorical factor (lower panels).

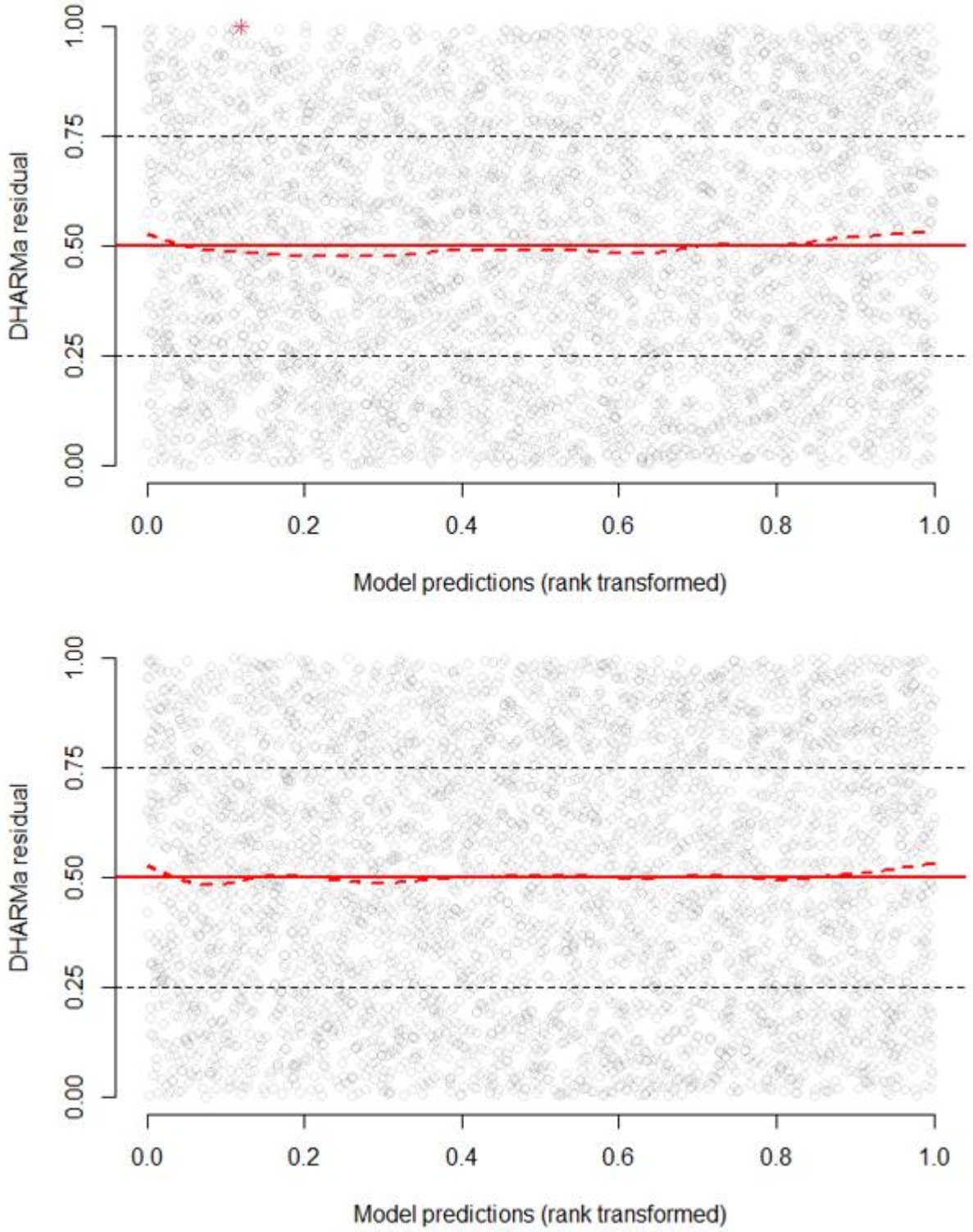


Figure 51: DHARMa residual plots for the models used to fit the presence and absence of Capelin in Greenland halibut and Atlantic cod stomach combined in the northern Gulf of St. Lawrence and considering temporal effect of year as a random effect drawn from a normal distribution (upper panel) or as a categorical factor (lower panel).

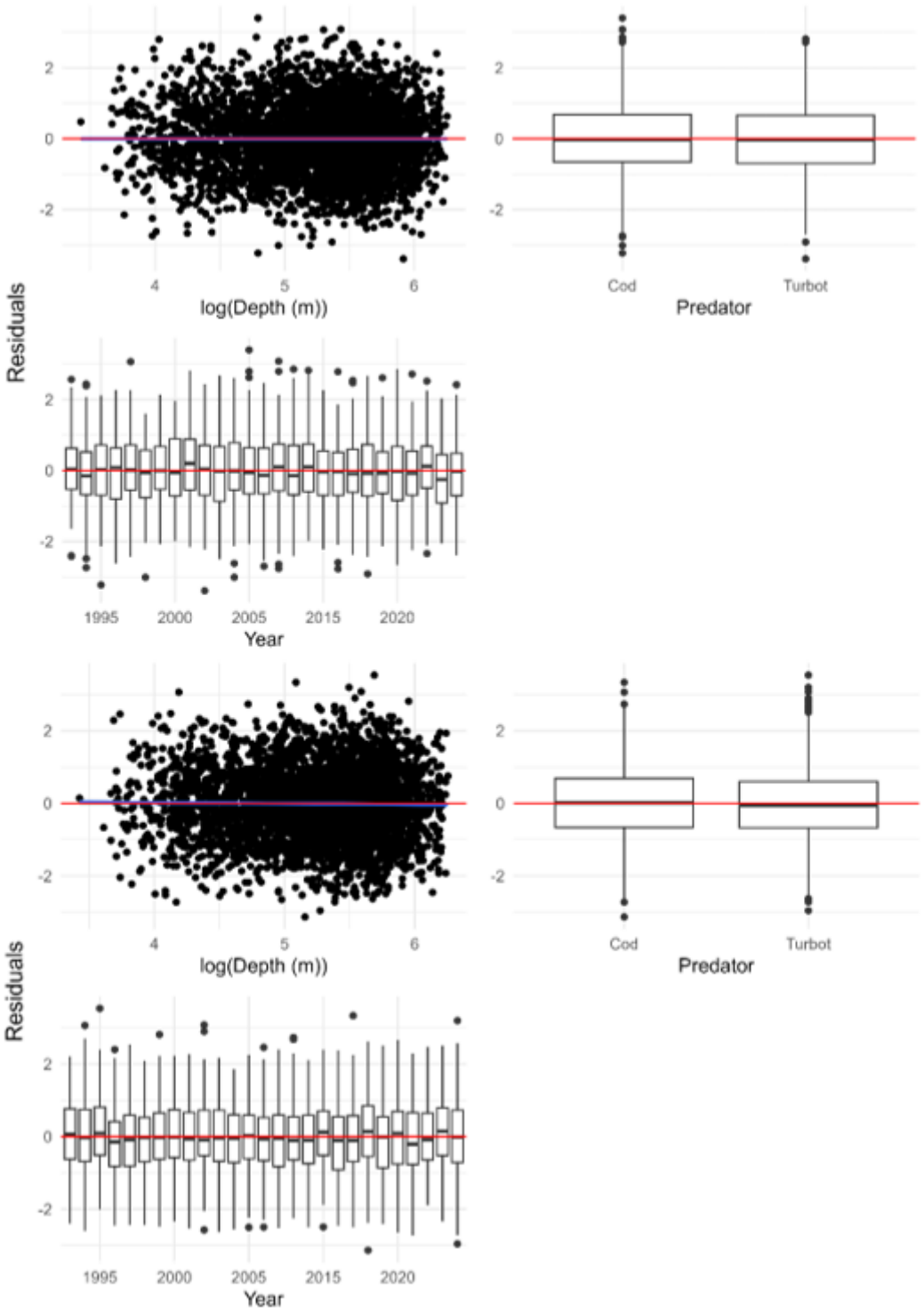


Figure 52: Quantile residuals in relation to the different predictive variables (log-transformed depth, predator and year) used to fit the presence and absence of Capelin in Greenland halibut and Atlantic cod stomach combined in the northern Gulf of St. Lawrence considering temporal effect of year as a random effect drawn from a normal distribution (upper panels) and as a categorical factor (lower panels). The horizontal red line indicates a value of 0, and the blue line represents a smoother distribution of residual values.

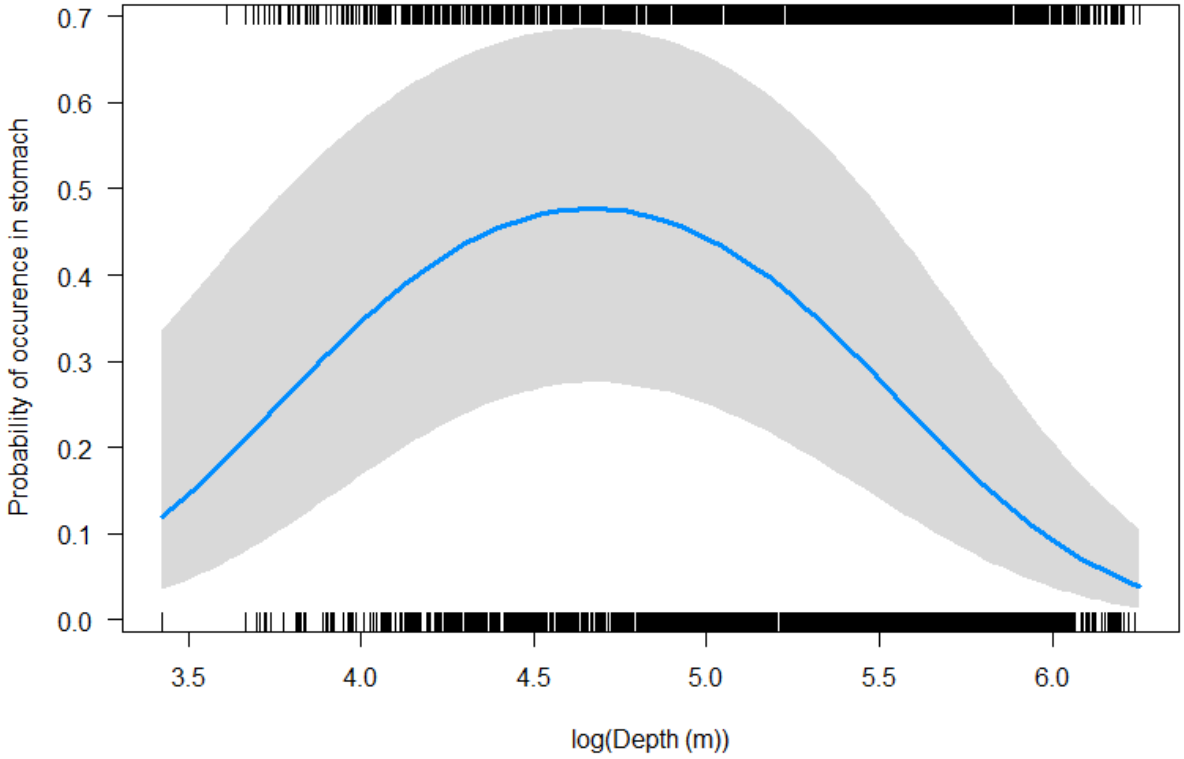


Figure 53: Conditional mean (blue line) and 95% confidence interval (shaded area) of the log-transformed depth effect on the Capelin probability of occurrence in predator stomach estimated with the sdmTMB selected model.

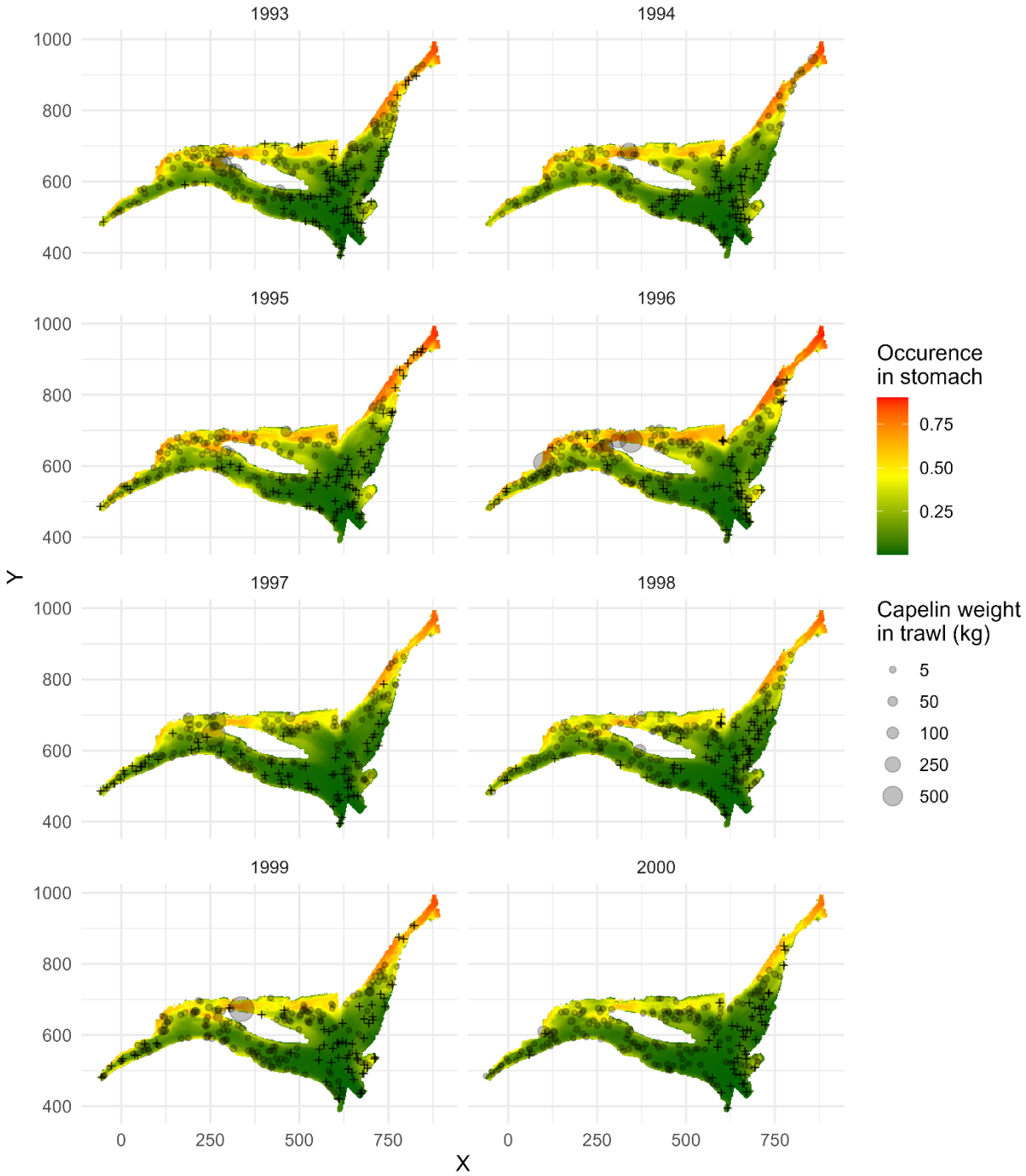


Figure 54: Maps of the capelin probability of occurrence in the stomachs of Greenland halibut and Atlantic cod estimated with sdmTMB in the northern Gulf of St. Lawrence and of the weight (bubble size) and absence of capelin (black cross) catches in the bottom trawl survey.

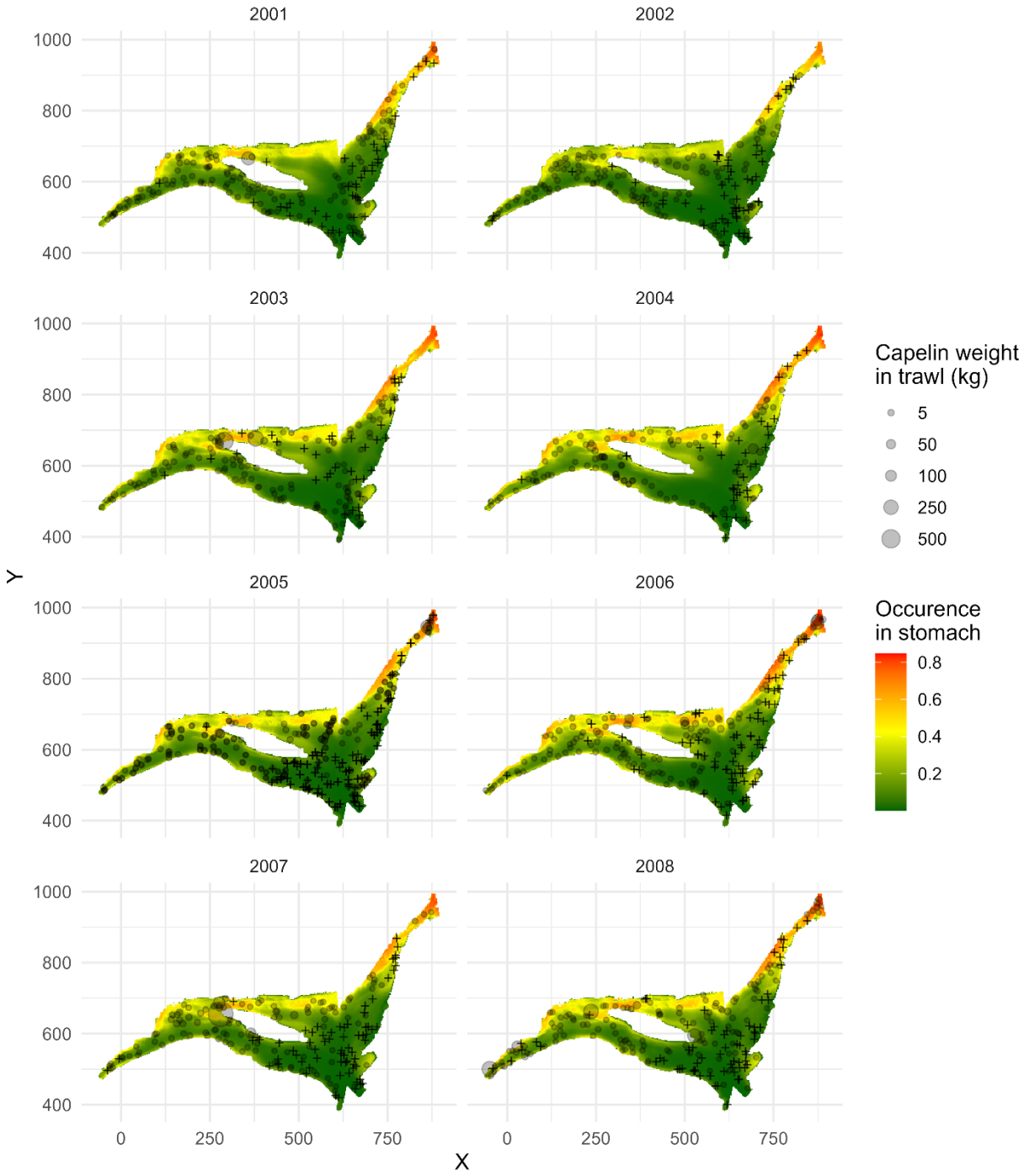


Figure 54: (continued)

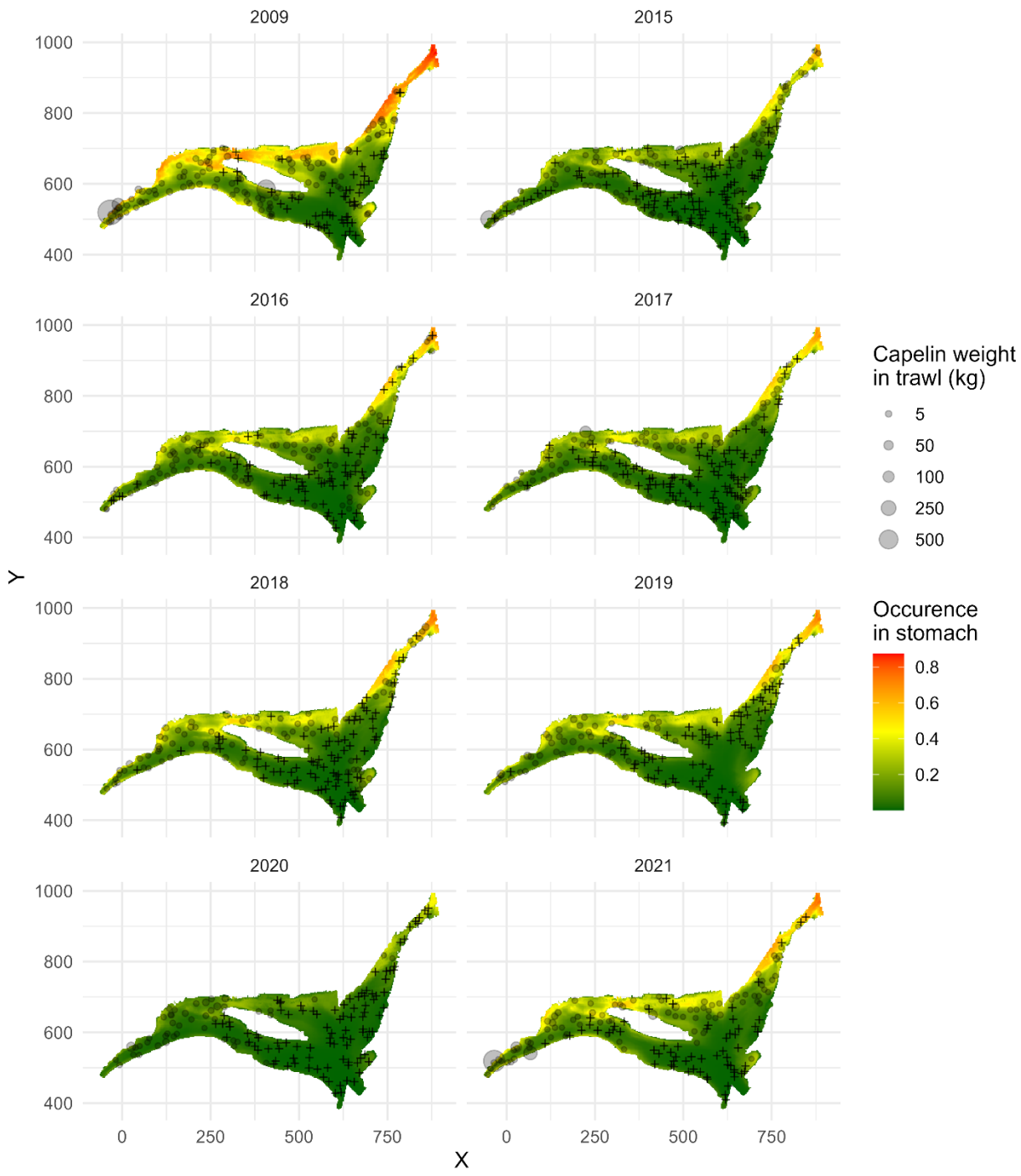


Figure 54: (continued)

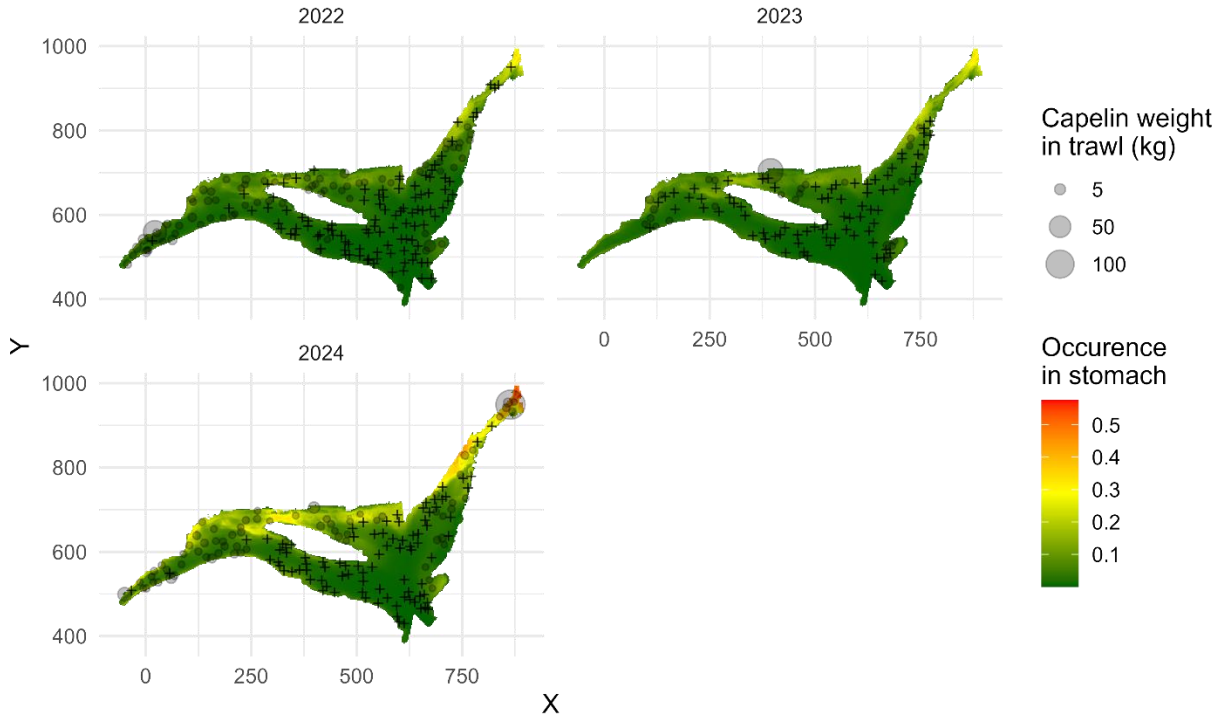


Figure 54: (continued)

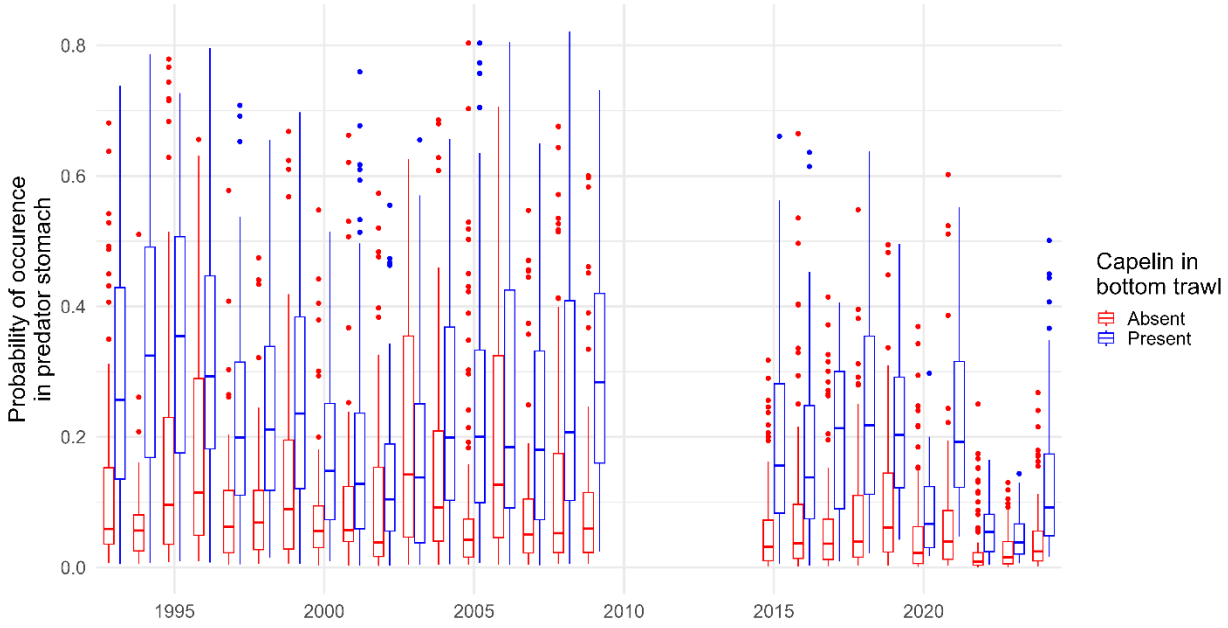


Figure 55: Capelin annual probability of occurrence in the stomachs of Greenland halibut and Atlantic cod predicted using sdmTMB and the 1x1 km² depth grid in cells where the northern Gulf of St. Lawrence survey recorded an absence or presence of capelin in the bottom trawl.

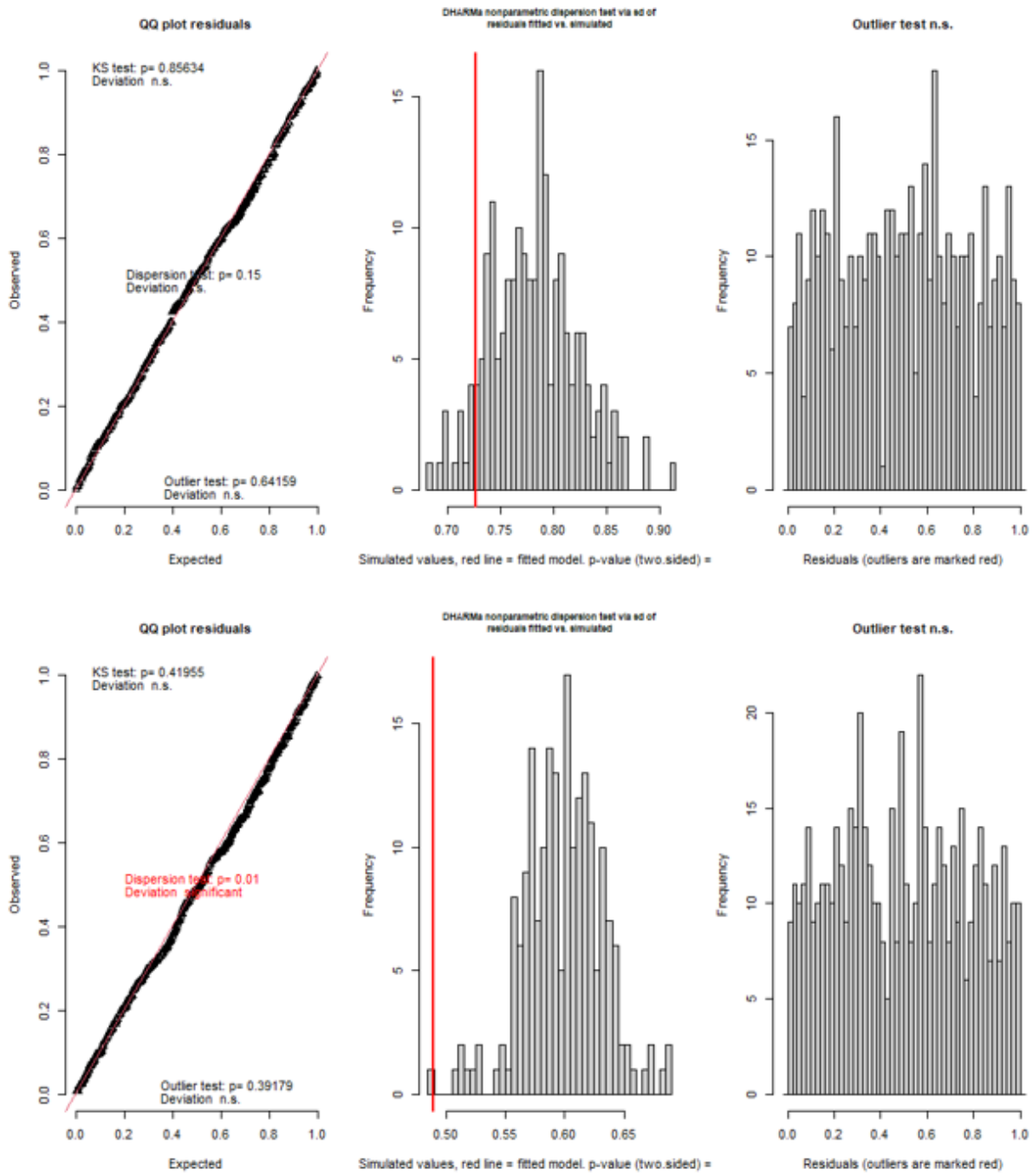


Figure 56: DHARMa diagnostic plots for the model used to fit the presence and absence of Capelin eDNA in the water column (upper panels) and at the bottom (lower panels) in the northern and southern Gulf of St. Lawrence.

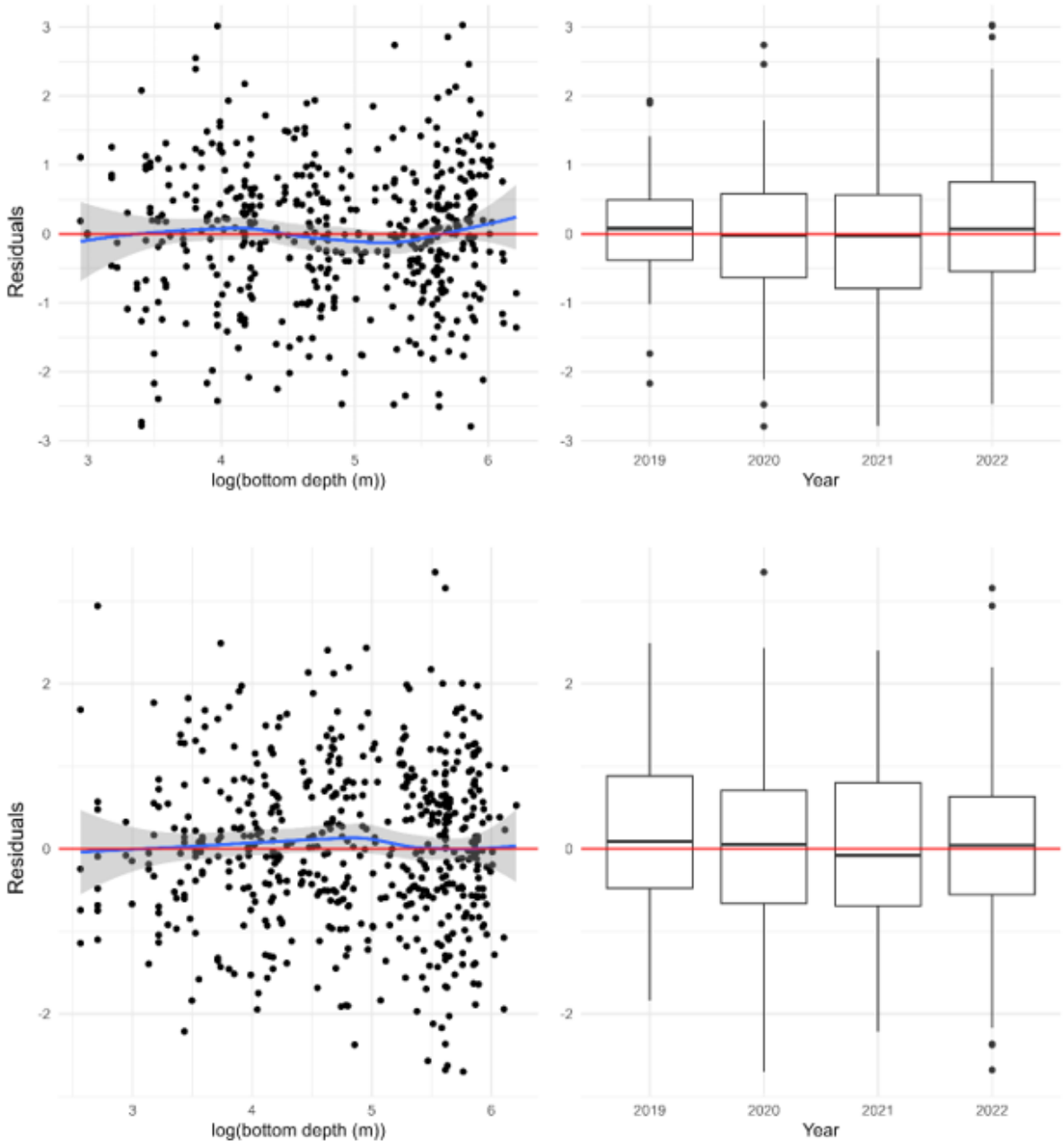


Figure 57: Quantile residuals in relation to the different predictive variables (depth and year) used to fit the presence and absence of Capelin eDNA in the water column (upper panels) and at the bottom (lower panels) in the northern and southern Gulf of St. Lawrence. The horizontal red line indicates a value of 0, and the blue line represents a smoother distribution of residual values.

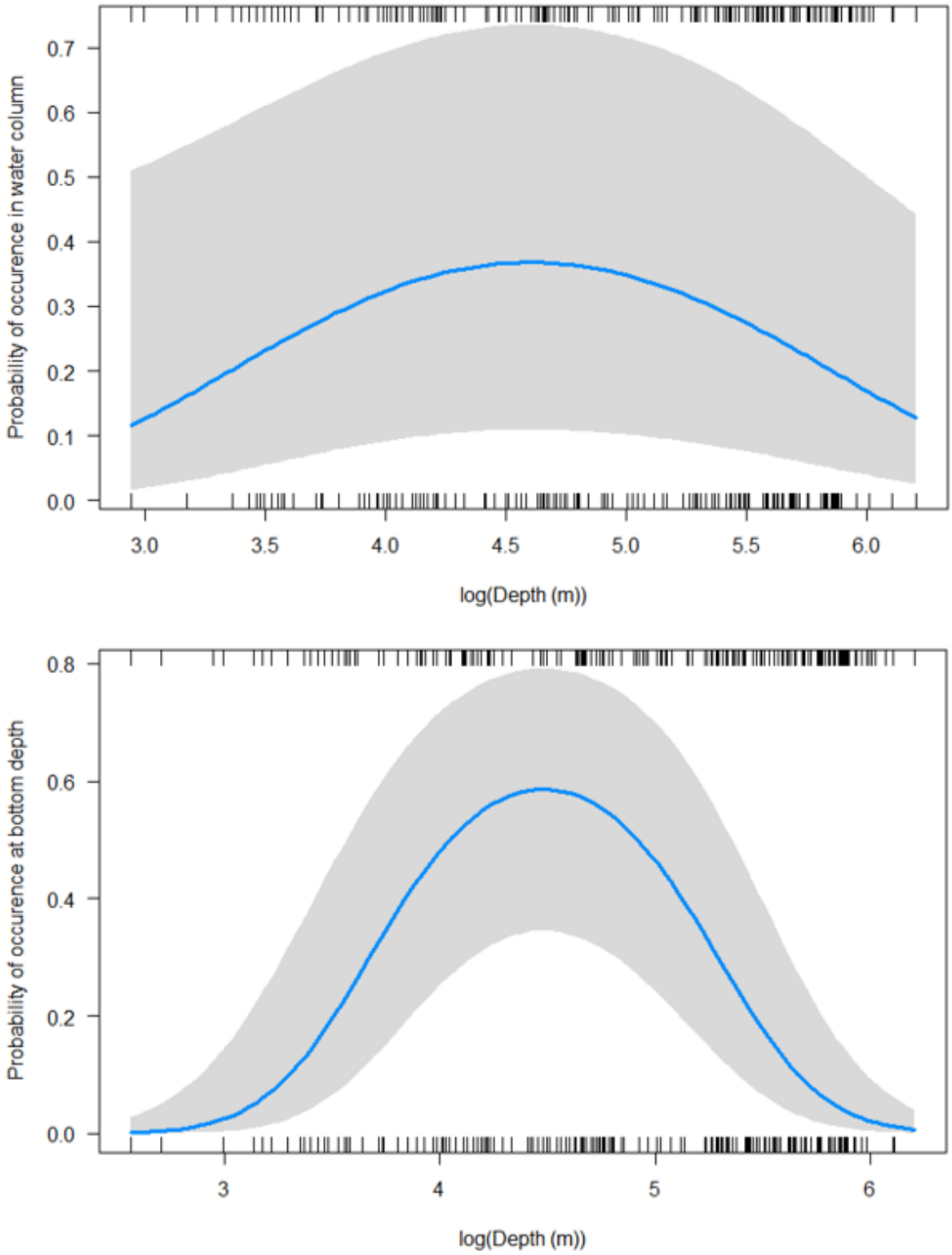


Figure 58: Conditional mean (blue line) and 95% confidence interval (shaded area) of the log-transformed depth effect on the Capelin probability of occurrence in the water column (upper panel) and at bottom depth (lower panel) estimated with the sdmTMB selected models.

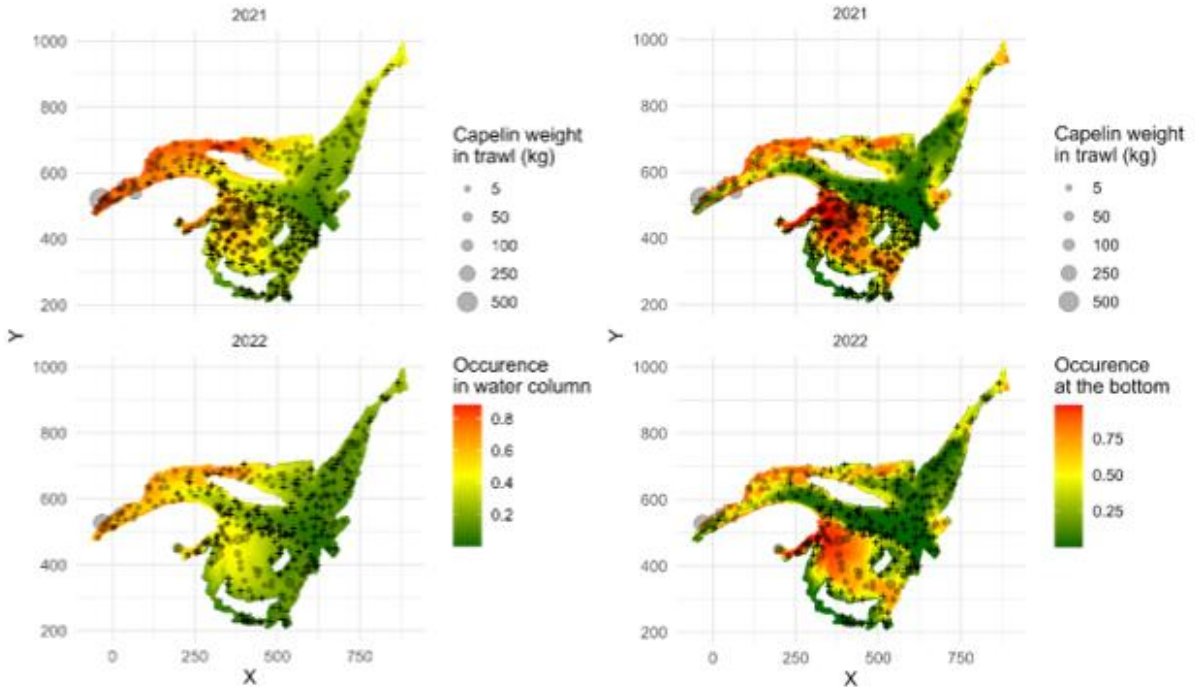


Figure 59: Annual maps of the probability of Capelin eDNA occurrence in the water column (left panels) and at the bottom (right panels) estimated with sdmTMB in the northern and southern Gulf of St. Lawrence and of the weight (bubble size) and absence of capelin (black cross) catches in the bottom trawl surveys for each year.

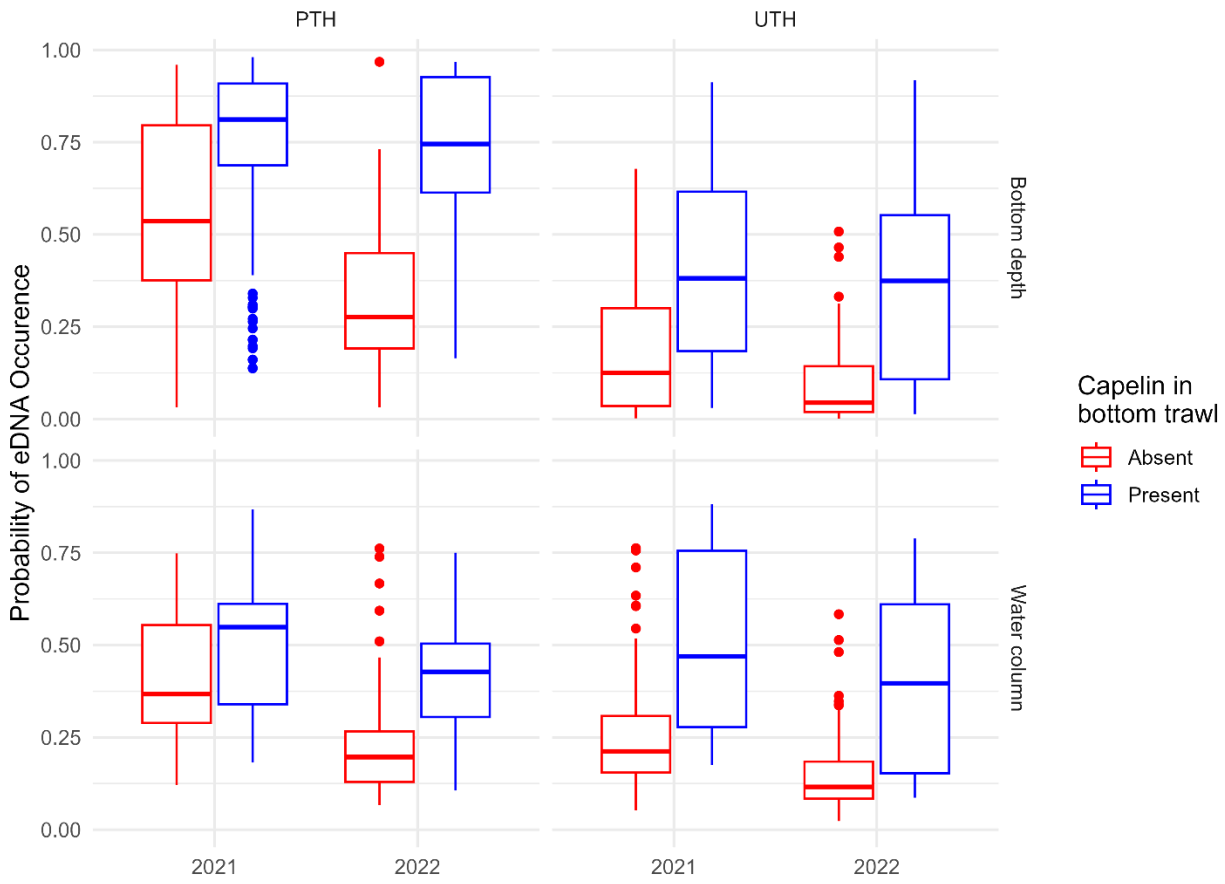


Figure 60: Annual probability of Capelin eDNA occurrence at the bottom and in the water column predicted with sdmTMB and the 1x1 km² depth grid in cells where the northern and southern Gulf of St. Lawrence survey recorded an absence or presence of Capelin in the bottom trawl in the preferred (PTH) and unfavorable (UTH) thermal habitat.

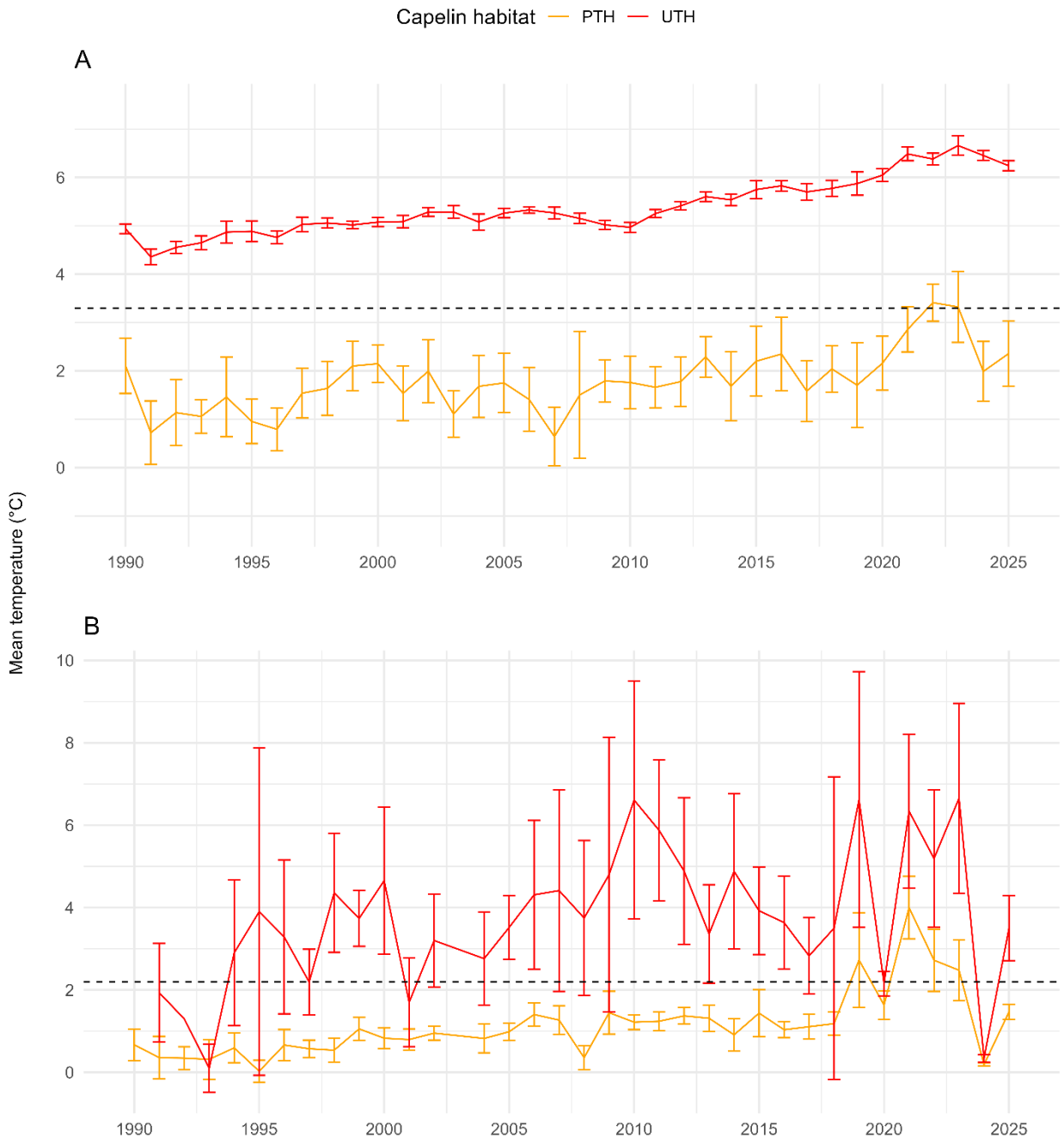


Figure 61: Mean bottom temperature recorded in trawl sets where capelin were captured during the A) northern and B) southern Gulf of St. Lawrence bottom trawl surveys, within capelin's preferred (PTH) and unfavourable (UTH) thermal habitat. The vertical lines represent the 95% confidence intervals. The horizontal dashed line represents the bottom temperature threshold associated with a major shift in the cumulative frequency distribution of capelin catches (3.3 and 2.2 °C in the nGSL and sGSL respectively) according to Chamberland et al. (2022).

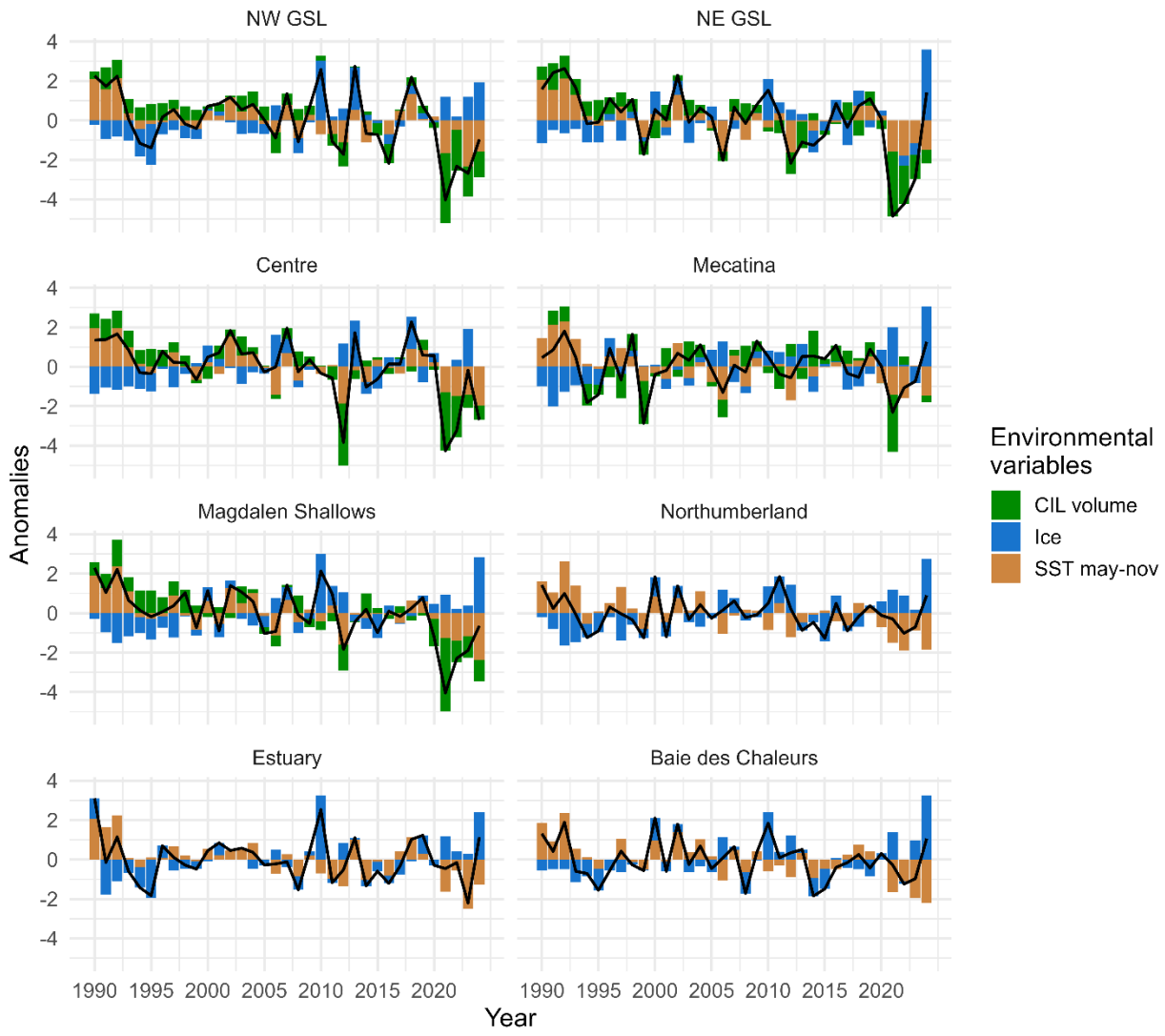


Figure 62: Annual values (bars) and cumulative sum (black line) of anomalies in the Cold Intermediate Layer (CIL) volume, the timing of the last occurrence of sea ice, and the sea surface temperature (SST) from May to November in the Gulf of St. Lawrence ecosystemic regions as defined by Duplisea et al. (2020).

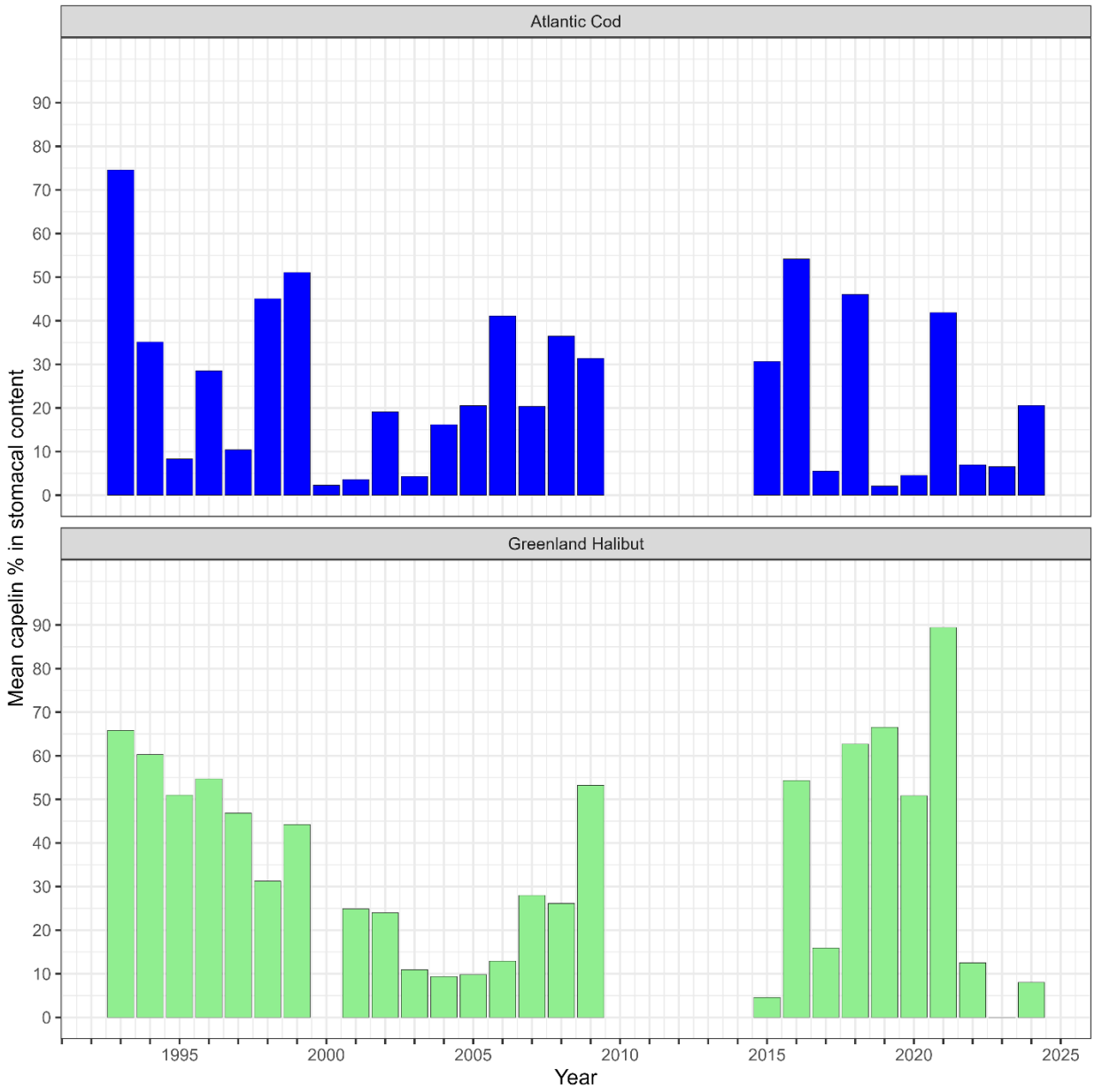


Figure 63: Percentage of stomach contents of Atlantic cod and Greenland halibut comprising Capelin, all predator length classes combined. No stomachs were collected during the period 2010–2014 (both predators) and in 2000 (Greenland halibut).